

ASSESSING THE IMPACT OF LAND USE CHANGES ON HYDROPOWER
PRODUCTION AND EROSION IN THE COCA RIVER BASIN. A
CONTRIBUTION TOWARDS INTEGRATED WATER RESOURCES
MANAGEMENT IN ECUADOR.

Zur Erlangung des akademischen Grades eines

DOKTOR-INGENIEURS

(Dr.-Ing.)

von der KIT - Fakultät für

Bauingenieur-, Geo- und Umweltwissenschaften

des Karlsruher Instituts für Technologie (KIT)

genehmigte

DISSERTATION

von

Carlos Alberto Zuleta Salmon

aus Ecuador

Tag der mündlichen Prüfung:

18. Mai 2021

Referent: Dr.-Ing. Uwe Ehret

Korreferent: Jun.-Prof. Dr.rer.nat. Andreas Braun

Karlsruhe 2021

Contents	
List of Figures	iii
List of Tables	iv
Abstract	v
German Abstract	vii
CHAPTER 1: Introduction	1
1.1- General overview	1
1.2.- Objectives	10
1.3.- Thesis outline	11
1.4.- Study area	12
1.5.- Integrated Water Resources Management – IWRM	18
1.5.1.- IWRM Process	19
CHAPTER 2. Data and Methods	21
2.1.- Available data	21
2.1.1.- Digital Elevation Model (DEM)	22
2.1.2.- Soil map and soil data	22
2.1.3.- Land-Use data	23
2.1.4.- Meteorological and Hydrological Data	23
2.1.5.- Data for LU/LUC analysis	26
2.2.- Uncertainty in IWRM	27
2.2.1.- Uncertainties and the Modeling role inside the IWRM Process.	27
2.2.2.- Modeling uncertainty sources	28
2.2.3.- Methodologies for uncertainty analysis in model-based IWRM process	29
2.2.4.- Methodology selection for uncertainty analysis	29
2.2.5.- Input and output uncertainties throughout the study area modeling process	30
2.3.- Methods for analyzing socioeconomic aspects and creating scenarios	31
2.3.1.- Historical Land-use Change analysis	32
2.3.2.- Markov Chain Model	32
2.3.3.- Cellular Automata Model (CA)	33
2.3.4.- The CA_Markov Chain Model	33
2.3.5.- CA_Markov parameter selection and modeling procedure	34
2.3.6.- Land-use modeling evaluation	38

2.4.- Methods for analyzing and modeling hydrological processes and creating scenarios.....	38
2.4.1.- Time series trend analysis methods	40
2.4.2.- The SWAT model.....	40
2.4.3.- SWAT model set-up for the study area	42
2.4.4.- Model Calibration, evaluation, and uncertainty procedures	45
2.4.5.- Calibration, Validation, Sensitivity, and Uncertainty analysis	47
CHAPTER 3.- Results and Discussion	50
3.1.- Land-use change (LUC) analysis and scenarios of socioeconomic aspects.....	50
3.2.- Hydrological analysis and scenarios	56
3.2.1.- Trend analysis	56
3.2.2.- Results of the SWAT modeling	58
3.2.3.- Effect of the different LUC scenarios on streamflow and water balance components	62
CHAPTER 4.- Summary, Conclusions, and Recommendations.....	72
Bibliography	76
Acknowledgments	88
Author’s declaration.....	89

List of Figures

Figure 1-1: Relevant chapters of the thesis structure.	12
Figure 1-2: Study Area – Upper Coca River basin.	13
Figure 1-3: Study Area main ecosystems.	14
Figure 1-4: Land-use cover map of 2016.....	15
Figure 1-5: Land-use cover changes (%) in the catchment between 1990 and 2016.	16
Figure 1-6: Total population and proportion (%) in economic activities in the study area.	17
Figure 1-7: The seven different steps with their main processes in the IWRM cycle.	20
Figure 2–1: Digital Elevation Model (DEM) (A) and Soil map of the Study Area (B).....	23
Figure 2-2: Land-use maps of the Study Area.....	24
Figure 2-3: Meteorological and Hydrological stations in the Study Area.....	25
Figure 2-4: Average daily precipitation (mm) and temperatures (°C) by month (1980 -2016).....	26
Figure 2-5: Average monthly flow (m ³ /s) of the Study Area (1980 – 2016).....	26
Figure 2-6: The Modeling role inside the IWRM process.	28
Figure 2-7: Standard 5 x 5-pixel contiguity filter.....	34
Figure 2-8: CA-Markov Model Flowchart.....	35
Figure 2-9: SWAT Model set-up process and model inputs.....	43
Figure 3-1: Land-use map of 2016 vs. Predicted Land-use map of 2016.....	50
Figure 3-2: Predicted LU maps of 2026 and 2036 Trend Scenario.....	52
Figure 3-3: Predicted LU maps of 2026 and 2036 Best-case Scenario.....	53
Figure 3-4: Predicted LU maps of 2026 and 2036 Worst-case Scenario.	55
Figure 3-5: Land-use coverage percentage according to the different LU maps and scenarios.....	55
Figure 3-6: Pettitt homogeneity tests of hydrometeorological variables.....	56
Figure 3-7: R ² analysis of Observed vs. Simulated Flows (m ³ /s) for calibration and validation.....	59
Figure 3-8: Uncertainty analysis with SUFI-2 algorithm for calibration and validation of streamflow.....	60
Figure 3-9: Calibration of the model and Uncertainty analysis of monthly streamflow (m ³ /s).....	61
Figure 3-10: Validation of the model and Uncertainty analysis of monthly streamflow (m ³ /s).....	62
Figure 3-11: Mean annual water-balance of the study area with different LU simulation scenarios.....	63
Figure 3-12: Average daily streamflow (m ³ /s) that reaches the HPP at the catchment outlet by scenario.	64
Figure 3-13: Changes on streamflow (%) by scenarios, relative to Trend Scenario 2026 and 2036.....	65
Figure 3-14: Agricultural areas (%) vs. Slope ranges in the catchment by scenario simulations.....	66
Figure 3-15: Soil Loss (T/Ha/Yr) in agricultural areas according to the scenario simulations.....	69

List of Tables

Table 2-1: Input data for hydrological and land-use analysis.	22
Table 2-2: Uncertainty analysis methodologies based on the modeling process and ambition level.	30
Table 2-3: Applicable methodologies for uncertainty analysis according to its Source and Type.	31
Table 2-4: Transition area probability matrix (2000 - 2008 – 2016).	36
Table 2-5: Weights of each factor based on AHP and Fuzzy standardization.	37
Table 2-6: Constraint Factors and suitability levels for LUC scenario analysis.	38
Table 2-7: Crop parameters /plant growth information and vegetation of the study area.	44
Table 2-8: Hydrological parameters considered for sensitivity analysis.	47
Table 2-9: Parameter description and ranges for calibration procedures with the model.	49
Table 2-10: General performance ratings for NSE and RSR statistics (monthly time step).	49
Table 3-1: Validation of the simulated Land-use (LU) map of 2016 based on the actual LU map of 2016.	50
Table 3-2: Validation analysis of the actual and simulated LU maps of 2016.	51
Table 3-3: Accuracy assessment of the simulated Land-use map of 2016.	51
Table 3-4: LU cover area (%) of Trend Scenarios (2026 – 2036) and gain/loss (%) estimation.	52
Table 3-5: LU cover area (%) of Best-Case Scenarios (2026 – 2036) and gain/loss (%) estimation.	53
Table 3-6: LU cover area (%) of Worst-Case Scenarios (2026 – 2036) and gain/loss (%) estimation.	54
Table 3-7: MK and Pettitt tests for the study area’s rainfall and streamflow data.	56
Table 3-8: Streamflow most sensitive parameters and final ranges for model calibration.	59
Table 3-9: Streamflow calibration, validation, and uncertainty analysis results.	59
Table 3-10: Mean annual water-balance results, according to the different scenario simulations.	63
Table 3-11: Agricultural areas (Ha and %) vs. Slope ranges, according to the LU scenario simulations. ...	66
Table 3-12: Agricultural area’s changes (%) vs. Slope ranges, regarding 2016 by scenario simulations. ..	67
Table 3-13: Soil Loss -SL- (T/Ha), Surface runoff -SurQ- (mm), and Regression analysis correlation (R²).	68

Abstract

The region with the highest rate of land-use change worldwide is the humid tropics, where deforestation of natural forest cover, caused by the aim to create space for agricultural lands and pastures, is a prevalent process. Furthermore, this region is well known for its great water availability and hydropower generation potential. Therefore, in recent decades, efforts to conserve and protect the natural forest cover of the tropic watersheds have become a priority within Integrated Water Resource Management (IWRM) processes.

Land-use change (LUC) influences the water balance of a basin, affecting the available water, along with the change in the other water balance components. Understanding the LUC and its implication on the hydrology of a basin is vital for the management and utilization of water resources in a watershed. Thus, understanding responses by changes in land use over the past decades on streamflow in a watershed is important for the proper water management and water resources planning within an IWRM framework in the future.

This study assesses the historical trends of rainfall and streamflow and analyzes the responses of streamflow for hydropower generation to changes in land use, under different scenarios and future projections, in the upper Coca River basin. Which is located on the eastern slopes of the Ecuadorian Andes and is part of the upper Ecuadorian Amazon region. Findings of the Mann-Kendall (MK) test indicate no statistically significant trend existed in the daily precipitation and monthly streamflow measurements in the watershed. The Pettitt test does not detect any jump point in the basin-wide precipitation series.

The land-use maps of 1990, 2000, 2008, and 2016 are used for LUC detection analysis, and the CA_Markov model is used to predict the future LUC projections under three different scenarios; Trend scenario, “Best-case” scenario, and “Worst-case” scenario, for the years 2026 and 2036, by taking into consideration the physical and socio-economic drivers of LUC dynamics in the catchment. The Trend scenario maintains the probabilities of change in land use that are predicted for the years 2026 and 2036. The “Best-case” scenario addresses the probabilities of change in land use towards a balanced scenario between conservation of natural ecosystems and productive activities within the basin. The “Worst-case” scenario addresses the probabilities of change in LU towards a scenario where extractive activities prevail and the productive areas in the watershed increase.

The LUC detection results show increases in agricultural lands and decreases in forest cover from 1990 to 2016. Statistically, natural forest cover decreased from 61.2% in 1990 to 57.12% in 2016, while the proportion of agricultural lands increased from 2.9% to 7.23% in 1990 and 2016, respectively. The LUC projection results, for the years 2026 and 2036, in relation to the year 2016, suggest that agricultural lands are predicted to increase by 9.3% in 2026, and by 19.2% in 2036 in the Trend scenario. For the “Best-case” scenario, agricultural lands are predicted to increase by 1.1% and 3% in 2026 and 2036, respectively. The “Worst-case” scenario results for the years 2026 and 2036 predict increases in agricultural lands by 26.1% and 54.3%, respectively. Furthermore, the natural forest cover in the catchment is predicted to decrease by 0.6% (2026) and by 1.5% (2036) for the Trend scenario, in relation to 2016. For the “Best-case” scenario, the forest cover is predicted to decrease by 0.2% (2026) and by 0.4% (2036). The “Worst-case” scenario results for the years 2026 and 2036 predicted decreases in natural forest cover by 2.6% and 5.8% respectively, in relation to 2016.

Results of hydrological modeling indicate that, due to the effects of LUC, the average daily streamflow increased by 1.04% (2026) and 1.45% (2036) for the Trend scenario, in relation to 2016. For the “Best-case” scenario, the

average daily streamflow decreased by 4.91% (-24.8m³/s) and 6.10% (-30.8m³/s) for the years 2026 and 2036 respectively, in relation to 2016. For the “Worst-case” scenario, in relation to the year 2016, the average daily streamflow is predicted to increase by 2.08% (2026) and by 2.37% (2036).

The findings on the effects of LUC on streamflow under the different proposed scenarios indicate that the changes in streamflow would not be a factor that could affect the hydropower generation in the watershed. Nevertheless, the results show that the water balance components are affected by the spatial and temporal distribution of LUC in the study area, which is useful for basin-wide integrated water resources management. However, the magnitude of these effects can be masked by uncertainties derived from the hydrological and LUC modeling processes. Hence, further land-use change optimization studies, and rainfall-runoff processes evaluation research are indispensable in the study area. Nevertheless, sustainability issues associated with the presence of the hydropower facility in the study area should not be neglected; and to be able to ensure sustainable development in the basin (which comprises the long-term hydropower production, ecosystems conservation, and the socio-economic well-being of the population in the watershed), other variables and processes that were not covered in this study must be analyzed in further work within an IWRM framework.

German Abstract

Zusammenfassung

Die Region mit der weltweit höchsten Rate an Landnutzungsänderungen sind die feuchten Tropen. Es ist ein weit verbreiteter Prozess in diesen Regionen durch Entwaldung Raum für landwirtschaftliche Flächen und Weiden zu schaffen. Darüber hinaus ist diese Region für ihre große Wasserverfügbarkeit und ihr Potenzial zur Erzeugung von Wasserkraft bekannt. Daher sind in den letzten Jahrzehnten Bemühungen zur Erhaltung und zum Schutz der natürlichen Waldbedeckung der tropischen Wassereinzugsgebiete zu einer Priorität innerhalb der Prozesse des integrierten Wasserressourcenmanagements (IWRM) geworden.

Landnutzungsänderungen (LUC) beeinflussen den Wasserhaushalt eines Einzugsgebiets, indem sie das verfügbare Wasser zusammen mit der Veränderung der anderen Wasserhaushaltskomponenten beeinflussen. Das Verständnis der LUC und ihrer Auswirkungen auf die Hydrologie eines Einzugsgebiets ist für das Management und die Nutzung der Wasserressourcen in einem Einzugsgebiet von entscheidender Bedeutung. Daher ist es wichtig, die Auswirkungen von Landnutzungsänderungen in den letzten Jahrzehnten auf die Abflussmenge eines Wassereinzugsgebiets zu verstehen, um in Zukunft - innerhalb eines IWRM-Rahmens - ein ordnungsgemäßes Wassermanagement und eine Wasserressourcenplanung durchführen zu können.

Diese Studie bewertet die historischen Trends von Niederschlag und Stromfluss und analysiert die Reaktionen des Stromflusses auf Landnutzungsänderungen unter verschiedenen Szenarien und Zukunftsprojektionen im oberen Coca-Einzugsgebiet. Dieses befindet sich am Osthang der ecuadorianischen Anden und ist Teil der oberen ecuadorianischen Amazonasregion. Die Ergebnisse des Mann-Kendall-Tests (MK) zeigen, dass kein statistisch signifikanter Trend in den täglichen Niederschlags- und monatlichen Flussabflussmessungen im Wassereinzugsgebiet existiert. Der Pettitt-Test kann keinen Sprungpunkt in den einzugsgebietsweiten Niederschlagsreihen feststellen.

Die Landnutzungskarten von 1990, 2000, 2008 und 2016 werden für die LUC-Erkennungsanalyse verwendet, sowie das CA_Markov-Modell, um die zukünftigen LUC-Projektionen unter drei verschiedenen Szenarien vorherzusagen: Trendszenario, "Best-Case-Szenario", "Worst-Case-Szenario".

Die Vorhersagen für die Jahre 2026 und 2036 werden unter Berücksichtigung der physischen und sozioökonomischen Treiber der LUC-Dynamik im Einzugsgebiet berechnet.

Das Trendszenario behält die für die Jahre 2026 und 2036 prognostizierten Wahrscheinlichkeiten für Landnutzungsänderungen bei. Das Best-Case-Szenario befasst sich mit den Wahrscheinlichkeiten für Änderungen der LUC in Richtung eines ausgewogenen Szenarios, zwischen der Erhaltung natürlicher Ökosysteme und produktiven Aktivitäten innerhalb des Einzugsgebiets. Das "Worst-Case-Szenario" befasst sich mit den Wahrscheinlichkeiten einer Änderung der LUC in Richtung eines Szenarios, in dem Rohstoffaktivitäten vorherrschen und die Produktionsbereiche in der Wasserscheide zunehmen.

Die LUC-Erkennungsergebnisse zeigen eine Zunahme der landwirtschaftlichen Flächen und eine Abnahme der Waldbedeckung zwischen 1990 und 2016. Statistisch gesehen, verringerte sich die natürliche Waldbedeckung von 61,2% im Jahr 1990 auf 57,12% im Jahr 2016, während der Anteil der landwirtschaftlichen Flächen von 2,9% auf 7,23% zwischen die Jahren 1990 und 2016 zunahm. Die Ergebnisse der LUC- Projektion für die Jahre 2026 und

2036 in Bezug auf das Jahr 2016 deuten darauf hin, dass die landwirtschaftlichen Flächen im Jahr 2026 voraussichtlich um 9,3% und im Jahr 2036 um 19,2% im Trendszenario zunehmen werden. Für das “Best-Case-Szenario” wird eine Zunahme der landwirtschaftlichen Flächen um 1,1% bzw. 3% im Jahr 2026 bzw. 2036 prognostiziert. Die Ergebnisse des “Worst-Case-Szenarios” für die Jahre 2026 und 2036 prognostizieren eine Zunahme der landwirtschaftlichen Flächen um 26,1% bzw. 54,3%. Darüber hinaus wird für das Trendszenario im Vergleich zu 2016 ein Rückgang der natürlichen Waldbedeckung im Einzugsgebiet um 0,6% (2026) und um 1,5% (2036) prognostiziert. Für das “Best-Case-Szenario” wird prognostiziert, dass die Waldbedeckung um 0,2% (2026) und um 0,4% (2036) abnehmen wird. Das “Worst-Case-Szenario” prognostiziert für die Jahre 2026 und 2036 einen Rückgang der natürlichen Waldbedeckung um 2,6% bzw. 5,8% gegenüber 2016.

Die Ergebnisse der hydrologischen Modellierung zeigen, dass aufgrund der Auswirkungen von LUC der durchschnittliche tägliche Stromfluss für das Trendszenario im Vergleich zu 2016 um 1,04% (2026) und 1,45% (2036) anstieg. Für das “Best-Case-Szenario” verringerte sich der durchschnittliche tägliche Stromfluss in den Jahren 2026 und 2036 gegenüber 2016 um 4,91% (-24,8 m³/s) bzw. 6,10% (-30,8 m³/s). Für das Szenario “Worst-Case” wird in Bezug auf das Jahr 2016 ein Anstieg des durchschnittlichen täglichen Stromflusses um 2,08% (2026) und um 2,37% (2036) prognostiziert.

Die Ergebnisse zu den Auswirkungen von LUC auf den Stromfluss unter den verschiedenen vorgeschlagenen Szenarien zeigen, dass die Änderungen des Stromflusses kein Faktor sind, der die Wasserkrafterzeugung im Einzugsgebiet beeinflussen könnte. Die Ergebnisse zeigen jedoch, dass die Wasserhaushaltskomponenten durch die räumliche und zeitliche Verteilung von LUC im Untersuchungsgebiet beeinflusst werden, was für ein einzugsgebietsweites integriertes Wasserressourcenmanagement nützlich ist. Das Ausmaß dieser Effekte kann jedoch durch Unsicherheiten verdeckt werden, die sich aus den hydrologischen und LUC-Modellierungsprozessen ergeben. Daher sind weitere Studien zur Optimierung von Landnutzungsänderungen und Untersuchungen zur Bewertung von Niederschlag-Abfluss-Prozessen im Untersuchungsgebiet unerlässlich.

Nichtsdestotrotz sollten Nachhaltigkeitsaspekte, die mit dem Vorhandensein der Wasserkraftanlage im Untersuchungsgebiet verbunden sind, nicht vernachlässigt werden. Um eine nachhaltige Entwicklung im Einzugsgebiet gewährleisten zu können (die die langfristige Wasserkraftproduktion, die Erhaltung der Ökosysteme und das sozioökonomische Wohlergehen der Bevölkerung im Einzugsgebiet umfasst), müssen in weiteren Arbeiten innerhalb eines IWRM-Rahmens weitere Variablen und Prozesse analysiert werden, die in dieser Studie nicht behandelt wurden.

CHAPTER 1: Introduction

1.1- General overview

The Amazon River system and its basin of 6'100.000 km² is the largest freshwater system in the world, providing critical benefits to local populations, national societies, and humanity at large (Tundisi et al. 2014). It comprises the most complex and extensive network of river channels on Earth and an exceptional diversity of wetlands, in terms of biodiversity, and primary and secondary productivity (Latrubesse et al. 2017). The river basin discharges approximately 16 to 18 % of the planet's freshwater flow to the Atlantic (Latrubesse et al. 2021). Four of the world's ten largest rivers are in the Amazon basin (the Amazon, Negro, Madeira, and Japurá), and twenty of the 34 largest tropical rivers are Amazonian tributaries (Latrubesse et al. 2017).

The hydrological connectivity of Amazon freshwater ecosystems enables the provision of several services that are vital for local, regional, and global communities. Key ecosystem services include biodiversity maintenance, water quality, climate, flow regulation; nutrient and carbon cycling; and food and fiber production. The diversity of freshwater ecosystems found in the Basin sustains a wealth of life forms. Much of this diversity occurs throughout river networks, as ecological corridors with specific environmental conditions determine species occurrence and mediate movement through the landscape (Castello et al. 2013). As rainwaters drain through terrestrial ecosystems, riparian zones regulate water quality by filtering the organic and inorganic materials that they carry (Lees et al. 2016). Terrestrial inputs are transported downstream, deposited, and remobilized in river floodplains until they are discharged into the ocean (Latrubesse 2015; Latrubesse et al. 2017). During this transport, freshwater ecosystems regulate water flows, buffering flows during high discharge periods and maintaining them during low discharge periods. This regulation of flows promotes soil infiltration, recharges groundwater stores, and facilitates regular river navigation and hydropower generation (Castello et al. 2013; Winemiller et al. 2016).

The Amazon is also the largest and most complex river system that transfers sediments and solutes across continental distances, building and sustaining the largest continuous belt of floodplains on Earth and a mosaic of wetlands, spanning more than 1,000,000 km² (Latrubesse 2014; Latrubesse and Rancy 1998). The sediment regimes of Amazon tributaries differ according to the dominant geotectonic regions they drain. Andean or Andean-forest rivers are rich in suspended sediment loads and solutes (Finer and Jenkins 2012; Tundisi et al. 2014). Lowland rivers drain sedimentary rocks and carry abundant suspended sediment loads entirely within the tropical rainforest (Latrubesse 2015). The fluvial channels and floodplain morphologies, the amount and characteristics of the sediments transported by the rivers, the annual flood-pulse, and the action of morphodynamic erosional-depositional processes in space and time, provide disturbance regimes that result in high habitat diversity of the alluvial landscape, high biotic diversity, and high levels of endemism for both, aquatic and non-aquatic organisms (Latrubesse et al. 2021; Latrubesse et al. 2017).

Despite the relatively conserved state of Amazonian watersheds compared to US or European rivers, these ecosystems are facing fast transformations caused by agricultural expansion, urbanization, overharvesting of animal and plant species, and infrastructure development (Fearnside 2016, 2014, 2013). A population of approximately 20 million people lives there and most of Brazil's remaining hydroelectric potential is located in that region (Tundisi et al. 2014). As a region that hosts enormous cultural and biological diversity, the Amazon is also a relatively untapped source of energy for Latin American countries reliant on hydroelectric energy (Timpe

and Kaplan 2017; Premalatha et al. 2014). However, the demand for energy in Brazil and countries that share the Amazon Basin has posed strong pressures on the Natural Resources of this basin (Santos et al. 2020a; Stickler et al. 2013; Athayde et al. 2019).

Amazon's natural resources and ecosystems are becoming increasingly degraded due to human development activities, including the construction of dams, and mining (IPCC 2008; Castello et al. 2013; Arantes et al. 2019). Many of these activities were historically driven by domestic markets and national development interests, which prompted the construction of roads and conversion of native forests and savannas to croplands and rangelands (Fearnside 2016; Andrade and dos Santos 2015). Although these internal forces remain strong, the growing participation of Amazonian countries in export-oriented markets for agricultural and mineral products has made the region increasingly susceptible to international forces (Ansar et al. 2014; Almeida Prado et al. 2016). For example, multilateral development initiatives, including the Initiative for the Integration of the Regional Infrastructure of South America (IIRSA), and the South American Council on Infrastructure and Planning (COSIPLAN), have invested heavily in the construction of waterways, hydroelectric dams, and other infrastructure in the Amazon (Castello et al. 2013; Fearnside 2014, 2016).

The result has been large-scale disruptions to the hydrological connectivity of Amazon freshwater ecosystems via a variety of mechanisms; including (i) storage of water in hydroelectric reservoirs, (ii) changes in seasonal flood dynamics, (iii) reduced rainfall, water quality, and evapotranspiration at regional scales, and (iv) increases in the frequency and intensity of extreme weather events, such as droughts and floods (Fontaine et al. 2001; Finer and Jenkins 2012; Ferreira et al. 2013; Fearnside 2016; Latrubesse et al. 2021).

While the negative environmental impacts of dams are fairly well understood, the development of new hydropower to support growing global energy demand (Koch et al. 2011; Andrade and dos Santos 2015) is widely viewed as a sustainable source of electricity (Kahn, Freitas, and Miguel Petrere 2014). Construction of large and small hydroelectric dams on tributaries of the Amazon River has advanced over the past two decades as a result of long-term governmental plans geared towards increased energy security, economic growth, industrialization, and improved living standards (Athayde et al. 2019; Premalatha et al. 2014). The number of hydroelectric dams operating in the Amazon region has grown at an increasingly rapid rate in recent years (Lees et al. 2016; Andrade and dos Santos 2015; Ansar et al. 2014). Including small-scale projects, the number of dams planned for construction over the next 30 years for the whole Amazon Basin may reach 277 (Timpe and Kaplan 2017).

In Brazil alone, the 2017–2026 Decadal Energy Expansion Plan foresees the construction of six new mega hydroelectric power stations in Amazonian ecosystems by 2026 (Santos et al. 2020a). This proliferation of hydroelectric projects, together with the facilitation of the environmental licensing process required for the construction of dams in the Amazon Basin, suggests that the environmental impacts being generated by these schemes may be underestimated (Pelicice et al. 2017; Premalatha et al. 2014; Kahn, Freitas, and Miguel Petrere 2014). The fast pace of planned development, the spatial scale of impact, and the potential for loss of globally important ecosystem services make this impending hydrological transformation unprecedented (Timpe and Kaplan 2017; Almeida Prado et al. 2016).

As Athayde et al. (2019) argue, water is the defining physical characteristic of the Amazon basin. Water quantity and quality are integrators of the coupled natural and human processes that occur within the watershed (R. Brown

et al. 2014), and both are directly and indirectly affected by hydropower (Arantes et al. 2019). Dam construction, land-use change, climate change, and their interactions have all been shown to play major roles in altering the hydrology in the Amazon (Ferreira et al. 2013; Fearnside 2016; Pelicice et al. 2017), with effects across social and ecological systems (Marengo et al. 2018). For example, changes in the hydrology and connectivity alter patterns of floodplain forest inundation and productivity, interrupt fish migrations, reduce fisheries production, and modify catchment sediment transport and biogeochemistry across vast spatiotemporal scales (Abe et al. 2018; Alho, Reis, and Aquino 2015; Andrade and dos Santos 2015; Athayde et al. 2019; Castello et al. 2013; Latrubesse et al. 2017; Latrubesse et al. 2021; Timpe and Kaplan 2017).

Despite being considered a source of clean energy, hydroelectric power plants have negative impacts on the fundamental ecological processes that sustain the biological diversity of aquatic ecosystems (Athayde et al. 2019). One of the principal impacts caused by these hydroelectric projects is the modification of the hydrological cycle of the river (Timpe and Kaplan 2017). Dams may also reduce the availability of nutrients in the floodplain (Zahar, Ghorbel, and Albergel 2008), alter the physicochemical characteristics of the water, and modify the morphology of river channels (Lobato et al. 2015; Latrubesse et al. 2017). Large dams are predicted to have widespread impacts on watersheds, forests, people, economies, and climate, from local to global scales (Almeida Prado et al. 2016; Ansar et al. 2014). Small dams are also modifying the Amazon landscape at an increasing rate, supported by international and national policies and regulations that often include less strict environmental licensing processes (Athayde et al. 2019; Arantes et al. 2019).

Dams alter the natural flow regime by changing the magnitude, frequency, duration, timing, and rate of change of flow (Castello et al. 2013), as well as by modifying the transport of sediments, nutrients, and biota (Fearnside 1995, 2014, 2016). Just upstream of a dam, the creation of a reservoir shifts the environment from lotic to lentic, affecting water quality (Fearnside 2016), and potentially increasing atmospheric flux of greenhouse gases from decomposing organic matter (Fearnside and Pueyo 2012; Ferreira et al. 2013). Reservoirs generally reduce biodiversity (Ferreira et al. 2013; Fearnside 2016), and are specifically detrimental to migratory species, because the lentic environment of the reservoir can act as a “filter” for species reliant on free-flowing water (FAO 2018; R. Brown et al. 2014; Araújo and J. Wang 2015).

Dams, even those associated with “runoff- river” dams, trap sediments (Arantes et al. 2019), reducing storage capacity and potentially causing backwater effects (Buytaert et al. 2006; Fearnside 2014), as well as causing that floodplains receive less nutrient and organic matter deposition downstream (Fearnside 2016, 2014). In addition to reduced sediment transport, the most conspicuous downstream impact of dam construction and operation is a permanent alteration of the flow regime (Latrubesse et al. 2017; Latrubesse et al. 2021). Stunted flood pulses and increased base flows reduce floodplain habitat and encourage the encroachment of upland vegetation, resulting in the degradation of floodplain forests and loss of biodiversity (Latrubesse 2015; Liermann et al. 2012). Frequent flow reversals and changes in flood timing, driven by energy demand, can disorient fauna, which relies on predictable flood timing and duration for migration and spawning cues (Lobato et al. 2015; Araújo and J. Wang 2015). Changes in flow, particularly if coupled with decreased sediment load, can also erode river channels and shorelines, resulting in vegetation disturbance and habitat loss (Notter et al. 2007; Santos et al. 2020a; Arantes et al. 2019).

Another type of impact resulting from the construction of hydroelectric dams is the blocking of fish migration routes (Araújo and J. Wang 2015; Pelicice et al. 2017; R. Brown et al. 2014). Dams may create insurmountable barriers to the movement of these organisms along fluvial corridors, affecting their reproduction patterns, and changing their whole life cycle (Winemiller et al. 2016; Araújo and J. Wang 2015). The interruption of migration routes may also affect the composition, abundance, and functional attributes of the local fish assemblages (Palmeirim, Peres, and Rosas 2014; Santos et al. 2020a). This process is especially preoccupying in the Amazon Basin, where many commercially important fish species -such as the catfishes (*Brachyplatystoma* spp. And *Pseudoplatystoma* spp.)- undertake systematic long-distance migrations throughout their life cycle (Anderson et al. 2018; Castello et al. 2013).

In addition to their negative impacts on fish populations, hydroelectric dams also affect the human populations that depend on fishery resources (Alho, Reis, and Aquino 2015). Approximately, 40.3 million people worldwide depend on artisanal fisheries for their livelihood, and this activity provides high-quality food for many of the planet's most vulnerable populations. Thus, it combats poverty, hunger, malnutrition, and inequality (FAO 2018). In the Amazon region alone, fisheries generate input of US\$200 million per annum and support a workforce of 200 000 fishers (Tundisi et al. 2014). Besides the overall impact on the aquatic and terrestrial ecosystems, the construction of Amazonian reservoirs results in the emission of greenhouse gases (Tundisi et al. 2014; Fearnside 2016). However, according to Keenan (2015), gas emissions from Amazonian reservoirs are below the greenhouse gas emissions by thermoelectric plants. Nevertheless, dam emissions need to be included in all accounting based on the best available data and calculation methods (Premalatha et al. 2014).

Tropical dams emit more greenhouse gases than do dams in other zones (Fearnside 2016; Fearnside and Pueyo 2012). Amazonian dams are being promoted, in part, based on a supposed benefit in mitigating global warming, including the intention of capturing mitigation funds on a large scale under the Kyoto Protocol's Clean Development Mechanism (IPCC 2008). Unfortunately, these dams can be expected to have cumulative emissions that exceed those of fossil-fuel generation for periods that can extend for several decades, making them indefensible based on global warming mitigation (Ferreira et al. 2013; Fearnside and Pueyo 2012; Fearnside 2016).

Beyond the river, terrestrial ecosystem transformations associated with dams are poorly understood in the Amazon and worldwide (Nepstad *et al.* 2008). It is well-established that dams cause direct deforestation via reservoir impoundment (Latrubesse et al. 2021; Latrubesse et al. 2017; Latrubesse 2015). Dams, however, cause significant indirect forest loss and degradation through at least three pathways (Grill et al. 2015; Marengo and Espinoza 2016; Oliveira et al. 2013). First, a land-use change associated with dams causes deforestation and degradation of upland forests (Padilla, Cruz, and Valero 2015; Santos et al. 2020b). Second, dams alter river and floodplain hydrology, which changes the structure and function of riparian and flood-plain forests (Timpe and Kaplan 2017; Zahar, Ghorbel, and Albergel 2008). Third, dam-associated infrastructure produces additional direct and indirect deforestation (Winemiller et al. 2016; Liermann et al. 2012). Together, these dam-induced terrestrial ecosystem impacts have cascading effects on biodiversity and ecosystem services (Latrubesse et al. 2017; Fearnside and Pueyo 2012), with evidence of wide-ranging impacts on birds (Ansar et al. 2014; Alho, Reis, and Aquino 2015), mammals (Araújo and J. Wang 2015), insects (Arantes et al. 2019), and reptiles (Ferreira et al. 2013).

Despite a history of hydropower development in the Amazon since the 1970s, the cumulative, synergistic, and long-term effects of dams on rivers, forests, and social systems are still underestimated in planning, decision-

making, and management (Athayde et al. 2019; Lees et al. 2016). Gaps in understanding those effects are largely due to lack of rigorous and independent research, and articulation and integration of existing data and knowledge, as well as due to a fragmented approach to studies informing environmental and social impact assessments and mitigation (Lees et al. 2016; Timpe and Kaplan 2017).

Sustainability science focuses on generating, articulating, and applying knowledge to development problems, governance, and decision-making, from local to global scales (Castello et al. 2013). In cases where to meet the needs of present generations without compromising those of future ones, as sustainability is defined, decision-makers need to map out and consider the best existing science and knowledge through Integrated Water Resources Management – IWRM - processes. This entails including multiple perspectives (i.e. embracing pluralism), options and trade-offs in planning and decision-making, and requires greater integration of different types of information and knowledge held by diverse social groups, scientists, practitioners, and other relevant actors (Andrade and dos Santos 2015; Anderson et al. 2018; Athayde et al. 2019).

In Amazonian countries, insufficient assessment and monitoring of social-ecological transformations associated with hydropower are worsened by the limited and/or inadequate participation of social actors in the planning, construction, monitoring, mitigation, and operational stages of dam implementation (Athayde et al. 2019; Alho, Reis, and Aquino 2015). Inconsistencies within and across government institutions and policies and poor communication between stakeholders (academics, civil society, government, private companies, communities) have exacerbated social conflicts, increased judicialization processes, and resulted in poor performance of mitigation and monitoring programs (Almeida Prado et al. 2016; Anderson et al. 2018).

All the previously mentioned effects of social-ecological transformations triggered by dams, such as resource extraction and associated infrastructure development in the Amazon basin, will be magnified in the near future because of the planned construction of 151 new dams in the six major Andean tributaries of the Amazon (Anderson et al. 2018; Tundisi et al. 2014). Andean landscapes, including the tropical Andes of Ecuador, provide a good opportunity for hydropower generation (Buytaert et al. 2006; Tundisi et al. 2014). Because of this, hydropower has become the principal source of energy in most of the Andean countries (Bradley et al. 2006; Stickler et al. 2013; Finer and Jenkins 2012).

As one type of renewable energy resource, hydropower development brings in some benefits for the countries, such as reduces diesel importations (for thermoelectric production), and provides the flexibility of electricity production and supply. However, sustainability issues associated with hydropower developments should not be neglected. Considering the numerous impacts of hydropower in the Amazon, a reduction of their expansion should be accounted as an economic, social, and ecological investment for the future. Nevertheless, with strong political and economic pressure to harness Amazon's hydropower potential, this is unfeasible.

Therefore, to be able to ensure sustainability in these basins, governments should perform a strategic analysis in order to plan, construct and monitor hydropower facilities in the future. This strategic analysis should contemplate (i) An in-depth understanding of the location of future dams, taking into consideration specific ecosystems and their services, as well as an appropriate Integrated Water Resources Management (IWRM); (ii) An analysis of the rivers where construction should occur, using criteria of conservation and ecological services of the whole basin; (iii) Adaptation and adoption of new technologies that mitigate ecological impacts and avoid fragmentation

preserving connectivity and forest loss. The key is the scientific understanding of the relationship between ecosystem services and hydropower benefits, which is strategic in a long-term policy.

Due to the high potential of the Ecuadorian river flows (Finer and Jenkins 2012), in 2007 the Ecuadorian government started the construction of several hydropower facilities; among them, the Coca Codo Sinclair hydropower plant (CCS-HPP). At that time, the Ecuadorian government expected hydropower to be the main source of electrical power by 2016, covering at least 90% of the national electricity demand with the exploitation of 20% of the country's total potential. This was estimated based on hydraulic considerations but without taking into account environmental needs and socioeconomic processes (Nolivos et al. 2015).

In 2008, the National Secretary of Water (SENAGUA) was created to reorganize the former Water Resources National Council (CNRH) and carry out the water resources planning and management at a national level (SENPLADES 2014). However, the institutional efforts of this Secretary to manage and plan the Ecuadorian water resources have been focused on a classical engineering approach, based entirely on water balance estimation derived from historical records, and not considering the potential influence of changes in climate and land use (Nolivos et al. 2015). In this sense, no attention has been paid to land-use changes (LUC) and climate change impacts regarding water availability for sustainable hydropower generation in the Ecuadorian watersheds (Hasan and Wyseure 2018).

Although progress has been made in assessing the impacts of LUC and climate change on tropic watersheds' hydrology, only a few studies have attempted to assess the attribution of changes in the water balance components and hydropower potential to changes in the land use of the watersheds (Buytaert, Iniguez, and Bièvre 2007). LUC can modify the rainfall path to generate basin runoff by altering critical water balance components, such as streamflow, groundwater recharge, infiltration, interception, and evaporation (van Griensven et al. 2012). It is important to highlight that streamflow is the main variable that determines the sustainability of hydropower production in a hydro-electrical plant (Winchell et al. 2013).

Over the past decades, climate change and LUC have affected the streamflow magnitudes all over the catchments of the world (Čerkasova 2019; Hasan and Wyseure 2018; Hassaballah et al. 2017). Effective planning, management, and the regulation of water resources development are therefore required to avert conflicts between the competing water users (Mekonnen et al. 2018). Only the understanding of the hydrological processes and sources impacting water quantity, such as LUC and climate change, can achieve an effective water resources management process, as they are the key driving forces that can modify the watershed's hydrology and water availability (Mango et al. 2011; Ludwig, van Slobbe, and Cofino 2014; Leta et al. 2016; J. Refsgaard et al. 2005).

In addition, it is necessary to have a water resources management system-oriented process, in which the relationships between the different elements that are part of the watershed -socioeconomic, physical, political, environmental, etc.- are considered, and where the different stakeholders and their interests are integrated into the planning and decision-making processes (Pahl-Wostl 2007). In this way, an integrated process of water resources management (IWRM) can be achieved, which will lead to an increase in the socio-economic well-being of the inhabitants, without compromising the sustainability of the natural ecosystems in the basin (Pahl-Wostl 2007, 2002).

Within the Integrated Water Resources Management (IWRM) framework, streamflow is an important hydrological variable needed for water resource planning, management, and ecosystem conservation. To manage water resources effectively at a local level, decision-makers need to understand how human activities and climate change may impact local streamflow (Jakeman 2003). Therefore, a proper IWRM process in a catchment requires an in-depth understanding of the aggregated and disaggregated effects of LUC on streamflow, regarding hydropower production, as well as of water balance components (Worku, Khare, and Tripathi 2017).

Within this context, by 2015, the construction of the Coca Codo Sinclair hydropower plant (CCS-HPP) was completed and became operational. It is the biggest hydroelectric facility in Ecuador, and it is considered a national priority, as it generates 1500 megawatts per hour, which supplies 35% of the annual domestic demand (CONELEC 2009). The CCS-HPP is located at the outlet point of the upper Coca River basin (CRB), which starts at the eastern slopes of the Ecuadorian Andes, and ends at the upper Ecuadorian Amazon region. The upper Coca River basin drains up to the gauging point, where the CCS-HPP is located, approximately 3600 km², and the mean annual flow is 450 m³/s, of which 375 m³/s are needed for hydroelectric production (ENTRIX S.A. 2009).

Historically, the hydrological conditions of the CRB have been favorable for the availability of water, supplying the necessities of people and ecosystems, especially due to the high degree of conservation of natural vegetation cover that exists within the basin (SENPLADES 2014). In the same way, the almost complete absence of degraded and eroded soils, as well as the humid tropical climate present in the basin, have been key factors for this positive scenario (Buytaert et al. 2006). However, in recent decades, this scenario has been affected by LUC, such as the increase of extensive agricultural production activities as well as of pasture establishment for livestock, urbanization, and illegal logging (Sierra 2013).

In general terms, from the beginning of the CCS-HPP construction in 2008, different processes associated with socioeconomic factors – such as job opportunities and new economic activities – and political decisions have influenced the dynamics of the population (e.g. migration processes and population increments) and promoted LUC in the CRB (Sierra 2013; SENPLADES 2014). In the future, these changes in the land coverage could lead to urban and agricultural areas expansion and reduction of natural forest cover, increasing the pressure on the natural resources and the ecosystems of the basin (Zahar, Ghorbel, and Albergel 2008). At the same time, flood risk in the lower parts of the basin and increments in the soil erosion and sediment rates of the catchment could be increased, generating decreases in soil fertility/agricultural production due to soil losses (Nie et al. 2011) with potential consequences for food security of the basin's population (FAO 2018), and affecting the electricity production of the CCS-HPP. On the same note, as van Griensven et al. (2012) and Stonestrom, Scanlon, and L. Zhang (2009) mentioned, LUC can alter critical water balance components of a watershed; among them, the streamflow, which is essential for ecosystem conservation and water resources planning (UN Water 2007).

Recently, Duque and Vazquez (2015) assessed the effect of land-use changes on streamflow on a sub-basin located southeast of the CRB. Their results show significant LUC where agricultural land has increased from 30% of the catchment in 2002 to 40% in 2008. The study attributes these changes to the increase in population, which increased the demand for agricultural land. The study also shows that farmers in the area are commonly clearing natural forest areas to create croplands, which caused a decrease in forest land from 52% in 2002 to 43% in 2008. These LUC have contributed to the high rate of soil erosion and land degradation in the sub-basin (Duque and Vazquez 2015). Since the CRB is neighboring Duque and Vazquez's sub-basin, there can be expected some

similarities of catchment characteristics, though differences cannot be excluded. Therefore, an in-depth understanding of the LUC effects on streamflow and the other water balance components in the basin is key.

When analyzing different LUC, the relation between socioeconomic processes –such as construction, agriculture, deforestation, and mining- and the management of natural resources can be understood (Guan et al. 2011). Materialized socioeconomic processes can be quantified efficiently with Geographic Information Systems (GIS) and remote sensing techniques (J. Brown 2004). The use of modeling tools allows the analysis of the land-use changes, since they enable the formulation of future scenarios, the understanding of the key processes that explain the changes, and the description of these in quantitative terms (Nath et al. 2020; Mishra, Rai, and Mohan 2014). In this context, the Cellular Automata – Markov chain model (CA-Markov) is used in this study to analyze the CRB changes in land use and the formulation of future scenarios. Furthermore, the analysis of historical trends of rainfall and streamflow can help to reveal the effect of climate change or variability on water resources (Guo 2008). For this purpose, the Mann-Kendall and Pettitt tests are used in this study.

Hydrologic modeling allows understand the impact of the changes in land use on the water balance components of a basin, providing several factors that should be considered at the IWRM process; both, at the present and in the future. In this sense, many models have been developed to simulate the impacts of LUC on streamflow (T. Li et al. 2011; Tamm 2016). During recent decades, several distributed hydrological models have been developed to simulate hydrological processes in basins, such as the Soil and Water Assessment Tool (SWAT) (J. G. Arnold et al. 1998), the European Hydrological System (SHE) (Abbott et al. 1986), the Topography-based Hydrological Model (TOPMODEL) (Beven and Kirkby 1979), and others like HEC, VIC, IHDM, and WATFLOOD. These are capable of simulating temporal-spatial variations in hydrological process and assisting in understanding the mechanisms of influence behind land-use impacts (B. Lin et al. 2015), because they allow for an approximate characterization of the spatial variability of a basin by use of data and parameters in a point-grid network (Wang et al. 2012).

The models can be categorized as empirical black-box, conceptual, and physically-based distributed. Each one of these types has its advantages and limitations. Several situations in practice demand the use of simple tools, such as linear system models or black-box models. Nevertheless, these basic models usually fail to mimic the non-linear dynamics, which are essential in the rainfall-runoff transformation process (Hassaballah et al. 2017).

Among the models mentioned above, the SWAT model has excelled in demonstrating its ability in detecting the impacts of land use and climate change on hydrological components in different areas (Nie et al. 2011; Guo 2008; P. W. Gassman et al. 2010; P. W. Gassman et al. 2007). SWAT has been applied in the investigation of the influence on water resources by simulating annual water yield for different periods that differed in land use (Nie et al. 2011; B. Lin et al. 2015). In this study, the SWAT model is used to analyze the historical and potential future effects of LUC on the water balance components and hydropower generation in the CRB.

Because of the uncertainty associated with hydrologic modeling, uncertainty should be accounted for in model application and evaluation (K. Abbaspour 2012). The analysis and consideration of uncertainty are particularly important, because decisions regarding water resource policy, management, regulation, and program evaluation are increasingly based on hydrologic modeling (Abbas 2016; Walker et al. 2003). The current modeling philosophy requires that calibration, validation, sensitivity, and uncertainty analysis are routinely performed as part of

modeling work. There is an intimate relationship between calibration and uncertainty since uncertainty analysis is essential to evaluate the strength of a calibrated model (K. Abbaspour et al. 2015). Furthermore, any analysis with a calibrated model must include the uncertainty in the result by propagating the parameter uncertainties (Neitsch et al. 2011).

Some of the Amazonian countries – among them Ecuador- are implementing water resource management laws to protect the availability and quality of water. Although these laws vary across countries, they rely on the common principle that water is a finite resource that is vulnerable to human activities and should be managed at the watershed scale (Winemiller et al. 2016). Because these laws focus almost exclusively on water as a resource to satisfy human needs, they cannot ensure preservation of freshwater ecosystems. Furthermore, they are generally national in their jurisdiction, contradicting the very principle of watershed-scale management, and ignoring the international connectivity of Amazon freshwater ecosystems (Castello et al. 2013).

Even though the CRB has great importance for the Ecuadorian Government in terms of its hydroelectric potential, and is considered a priority for the country's economic development, there is no management plan with an integrated approach in the basin. In this sense, the hydropower generation in the future cannot be assured, as well as the increase of the socio-economic wellbeing of the inhabitants, without compromising the sustainability of the natural ecosystems in the basin. Likewise, there is no record of studies that analyze the potential effects on the water balance components and ecosystem health in the basin due to the presence of the CCS-HPP and its associated effects, such as changes in land use. At this point, it is important to highlight that understanding the impacts of LUC on the natural resources and the ecosystems of the basin, and incorporating this understanding into an IWRM process, is essential for the sustainable development of the CRB in the future.

An adequate IWRM process is composed of a political and a technical part, where plans, programs, and projects must be complemented and fed with the results from different scientific methods and tools (UN Water 2007). An IWRM process aims to ensure the management of water, land, and related resources of a basin; looking to maximize the economic and social welfare of its population without compromising the sustainability of the ecosystems (UN Water 2013).

In that sense, sustainability is a broad term that according to the UN WCED (1987) is defined as “the integration of environmental health, social equity, and economic vitality in order to create thriving, healthy, diverse and resilient communities for this generation and generations to come. The practice of sustainability recognizes how these issues are interconnected and require a systems approach and an acknowledgment of complexity”. The goal of sustainability is to, “create and maintain conditions, under which humans and nature can exist in productive harmony, that permit fulfilling the social, economic, and other requirements of present and future generations” (UN WCED 1987). This means that sustainable approaches need to consider the fundamental interplays between actions that affect the environment, society, and the economy; which comprise the three pillars of sustainability (Escrig-Olmedo et al. 2019).

In that regard, it is beyond the scope of this work to analyze the sustainability of the CRB; because of the unavailability of information -or the difficulty of accessing it- to support an analysis of this magnitude in the basin. Thus, this study only addresses certain criteria related to the environmental, social, and economic aspects of sustainability, which are; erosion and sediments, hydrology and water availability, population dynamics, and the

benefits for Ecuadorian economic development; focusing mainly on the analysis of the CCS's induced LUC and their impacts on the hydrological and erosive processes inside the basin. The specific variables to be analyzed will be streamflow -among other water balance components- and soil losses.

The results of this work will provide relevant technical information for a further IWRM process in the CRB. However, it is important to highlight that a future IWRM process in the CRB must address all the necessary environmental, social, and economic criteria to guarantee sustainable development in the basin; which comprises hydroelectric production, the health of the ecosystems, and the well-being of the population.

1.2.- Objectives

The main objective of this study is to analyze the effects of historical and future land-use changes on the hydrological components of the upper Coca River basin, towards a long-term hydropower production, ecosystem conservation, and the socio-economic well-being of the population; with the potential to help in answering questions of the decision-makers about the CCS's induced land-use change impacts on the watershed dynamics, facing an effective IWRM process in future.

In order to address the main objective, the following tasks were carried out, taking into account the different steps inside the IWRM process cycle (Chapter 1.5.1; Figure 1-7) and applying different methods for hydrological and socio-economical analysis.

- Historical socio-economic factors and processes analysis of the study area (Chapter 1.4), and future socio-economic scenarios formulation (Chapter 2.3.5). These tasks are directly linked to the process of *Analyzing Gaps* (Step 3) in the IWRM process cycle.
- Historical land-use changes analysis in the watershed (Chapter 2.3.1), which is also related to Step 3, and, at the same time, is linked to the *Prepare a Strategy and Action Plan* process (Step 4) in the IWRM process cycle. To accomplish this task, the Geographic Information System (GIS) ArcGIS – ArcMap software is used.
- Also linked to Step 3 and Step 4 of the IWRM process cycle, the precipitation and streamflow historical time-series trend analysis, and medium-long term precipitation scenario formulation are executed using the Mann-Kendall and Pettitt tests (Chapter 2.4.1).
- Medium-Long term future land-use changes scenarios formulation (Chapter 2.3.4). This task is related to the *Implement Frameworks* (Step 6) and *Monitor and Evaluate Progress* (Step 7) and, at the same time, is linked to Step 3 and Step 4 of the IWRM process cycle. This activity is executed using the Cellular Automata – Markov chain model (CA-Markov), which is part of the TerrSet GIS software.
- In the same way, the analysis of the effects of the formulated land-use change scenarios on the streamflow for hydropower production in the Coca Codo Sinclair Hydropower plant (Chapter 3.2.2) is directly linked to Steps 3, 4, 6, and 7 of the IWRM process cycle. To complete this task, the physically-based/spatially distributed SWAT model (Soil and Water Assessment Tool) is used.
- Uncertainty assessment of the hydrological and land-use change modeling processes (Chapters 2.4.4 and 2.3.6), which is also related to Steps 3, 4, 6, and 7 of the IWRM process cycle. The Sequential Uncertainty Fitting Method version 2 (SUFI-2) algorithm and the Kappa variation/statistic index are used to assess

the uncertainties in parameters of the hydrological modeling process and the land-use change modeling evaluation, respectively.

- The Effects analysis of the formulated land-use change scenarios on the hydrological components of the upper Coca River basin, within the IWRM framework (Chapter 3.2.3), is directly linked to Steps 3, 4, 6, and 7 of the IWRM process cycle as well. For this task, the SWAT model is used.
- Formulation of recommendations regarding future scenarios and LU decisions that could lead to an effective IWRM process and sustainable hydropower production in the upper Coca River basin (Chapter 4). This activity is related to Steps 6 and 7 of the IWRM process cycle.

1.3.- Thesis outline

This dissertation is structured into four chapters. Figure 1-1 shows relevant chapters associated with the main objective and the carried out tasks of this work.

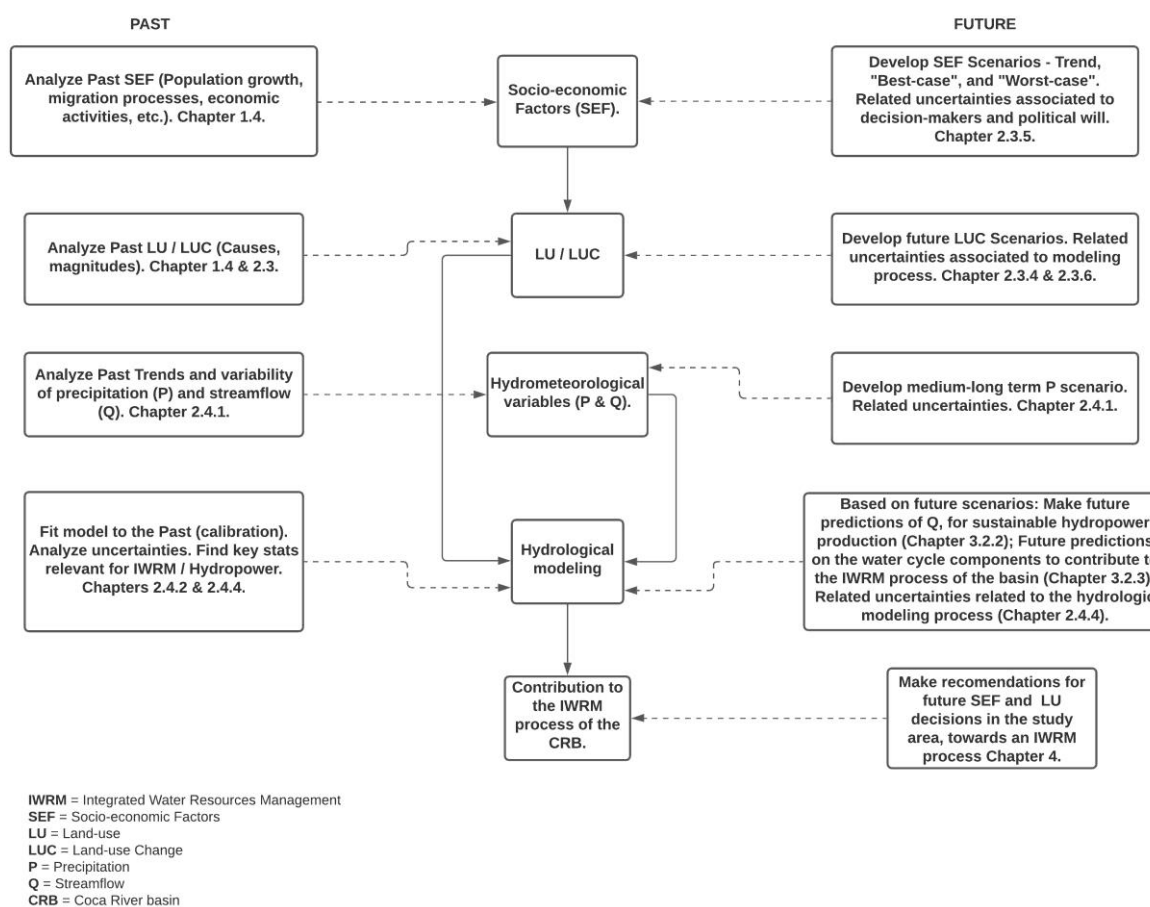
In Chapter 1, the reader has been introduced to the research topic by clarifying the study's objectives. After the general situation, this chapter describes the main characteristics of the study area, such as the environmental components and historical socio-economic factors/processes. Furthermore, a general introduction to the Integrated Water Resources Management (IWRM) takes place in the chapter, explaining why IWRM is a suitable framework for this work, and giving an outline of the study along the IWRM process, including the tools and methods that are used in each step.

Chapter 2 focuses on the data and methods used in this study. First, the available data for this study is provided, such as time series and Land-use maps. Then, an approach for the uncertainties inside the IWRM process is developed, where the different sources and methods that consider uncertainties inside the IWRM process are presented. Next, a description of the methods used to analyze socio-economic factors and create scenarios takes place. Here, the land-use change modeling tools, the modeling process, and the evaluation procedure executed in this study are explained. Then, the methods for analyzing and modeling hydrological processes and creating scenarios are shown. In this context, the rainfall and streamflow time series trend analysis method and the SWAT model for hydrological analysis are explained. Furthermore, this chapter presents the study area model calibration, validation, sensitivity, and uncertainty analysis procedures.

Chapter 3 presents and discusses results from the LUC modeling, the rainfall and streamflow time series trend analysis, and the results of the model calibration, validation, sensitivity, and uncertainty analysis procedures of the hydrologic model of the study area. In the same section, the hydrological modeling results and analysis of the different LUC scenarios are shown.

In Chapter 4, the summarized results, conclusions, recommendations, and suggestions for further work are presented.

Figure 1-1: Relevant chapters of the thesis structure.

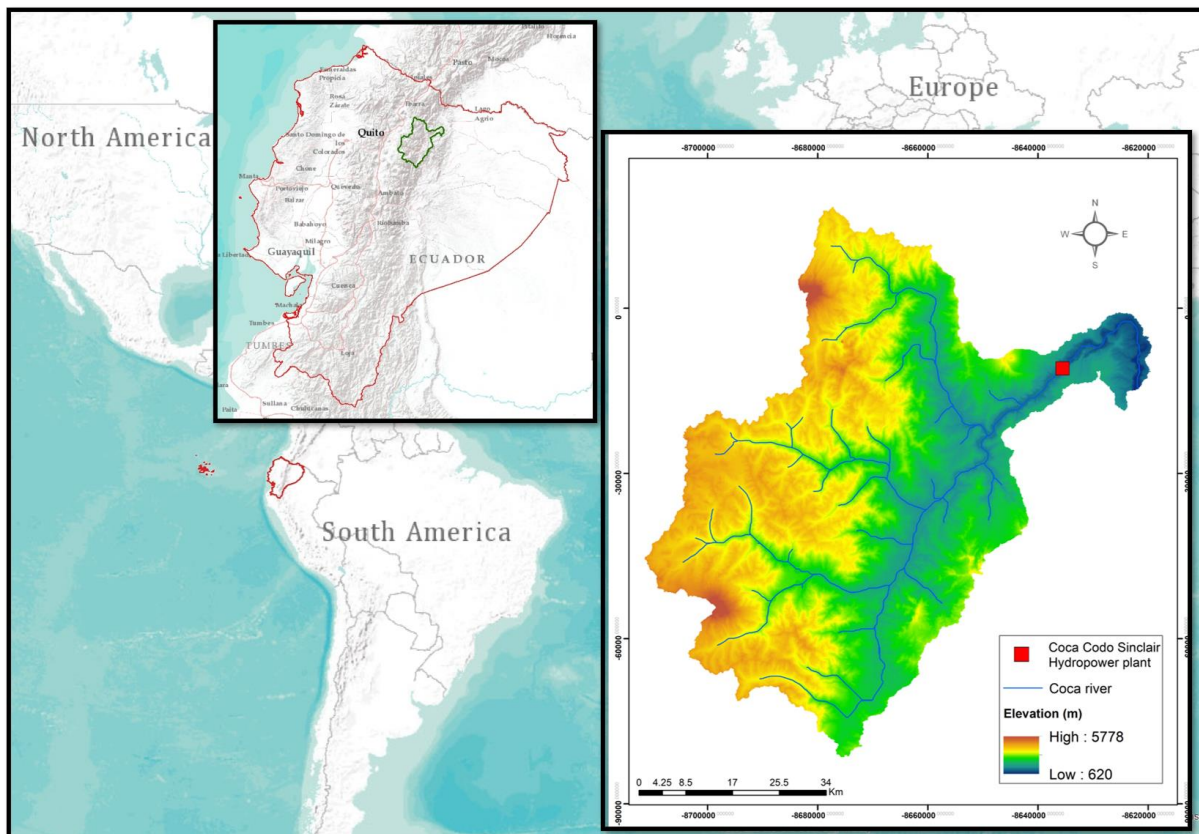


1.4.- Study area

The study area (Figure 1-2) spans the Coca River upper basin. It is located in the Ecuadorian Amazon region, which is part of the Amazon River watershed. The watershed area is 4081 Km², and the drainage area of the basin is approximately 3600 km² (Within 805450.905E - 9954916.565N and 877430.899E - 9984488.481N) up to the outlet point of the catchment (gauging station), where the hydroelectric project Coca Codo Sinclair is located. At this place (basin outlet) the average annual flow is 450 m³/s, of which 375 m³/s are needed for hydropower generation at the plant (ENTRIX S.A. 2009). The average range of precipitation in the basin goes from 3500 to 6000 mm/year, the mean annual temperature (over space) is 19°C, the mean evaporation is 1200 mm/year, and the average annual relative humidity value in the catchment is 90% (ENTRIX S.A. 2009).

The study area starts at 5759 m.a.s.l. at the Antisana volcano, which is the highest point of the catchment, and ends at the outlet of the watershed, at the Coca Codo Sinclair Hydro Power Plant (CCS-HPP) with 640 m.a.s.l., which is the lowest point of the study area. As we can see, the altitudinal difference between the beginning and the end of the watershed is very steep, because in less than 100 kilometers we have an altitudinal difference of 5120 meters approx., starting on the eastern slope of the Ecuadorian Andes and ending at the upper Ecuadorian Amazon region.

Figure 1-2: Study Area – Upper Coca River basin.



Data source: ESRI 2020; Militar Geographic Institute of Ecuador (IGM) 2017.

Due to this extreme altitude difference, we find different ecosystems (Figure 1-4) as we descend into the valley, starting with the volcanos, where there is no vegetation because of the relatively new soils formed from volcanic lava, also know as Barren volcanic soils (Figure 1-3 and 1-4). In these areas, the presence of ice and snow is reduced and is confined to the volcanic structures, such as the Antisana, Cayambe, and Reventador volcanoes in the catchment.

A few meters below the Barren areas, we find the Andean Páramo/Andean Moorland (Figures 1-3 and 1-4), where the average altitude in the study area is 3770 m.a.s.l. It is an ecosystem characterized by its dense and predominant herbaceous plant cover, high humidity, steep slopes (greater than 50% in 40% of the ecosystem area), and deep soils with high organic matter content, water retention capacity, infiltration rates, and porosity (Chuncho 2019; Buytaert et al. 2006).

After the Páramo areas, we find the Natural Forest cover (Figures 1-3 and 1-4) of the study area, which is the dominant ecosystem in the catchment, with 57% of the total area of the basin (Figure 1-5). This ecosystem is characterized by steep slopes and shallow soils.

Figure 1-3: Study Area main ecosystems.



Barren Soils and Volcano



Andean Páramo



Forest Cover of the Study area (Basin Outlet)

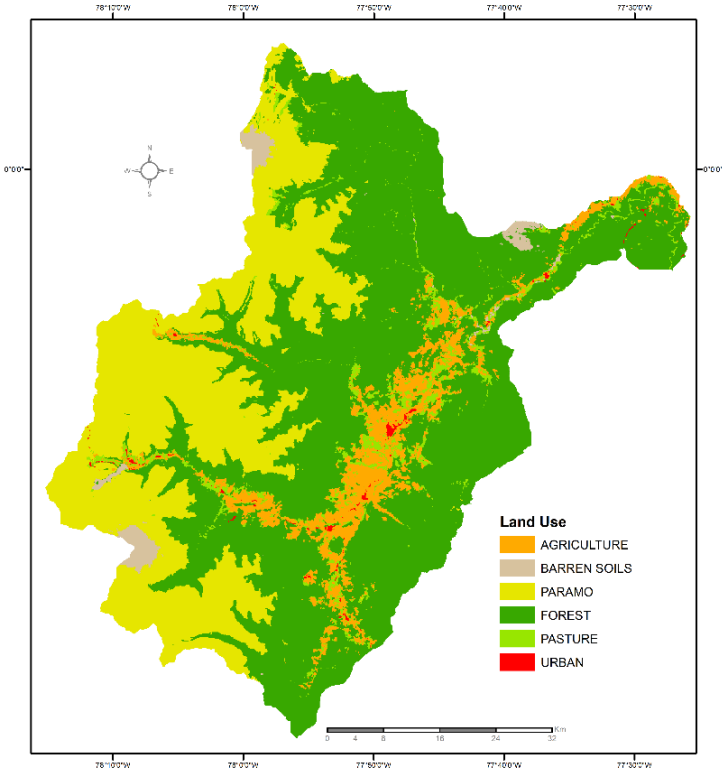
The high organic matter content in the soil makes them have high water storage and infiltration capacities. The high level of cloudiness throughout the year and the constant rainfall causes that the soils remain saturated almost

all year round. The predominant vegetation in these forests is very dense and captures most of the precipitation in its canopy. Therefore, the evaporation rate is 1200 mm/year on average (Chuncho 2019; ENTRIX S.A. 2009).

By the year 2016, the land-use cover (LU) of the study area was represented as follows. Agricultural areas represented 7% of the total of the catchment, Forest areas 57%, Pasture areas 3.5%, Andean Páramo (Moorland) represented 30%, Barren soils (volcanic landscapes) 1.5 %, and Urban areas represented 0.28% of the total of the catchment (Figure 1-5).

However, over the last decades, different socio-economical factors, such as population growth, migration, and economic activities, have been triggering Land-use change (LUC) processes in the study area. Figure 1-5 shows how land-use covers changed in area and proportion over time. Between 1990 and 2000, migration processes occurred because of the need to search for jobs outside the study area, due to low incomes coming from agricultural practices. This led to a situation where only a few members of the family stayed in charge of the lands, however, this is not reflected in the Ecuadorian Population and Housing National Census (1990, 2001, or 2010). At that time, the land redistribution policies of the Ecuadorian Amazon region required that, in order to legalize the land ownership, the farmer had to prove the capability of production of their land. In that sense, families started to deforest areas inside their properties adopting agricultural practices that do not require a large number of people to maintain and produce, such as livestock and short-cycle crops.

Figure 1-4: Land-use cover map of 2016.



Data Source: Ecuadorian Ministry of the Environment (MAE)

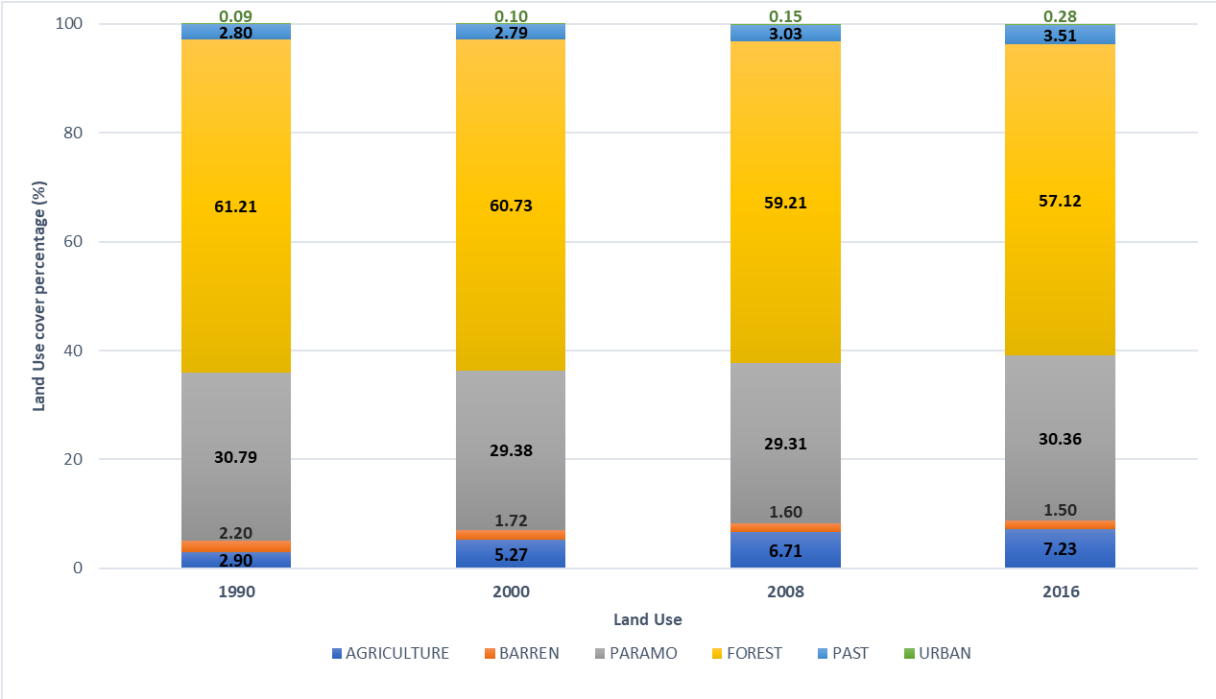
From 2000 to 2010, there was a gradual increase in income derived from agricultural activities in the basin, due to large industries buying and exporting milk, meat, and agricultural products directly from farmers (Sierra 2013). Additionally, the Central Government initiated payment programs for environmental services that allowed

maintaining the natural forest cover and promoted the reforestation and regeneration of the areas that were deforested before (Sierra 2013).

In 2008, the construction of the Coca Codo Sinclair Hydropower Plant (CCS-HPP) started and with that, migration processes to the catchment were initiated. Services and commerce activities increased. Furthermore, people from the catchment and other cities came to work at the construction site. With the CCS-HPP construction, there were approximately 3000 new workers at the catchment. The Central Government assumed that 20% of those workers would stay in the area with their families, which implies that the population in the catchment would increase significantly after the HPP construction, and, with that, the necessity of more urban settlements, agricultural areas to produce, and more pressure on the natural resources in the study area (SENPLADES 2014).

As Figure 1-6 shows, according to the Ecuadorian Population Census of 2010, there were 23553 inhabitants inside the catchment by the year 2010, with an economically active population of 10071. The government projections expect that by the year 2020, the population will reach 27000 inhabitants approximately inside the catchment (Figure 1-6 A). The main economic activities inside the catchment are agriculture and livestock, commerce, industries, the public sector (Government entities, police, and army), and a proportion of the population are related to mining, construction, transport, hotels, restaurants, tourism, and teaching, which are listed as “Others” in Figure 1-6 B. Over the years (1990, 2001, and 2010), Agriculture and livestock, and “Others” were the activities with the most people engaged in the catchment; followed by the number of people working in the public sector.

Figure 1-5: Land-use cover changes (%) in the catchment between 1990 and 2016.

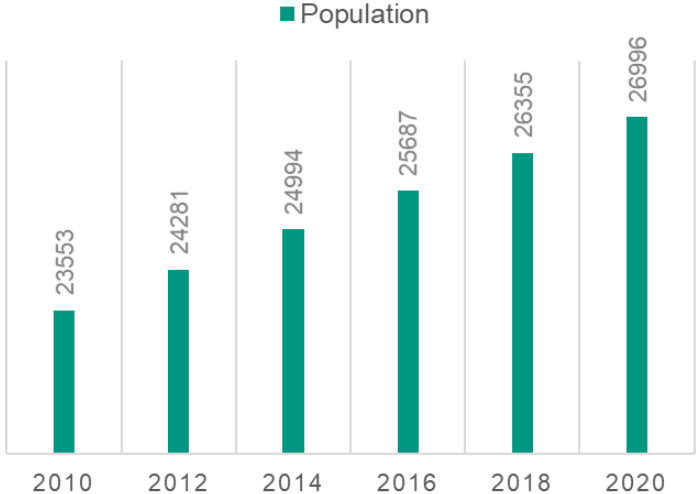


Data source: Ecuadorian Ministry of the Environment (MAE)

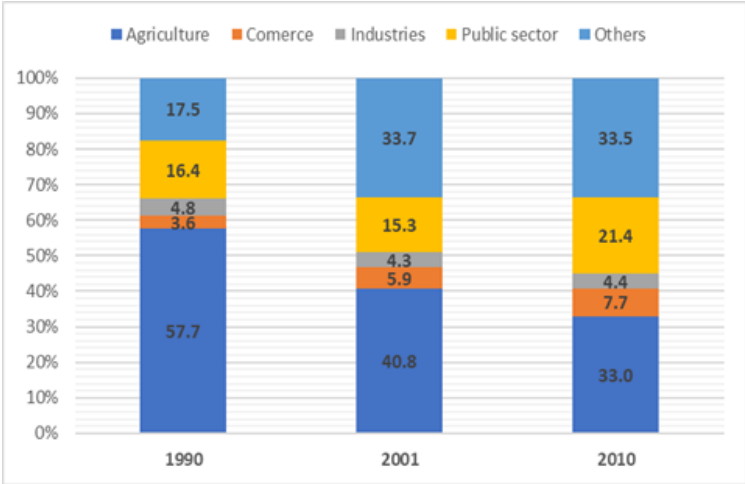
The percentage of the population involved in Agricultural activities decreased from 57.7% in 1990 to 33% in 2010. Additionally, the number of people involved in activities related to the Public sector and “Others” increased between 1990 and 2010. Furthermore, people engaged in the public sector, as well as in the category marked as “Others”, increased from 1990 to 2010, going from 16.4% to 21.4% and from 17.5% to 33.5%, respectively. As

mentioned before, this phenomenon occurred because the low income derived from agricultural activities made people look for alternative sources of income within the construction of the HPP, as well as other associated activities inside the study area (Sierra. R, 2013).

Figure 1-6: Total population and proportion (%) in economic activities in the study area.



1-6 A



1-6 B

Data Source: Population and Housing National Census – Ecuador, 1990 -2010.

In general terms, it can be observed that in the Coca River basin, over the years, different processes associated with socioeconomic factors and political decisions have influenced the socio-economic dynamics of the population and promoted land-use change processes in the basin. Socio-economic dynamics have evolved according to land tenure and legalization policies, income from agricultural activities, population growth, and migratory phenomena related to new job opportunities within the basin since the construction of the hydropower plant.

Therefore, over the years, agricultural activities ceased to be the main source of employment in the study area, and activities related to commerce, construction, public sector, industry, among others, began to have greater participation in terms of the number of inhabitants involved into these activities. This can be related to the incomes received from these new economic activities and the central government's natural resources conservation policies and programs within the basin.

Thus, it can be said that the trend scenario within the basin in the short and medium-term leads to economic activities diversification, human settlements consolidation, and conservation of natural resources to ensure hydropower generation.

1.5.- Integrated Water Resources Management – IWRM

Challenges faced by more and more countries in their struggle for economic and social development are increasingly related to water. Water shortages, quality deterioration, and flood impacts are among the problems which require greater attention and action. Integrated Water Resources Management (IWRM) is a process that can assist countries in their endeavor to deal with water issues cost-effectively and sustainably (UN Water 2007).

The four Dublin principles, that aim for the improvement of water resources management, are the principles on which the IWRM is based. Those principles are; A) Freshwater is a finite and vulnerable resource, essential to sustain life, development, and the environment. B) Water development and management should be based on a participatory approach, involving users, planners, and policymakers at all levels. C) Women play a central part in the provision, management, and safeguarding of water. D) Water has an economic value in all its competing uses and should be recognized as an economic good (Brouwer 2005).

The IWRM is considered state of the art in water resources management, and its definition goes as follows: “IWRM is a process that promotes the coordinated development and management of water, land, and related resources, to maximize the resultant economic and social welfare equitably without compromising the sustainability of vital ecosystems” (UN Water 2007).

Many of the world’s socio-economic systems are becoming linked at an unprecedented rate. As Easterling. D (2000) described, the impacts of extreme climates in flood and drought conditions are increasingly witnessed. Therefore, water managers need to manage an increasingly scarce resource that varies in space and time. According to (Pahl-Wostl 2007), IWRM processes will need to be responsive to change and be capable of adapting to new economic, social, and environmental conditions as well as to changing human values. An IWRM system-oriented approach addresses the need to consider connections between elements (upstream-downstream, water quality, and quantity and aquatic ecology, governance and technical management, etc.) and the inclusion of stakeholder interests in planning and decision making (Pahl-Wostl 2007, 2002).

In recent years, awareness is being developed: natural systems cannot be studied in isolation and human activities influence natural systems at all scales (van der Keur et al. 2008). Due to that, the large uncertainties usually connected to water management (physical settings, climate, socio-economics, and political environment) make it difficult to develop a consistent water management strategy.

Integrated Water Resources Management requires making a large number of decisions based on the available information. Most of the time, this information is deficient, incomplete, and characterized by uncertainties of different kinds due to the social, economic, environmental, political, and technical factors involved in the process (J. Refsgaard et al. 2005). That is why knowledge about the different types of uncertainties is a key factor inside the IWRM process to avoid taking wrong decisions. Water problems are understood as knowledge challenges, and the aim is to reduce uncertainties by the integration of scientific and stakeholder knowledge (Ludwig, van Slobbe, and Cofino 2014).

The watershed can be defined as the basic planning and management unit (Jønch-Clausen 2004); water follows its own boundaries (the river or lake basin, or the groundwater aquifer), and analyses and discussions of water allocation between users and ecosystem make sense only when is addressed at the watershed or basin level. Hence, a lot of the “integration” in IWRM takes place at the basin scale, whether at the local catchment or aquifer, or the multi-state or multi-country river basin. Many countries have realized this and organized their water management at the basin level years ago (the Spanish river basin management structure recently celebrated its 75th anniversary; the first Mekong River Basin structures were established in the 1950s). Several countries are now setting up various river and lake basin management structures. With the EU Water Framework Directive in Europe, basin-level management has become law for an entire region (UN Water 2007; Jønch-Clausen 2004).

In Ecuador, water resources management has been carried out at the watershed level since 2008 with the creation of the National Water Secretariat (SENAGUA) (SENPLADES 2014). However, the lack of coordination between the government and watershed stakeholders in terms of natural resources management, the lack of scientific information related to natural resources and the effects of changes in land use and climate variability on them, and the uncertainties derived from the different political and socio-economic processes (such as population growth, economic development, and lifestyle changes), increase the pressure on natural resources and accelerate watershed degradation processes.

The upper Coca River basin is one of the most important watersheds for Ecuador's economic development due to the presence of the Coca Codo Sinclair hydroelectric project and its great potential for hydropower generation (SENPLADES 2014; ENTRIX S.A. 2009). In recent decades, different socioeconomic factors and political decisions within the basin have generated land-use change processes (Sierra 2013), thus increasing pressure on natural resources, which in the medium term could lead to their accelerated degradation, endangering the sustainability of hydropower generation and the economic development of the watershed and Ecuador.

It is, therefore, necessary to have a natural resources management system-oriented, in which the relationships between the different elements that are part of the watershed (socioeconomic, physical, political, technical, etc.) are considered, and where the different stakeholders and their interests are integrated into the planning and decision-making processes (Pahl-Wostl 2007). In this way, an integrated and coordinated process of natural resource management will be achieved, which will lead to an increase in the socio-economic wellbeing of the inhabitants, without compromising the sustainability of the natural ecosystems in the basin.

An adequate IWRM process within the upper Coca River basin, complemented and fed with the results from the different scientific tools and methods used in this study, could guarantee the future sustainability of hydropower production and natural resources of the watershed, and the increase of the socio-economic wellbeing of its population. Therefore, the IWRM framework is not only appropriate for this study but can also be replicated (with its limitations) in other economic development strategic watersheds of Ecuador.

1.5.1.- IWRM Process

As Jønch-Clausen (2004) says, the IWRM process is a sequence of stages making up the IWRM cycle (Figure 1-7) and is essentially a process of moving towards an enabling environment of appropriate policies, strategies, and legislation for sustainable water resources development and environment, i.e. creating an institutional framework through which policies, strategies, and legislation can be implemented.

The cyclic IWRM process starts with the planning process and continues into the implementation of the framework and action plans and monitoring of progress (Figure 1-7). Active stakeholder involvement is the key to providing feedback at any stage in the IWRM cycle and may result in adjustments and parts of the cycle to be repeated. Moreover, there is a need to take uncertainty into account as argued before.

Figure 1-7: The seven different steps with their main processes in the IWRM cycle.



Modified from Jønch-Clausen 2004.

The main objective of this study and the different carried out activities to achieve it are directly related to steps 3, 4, 6, and 7 of the IWRM process cycle. Therefore, the historical socio-economic factors/processes analysis of the study area and future socio-economic scenarios formulation are directly linked to the Gap Analysis (Step 3) process. The historical land-use changes analysis in the watershed, the precipitation and streamflow historical time-series trend analysis, and the medium-long term precipitation scenario formulation are linked to the Gap Analysis (Step 3) and the Strategy and Action Plan Preparation (Step 4) processes.

The Medium-Long term future land-use changes scenarios formulation, the analysis of the effects of the formulated land-use change scenarios on the streamflow for hydropower production, the uncertainty assessment of the hydrological and land-use change modeling processes, and the analysis of the effects of the formulated land-use change scenarios on the hydrological components of the upper Coca River basin, are directly linked to step 3 and step 4, but also provide information relative to the Implementation of the IWRM framework and action plan (Step 6) process, and the Progress monitoring and evaluation (Step 7) process of the IWRM cycle. Likewise, the given recommendations that could lead to an effective IWRM process and sustainable hydropower production in the upper Coca River basin in the future are linked directly to steps 6 and 7 of the IWRM process cycle.

During the execution of the different activities mentioned above, statistical methods and spatial analysis tools (such as geographic information systems, land-use change models, and hydrological models) will be used to obtain information that allows us to fill and identify the information gaps required to carry out diagnoses and projections, which will help to prioritize programs and recommend actions with acceptable uncertainties inside the water

resources management action plans of the study area. For a more detailed description of these methods and tools, see Chapters 2.3 and 2.4.

A brief description of the IWRM process cycle components based on Jønch-Clausen (2004) can be found below.

1. *Establish Status and Overall Goals.* The starting point of the IWRM process is the burning and urgent water resources issue seen in the national context. Chart the progress towards a management framework within which issues can be addressed and agreed upon and overall goals are achieved. Do international agreements with the neighbors present potentials/constraints? Pragmatism is key.
2. *Build Commitment to Reform Process.* The political will is a prerequisite and building or consolidating a multi-stakeholder dialogue comes high on the list of priority actions. The dialogue needs to be based on knowledge about the subject matter and awareness-raising is one of the tools to establish this knowledge and the participation of the broader population.
3. *Analyze Gaps.* Given the present policy and legislation, the institutional situation, the capabilities and the overall goals, gaps in the IWRM framework can be analyzed in the light of the management functions required by the urgent issues.
4. *Prepare a Strategy and Action Plan.* The strategy and action plan will map the road towards completion of the framework for water resources management and development and related infrastructural measures. A portfolio of actions will be among the outputs, which will be set in the perspective of other national and international planning processes.
5. *Build Commitment to Actions.* Adoption of the action plan at the highest political levels is key to any progress and full stakeholder acceptance is essential for implementation. Committing finance is another prerequisite for taking planned actions to implementation on the ground.
6. *Implement Frameworks.* Taking plans into reality poses huge challenges. The enabling environment, the institutional roles, and the management instruments have to be implemented. Changes have to be made in present structures and building of capacity and capability also taking into account infrastructure development need to take place.
7. *Monitor and Evaluate Progress.* Progress monitoring and evaluation of the process inputs and outcomes serve to adjust the course of action and motivate those driving the processes. Choosing proper descriptive indicators is essential to the value of the monitoring.

CHAPTER 2. Data and Methods

2.1.- Available data

The methodology that we will use in this research is based on a historical analysis of the basin in terms of Land-use (LU) and Land-use Changes (LUC), as well as an analysis of the effects on water resources observed over time. It combines computer science, Geographical Information Systems (GIS), and hydrological and LU/LUC modeling tools to analyze the hydrological behavior of the study area in the past, present and future.

To analyze the hydrological behavior of the study area, the ArcView GIS 10.4 interface for SWAT2012 (Winchell et al. 2013) was used to configure and parameterize the SWAT model (See Chapter 2.4.2). Table 2-1 shows the description and sources of the input data used to analyze the hydrological behavior of the catchment. The model inputs included a 30 x 30 meters spatial resolution digital elevation model (DEM) of the watershed (Figure 2-1 A), Soil data and soil map (Figure 2-1 B), Land-use data, and Land-use maps of four different years (1990, 2000, 2008, and 2016) (Figure 2-2), daily time series of precipitation and minimum-maximum temperature from 1980 to 2016 (Figure 2-4), and monthly discharge time series (Figure 2-5) from 1980 to 2016.

Table 2-1: Input data for hydrological and land-use analysis.

Data Type	Description	Source	LUC Input
Topography	30 x 30m spatial resolution, digital elevation model (DEM). (Fig. 2-1 A)	Ecuadorian Geographic Military Institute (IGM).	Slope map (degree) Elevation map (meter)
Soil	Soil map Scale 1:250.000	Ecuadorian Agriculture and Livestock Ministry (MAGAP-PRONAREG)	
Land-use	A) LU maps Scale 1:250.000. Years: 1990, 2000, 2008, and 2016. (Fig. 2-2). B) Crop parameters and vegetation information of the watershed.	Ecuadorian Ministry of the Environment (MAE) and the Ecuadorian Space Institute (IEE).	LU maps (1990, 2000, 2008, 2016). Proximity to forest (m) Proximity to agricultural lands (m) Proximity to urban areas (m) Proximity to pasture (m)
Meteorological	Daily precipitation (1980 – 2016) of four stations. (Fig. 2-4)	National Institute of Meteorology and Hydrology of Ecuador (INAMHI) and the National Water Secretariat of Ecuador (SENAGUA).	Rainfall (mm)
Hydrological	Monthly discharge (1980 – 2016).	National Water Secretariat of Ecuador (SENAGUA) and the Ecuadorian Ministry of the Environment (MAE)	
Population	Population and housing year 2010.	INEC 2010.	Population density (Sq Km)
Road network	Road maps Scale 1:50000	National Information System (SNI) Ecuador	Proximity to roads (m) map
River network	River network map Scale 1:50000	SNI Ecuador	Proximity to river (m)

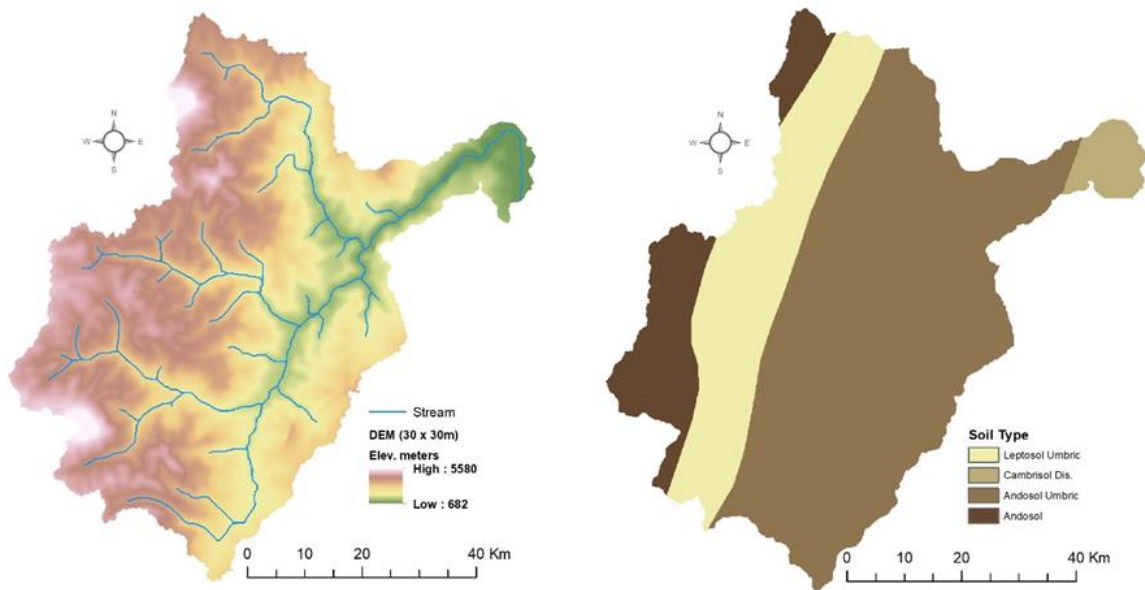
2.1.1.- Digital Elevation Model (DEM)

To describe the topography, a digital elevation model (DEM) of the watershed (Figure 2-1 A) with a spatial resolution of 30 x 30 meters was obtained from the Ecuadorian Geographic Military Institute (IGM). To acquire pertinent information about stream network and length, drainage pattern of the watershed, channel width within the watershed, slope, and reach length, DEM was employed.

2.1.2.- Soil map and soil data

The soil map (1:250.000) of the study area (Figure 2-1 B) and the physical properties of the four identified soil classes (Leptosol, Cambisol, Andosol, and Andosol umbric), such as available water content, soil texture, soil bulk density, hydraulic conductivity, and organic matter, were acquired from the Ecuadorian Agriculture and Livestock Ministry (MAGAP-PRONAREG).

Figure 2–1: Digital Elevation Model (DEM) (A) and Soil map of the Study Area (B).



Date Source: Ecuadorian Geographic Military Institute (IGM) / Ecuadorian Agriculture and Livestock Ministry

2.1.3.- Land-Use data

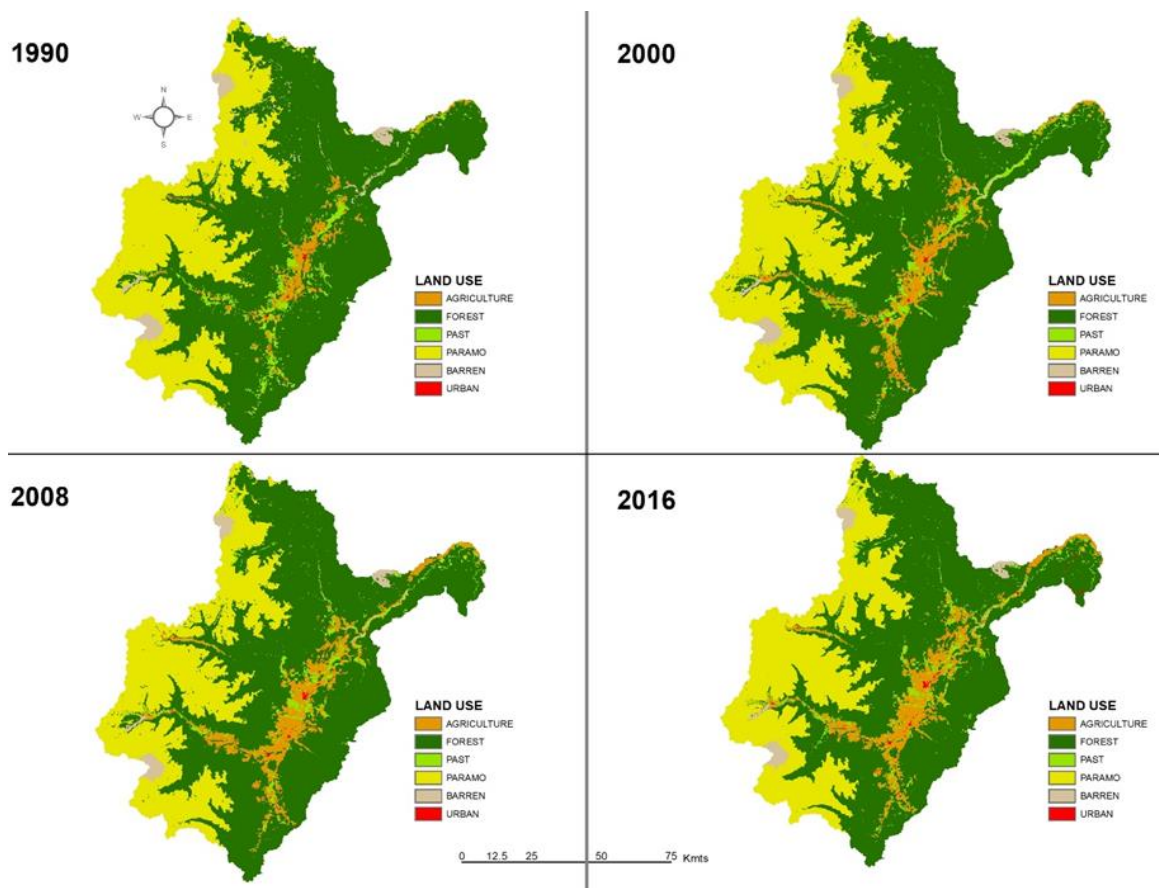
The land-use maps (1:250.000) for the years 1990, 2000, 2008, and 2016 (Figure 2-2) were obtained from the Ecuadorian Ministry of the Environment (MAE) and the Ecuadorian Space Institute (IEE).

The SWAT model (See Chapter 2.4.2) has limitations in simulating the seasonal growth cycles for trees and perennial vegetation in the tropics, where rainfall rather than temperature is the dominant plant growth controlling factor (van Griensven et al. 2012; Alemayehu et al. 2017). Arnold et al. (J. Arnold et al. 2012) underscored the need for a realistic representation of the local and regional plant growth processes to reliably simulate the water balance, erosion, and nutrient yields using SWAT. With that being said, the crop parameters/plant growth information (such as leaf area index, canopy height, biomass, or crop yields) and vegetation data of the watershed for the simulations were obtained from the National Forest Inventory and the Catholic University of Ecuador (See Table 2-7 in Chapter 2.4.3).

2.1.4.- Meteorological and Hydrological Data

For this study, we collected data from four meteorological stations and one hydrological station (Figure 2-3) inside the catchment. For purposes of this study, the name of the four meteorological stations will be ST1, ST2, ST3, and ST4; and the name of the hydrological station will be Station Low. The spatial distribution of the meteorological stations is mainly along the watershed valley (Figure 2-3), and their altitudinal location within the basin is as follows: ST1: 1570 m.a.s.l; ST2: 1310 m.a.s.l; ST3: 1615 m.a.s.l; ST4: 1960 m.a.s.l.

Figure 2-2: Land-use maps of the Study Area.



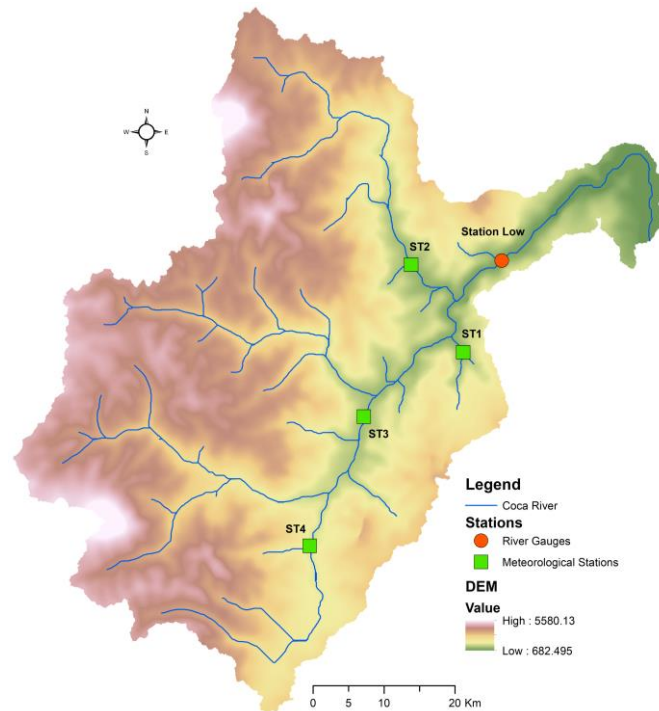
Data Source: Ecuadorian Ministry of the Environment (MAE)

As Figure 2-3 shows, all four meteorological stations in this study are spatially distributed along the Coca River valley, in the east part of the watershed. Precipitation is a major driving force of hydrological processes (Tuo et al. 2016; Worku, Khare, and Tripathi 2017; Yusuf, Biswajeet Pradhan, and Idrees 2014), and therefore reliable precipitation data is important for hydrological modeling (M. Volk 2016; M. Volk, Lorz, and M. Strauch 2012; Nie et al. 2011; Mekonnen et al. 2018). Therefore, an accurate representation of the temporal and spatial variability of precipitation is of importance to achieve an accurate river basin model. In other words, physically-based hydrological models such as SWAT cannot generate accurate predictions of hydrological processes without adequate representations of the regional precipitation distribution. Subsequently, without an accurate simulation of hydrological processes, reliable predictions of other relevant behaviors such as water quality and erosion cannot be achieved because of the uncertainties related to this issue (Chaplot, Saleh, and Jaynes 2005).

The sparse and heterogeneous spatial distribution of rain gauges often results in inaccurate precipitation inputs for the SWAT modeling process, especially when modeling large river basins with complex heterogeneous terrains like mountainous regions (e.g. Andes catchments) where the assumption of spatially uniform rainfall is not valid (dos R. Pereira et al. 2016b; Ficklin et al. 2009; Galván et al. 2014). Therefore, improved precipitation inputs that consider regional spatial variations are crucial for achieving reliable modeling results (Ficklin et al. 2009; Fan, Y. Wang, and Z. Wang 2008). To consider the orographic effects on precipitation and temperature in mountainous areas, SWAT uses the elevation bands method to simulate precipitation variability in a subbasin due to orographic

effects (Neitsch et al. 2011). In this work, five elevation bands have been applied to all the 83 sub-basins in the study area for the SWAT model (Chapter 2.4.3).

Figure 2-3: Meteorological and Hydrological stations in the Study Area



All the information related to climatic data such as daily time series of precipitation and the minimum-maximum temperature from 1980 to 2016 (Figure 2-4) from the National Institute of Meteorology and Hydrology of Ecuador (INAMHI) and the National Water Secretariat of Ecuador (SENAGUA). Then, these datasets were processed according to the model input format as (J. Arnold et al. 2012) explain. The monthly discharge data series from 1980 to 2016 (Figure 2-5) were collected from the National Water Secretariat of Ecuador (SENAGUA) and the Ecuadorian Ministry of the Environment (MAE).

In the hydroclimogram (Figure 2-4), we find the average daily precipitation (mm) values by month. Values plotted in bars with a blue color, corresponding to each of the four stations in the catchment. As we can see, there are two periods in the watershed with high precipitation values; the first one from March to May and the second one from September to December. As shown in Figure 2-4, Station 2 (ST2 in Figure 2-3) receives more precipitation per day than the other stations especially during the period between September to December. This can be explained because this station is located in the proximities of the Reventador volcano, which is an area characterized by high average precipitation values over the year due to its orography and the proportion of cloudy days in the area, which is 7/8 of the total year.

Plotted in lines with an orange color, we find the average daily Max temperature (°C) by month, which goes from 21°C to 23 °C, of the four stations in the study area. Lines plotted with a green color show the average daily Min temperature (°C) by month, which goes from 13°C to 15°C, corresponding to each of the four stations in the catchment.

Figure 2-4: Average daily precipitation (mm) and temperatures (°C) by month (1980 -2016).

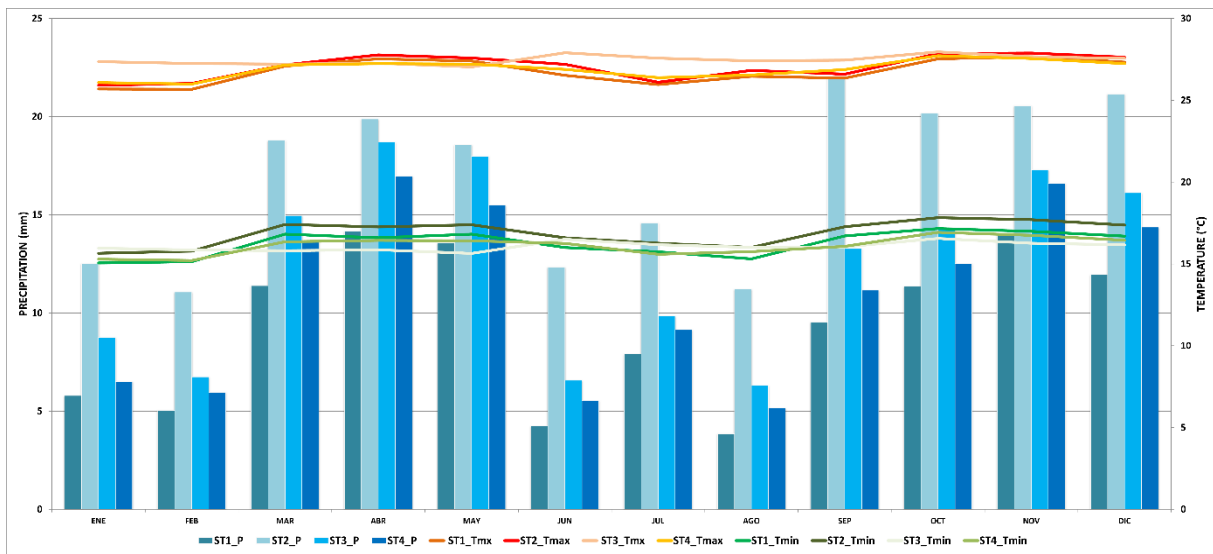
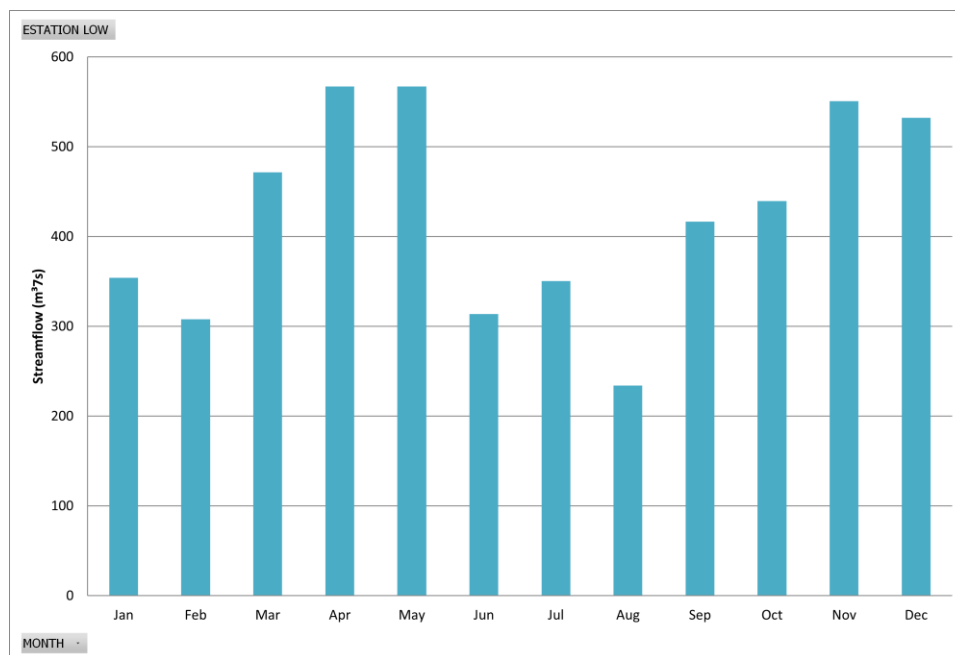


Figure 2-5 shows the average monthly flow (m³/s) of the available station in the study area from 1980 to 2016. Plotted in bars with blue color, we find the average monthly flow values corresponding to the Station Low. The drainage area of the basin is approximately 3600 km².

Figure 2-5: Average monthly flow (m³/s) of the Study Area (1980 – 2016).



2.1.5.- Data for LU/LUC analysis

Predictions of future LUC dynamics require a substantial amount of earth observation data to conduct an effective analysis (Araya and Cabral 2010; Mango et al. 2011; Keshtkar and Voigt 2016). For instance, earth observation data sets serve as a great source of data, from which updated Land-use maps and changes can be analyzed and predicted (Keshtkar and Voigt 2016). Hence, the LUC data for this study were prepared using the Ecuadorian Ministry of the Environment (MAE) and the Ecuadorian Space Institute (IEE) maps of the years 1990, 2000, 2008, and 2016. MAE and IEE reported six major LU types, which include Agriculture, Forest, Pasture, Andean Páramo

- Moorlands, Barren soils, and Urban areas. These data sets were used as a baseline for predicting future LUC dynamics.

Also, In this study, socio-economic data such as population, roads, and rivers were gathered from the Ecuadorian Institute of Statistics and Census (INEC) and the National Information System (SNI) of Ecuador. These data sets were used as one of the socio-economic driving forces of LU dynamics to prepare the suitability maps for running the CA_Markov model (See Chapter 2.3). More details about the input data used for this analysis are detailed in Table 2-1.

2.2.- Uncertainty in IWRM

There are many concepts, definitions, and interpretations regarding uncertainty. For this study, we took the definition of Vanrolleghem et al. (2010) that establishes uncertainty as “The degree of confidence that a decision-maker has about possible outcomes and/or probabilities of these outcomes”. Within the IWRM cycle (Figure 1-5), uncertainty emerges at every stage of the process. They arise because of the conflicting interests between stakeholders and the different sectors. During the assessment of present and future situations using monitoring and environmental models, where uncertainties arise from the limited knowledge of the data, model structures, and extrapolation data to the future. Also, uncertainties come from the political system and pressures from the different population sectors.

2.2.1.- Uncertainties and the Modeling role inside the IWRM Process.

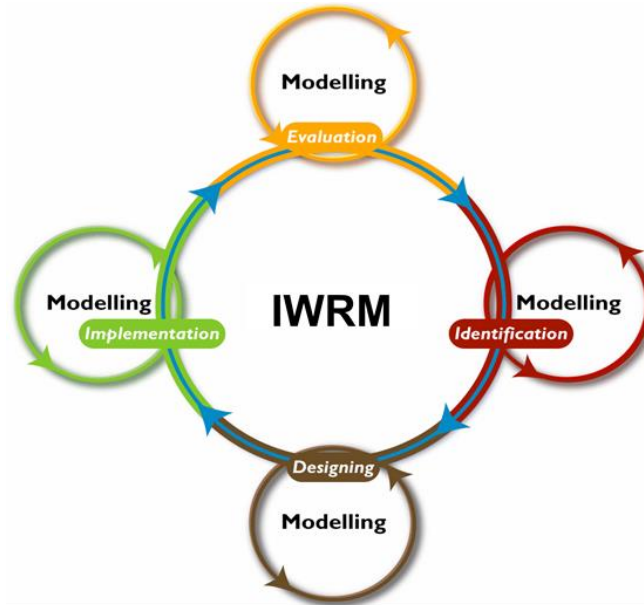
Models describing water flows, water quality, ecology, and economy are being developed and used in increasing numbers and variety. Due to the IWRM processes, the trend in recent years to base water management decisions to a larger extent on model studies and to use more sophisticated models is likely to be reinforced. It is important to note that the modeling studies typically do not address the entire water resources management decision process, such as the IWRM process, but rather support certain elements of the process (Vanrolleghem et al. 2010; Refsgaard et al. 2007; J. Refsgaard et al. 2005).

Modeling has been used as a tool at various stages of the IWRM process (Jønch-Clausen 2004). The role of modeling as part of the IWRM process can be illustrated schematically as in Figure 2-6. The inner circle in the figure depicts a simplified version of the IWRM planning process with the main elements.

- *Identification* including assessment of present status, analysis of impacts and pressures, and establishment of environmental objectives. Here modeling may be useful for example for supporting assessments of what are the reference conditions, for assessment of the pressures, and what are the impacts of the various pressures in combination with monitoring data and expert judgment (WFS 2004).
- *Designing* including the setup and analysis of programs of measures designed to be able in a cost-effective way to reach the environmental objectives. Here modeling will typically be used for supporting assessments of the effects and costs of various measures under consideration.
- *Implementing* the measures. Here online modeling in some cases may support the operational decisions to be made.

- *Evaluation* of the effects of the measures on the environment. Here modeling may support the monitoring to extract maximum information from the monitoring data, e.g. by indicating errors and inadequacies in the data and by filtering out the effects of climate variability.

Figure 2-6: The Modeling role inside the IWRM process.



Modified from (Refsgaard et al. 2007)

Uncertainty analysis of modeling results is crucial in every step of the IWRM process because, as soon as the modeling process starts, uncertainties show up and must be assessed by the modeler to reach the previously defined accuracy of the modeling predictions. In this study, uncertainty arises during the evaluation, identification, and designing modeling phases, in that sense, the uncertainty assessment of the hydrological and land-use change modeling processes has been performed. See Chapters 2.4.4 and 2.3.6.

2.2.2.- Modeling uncertainty sources

Walker et al. (2003) describe the uncertainty as manifesting itself at different locations in the model-based water management process. These locations, or sources, may be characterized as follows:

- *Context (Model)*: i.e. at the boundaries of the system to be modeled. The model context is typically determined at the initial stage of the study where the problem is identified and the focus of the model study selected as a confined part of the overall problem. This includes, for example, the external economic, environmental, political, social, and technological circumstances that form the context of the problem.
- *Input uncertainty*: in terms of external driving forces (within or outside the control of the water manager) and system data that drive the model such as Land-use maps, pollution sources, and climate data.
- *Model structure (Conceptual) uncertainty*: due to incomplete understanding and simplified descriptions of processes inside the model as compared to nature.
- *Parameter uncertainty*: i.e. the uncertainties related to parameter values.

- *Model technical uncertainty*: is the uncertainty arising from computer implementation of the model, e.g. due to numerical approximations and bugs in the software.
- *Model output uncertainty*: i.e. the total uncertainty on the model simulations taken all the above sources into account, e.g. by uncertainty propagation.

2.2.3.- Methodologies for uncertainty analysis in model-based IWRM process

Assessment of uncertainty in model simulations is important when such models are used to support decisions in IWRM (Beven and Binley 1992; Jakeman 2003; Pahl-Wostl 2002; J. Refsgaard and H. Henriksen 2004). There are many methodologies and tools reported in the scientific literature that can be used to assess uncertainties during the model-based IWRM process. No methodology is applicable to address all the different aspects of uncertainty assessment (Vanrolleghem et al. 2010). According to (van der Sluijs, J. et al. 2004), the methodologies can roughly be divided into three groups that differ according to their purpose.

- *Methods to characterize and prioritize uncertainty*. This group includes methods for handling data uncertainty, methods of expert elicitation, parameter estimation through inverse modeling, sensitivity analysis, the NUSAP method, and the uncertainty matrix.
- *Methods aiming to increase the quality of information*. This group includes procedures for quality assurance, extended peer review, and stakeholder involvement.
- *Methods to quantify and propagate uncertainty in model calculations to produce uncertainty in the model outcome*. This group includes the error propagation equations, Monte Carlo analysis, inverse modeling (parameter estimation and predictive uncertainty), multiple model simulation, various forms of sensitivity analysis, and scenario analysis.

These methods are not necessarily valid for only one of the listed groups. Sensitivity analysis may, for instance, be used both to identify the importance of a given uncertainty source at an early stage in the modeling process and again at a later stage to quantify the uncertainty for the model results. More detailed and extensive descriptions of those methodologies are available in the (van der Sluijs, J. et al. 2004) research.

2.2.4.- Methodology selection for uncertainty analysis

As we have seen, there are different methodologies and associated tools that may be applied for assessing uncertainties during the modeling phase of an IWRM process, but the question to answer is which methodology should be selected for a particular purpose and task of the modeling process.

The selection of an adequate methodology depends on:

- Where in the modeling process the analysis should be carried out.
- The type, nature, and source of uncertainty.
- The priority that addressing each of the identified sources of uncertainty has, according to their importance for the decision-making process (“policy relevance”).
- The available resources and level of ambition for the completeness of the analysis.

Table 2-2: Uncertainty analysis methodologies based on the modeling process and ambition level.

Type of uncertainty aspect	Task in the modeling process	Level of ambition / Available resources	
		Basic	Comprehensive
Identify and characterize sources of uncertainty	Describe Problem and Context	UM	EPE, SI, UM
	Determine Requirements		
Modeler reconsiders uncertainty and performance criteria	Prepare and Evaluate Tender	(Update of) UM + Common sense	
	Reporting		
	Specify or Update Calibration and Validation Targets and Criteria		
Reviews - dialogue - decisions	Agree on Model Study Plan and Budget	QA	EPR, QA
	Review		
Uncertainty assessment and propagation	Uncertainty Analysis of Calibration and Validation	DA, EPE, SA	DA, EPE, EE, INPA, IN-UN, MCA, MMS, NUSAP, SA
	Uncertainty Analysis of Simulation	DA, EPE, SA	DA, EPE, EE, INPA, IN-UN, MCA, MMS, NUSAP, SA

Methodologies Abbreviations

DA Data Uncertainty	MMS Multiple Model Simulation
EPE Error Propagation Equations	NUSAP NUSAP Model
EE Expert Elicitation	QA Quality Assurance
EPR Extended Per Review (by stakeholders)	SC Scenario Analysis
IN-PA Inverse modeling (parameter estimation)	SA Sensitivity Analysis
IN-UN Inverse modeling (predictive uncertainty)	SI Stakeholder Involment
MCA Monte Carlo Analysis	UM Uncertainty Matrix

Inside Table 2-2, constructed from the information of (J. Refsgaard et al. 2005) and (Vanrolleghem et al. 2010), a list of applicable methodologies that are considered to be adequate for the different tasks/steps in the modeling process is shown. Also, it includes hints for which methodologies are more suitable for comprehensive analysis with relatively large economic resources for the study and which methodologies correspond to a lower level of ambition; which is denoted as “Basic”.

2.2.5.- Input and output uncertainties throughout the study area modeling process

As mentioned before, during the modeling process of a catchment, models suffer from large model uncertainties, such as conceptual model uncertainty (structural uncertainty), input uncertainty, and parameter uncertainty (K. Abbaspour 2012). Conceptual model uncertainties refer to simplifications in the conceptual model, processes occurring in the watershed but not included in the model, processes that are included in the model, but their occurrences in the watershed are unknown to the modeler, and processes unknown to the modeler and not included in the model.

Inside Table 2-3, constructed from the information of (van der Sluijs, J. et al. 2004), we find a list of applicable methodologies for addressing the uncertainty of different types and originating from different sources. Reporting the uncertainty is a necessity because, without it, model calibration is meaningless and misleading. Any analysis with a calibrated model must include the uncertainty in the result by propagating the parameter uncertainties. Input uncertainty is a result of errors in input data such as rainfall, and, more importantly, extension of point data to large areas in distributed models. Parameter uncertainty is usually caused as a result of inherent non-uniqueness of parameters in inverse modeling. Parameters represent processes, and the fact that processes can compensate for

each other gives rise to many sets of parameters that produce the same output signal (K. Abbaspour 2012; K. Abbaspour, Johnson, and van Genuchten 2004).

Table 2-3: Applicable methodologies for uncertainty analysis according to its Source and Type.

Source of uncertainty		Taxonomy (types of uncertainty)			
		Statistical Uncertainty	Scenario Uncertainty	Qualitative Uncertainty	Recognized ignorance
Context	Natural, technological, economic, social, political	EE	EE, SC, SI	EE, EPR, NUSAP, SI, UM	EE, EPR, NUSAP, SI, UM
Inputs	System data	DA, EPE, EE, MCA, SA	DA, EE, SC	DA, EE	DA, EE
	Driving forces	SA	DA, EE, SC	DA, EE, EPR	DA, EE, EPR
Model	Model structure	EE, MMS, QA	EE, MMS, SC, QA	EE, NUSAP, QA	EE, NUSAP, QA
	Technical	QA	QA	QA	QA
	Parameters	IN-PA, SA, QA	IN-PA, SA, QA	QA	QA
Model Outputs		EPE, EE, INUN, MCA, MMS, SA	EE, IN-UN, MMS, SA	EE, NUSAP	EE, NUSAP

Taxonomy – Types of uncertainty

- Statistical Uncertainty:** All probabilities are known
- Scenario Uncertainty:** Some outcomes and probabilities are known
- Qualitative Uncertainty:** Some outcomes, but NO probabilities are known
- Recognized Ignorance:** No outcomes

In this study, uncertainty in parameters of the modeling process will be reported using the SUFI-2 (K. Abbaspour 2012) uncertainty analysis routine (See Chapters 2.4.3 and 2.4.4). In SUFI-2, uncertainty in parameters, expressed as ranges (uniform distributions), accounts for all sources of uncertainties such as uncertainty in driving variables (e.g., rainfall), conceptual model, parameters, and observed data (K. Abbaspour 2012; Vilaysane et al. 2015). Propagation of the uncertainties in the parameters leads to uncertainties in the model output variables, which are expressed as probability distributions (certain parameter ranges), calculated using Latin hypercube sampling (K. Abbaspour et al. 1997; K. Abbaspour 2012).

2.3.- Methods for analyzing socioeconomic aspects and creating scenarios

Historically, the hydrological conditions of the upper Coca River basin have been favorable for the availability of water, supplying the necessities of people as well as of ecosystems, especially due to the high degree of conservation of natural vegetation cover that exists within the basin (SENPLADES 2014). In the same way, the almost complete absence of degraded and eroded soils have been key factors for this positive scenario (Buytaert et al. 2006). However, in recent years this scenario has been affected by the increasing extensive agricultural production activities, as well as pasture establishment for livestock, and illegal logging (Sierra 2013).

In the future, these negative elements together could increase flood risk in the lower parts of the basin, and increments in the soil erosion and sediment rates of the catchment, generating damages in the reservoir area of the CCS-HPP and decreases in soil fertility/agricultural production due to soil losses. In that sense, the future behavior of water resources should be studied taking into account the future land-use changes (LUC) effects on the hydrological components of the watershed (Juckem et al. 2008). The use of land-use change modeling tools allows

the formulation of future LUC scenarios, the understanding of the key processes that explain the changes, and the description of these in quantitative terms (Mas, J.F y Sandoval, F. 2011; M. Camacho, Molero, and Paegelow 2010).

The land-use change models used to simulate, explore and predict probable future LUC scenarios can be divided into three categories: (a) statistical and empirical models, such as logistic regression model (Al-sharif and B. Pradhan 2013, 2014) and Markov chains model (Arsanjani, Kainz, and Mousivand 2011); (b) dynamic models, e.g. agent-based model and Cellular Automata (CA) model (Al-shalabi et al. 2007; Naghibi, Delavar, and Pijanowski 2016) (c) integrated model, e.g. the conversion of Land-use and its effects model CLUE (P. H. Verburg et al. 2002).

2.3.1.- Historical Land-use Change analysis

The historical land-use change analysis was carried out to assess the different temporal changes in land-use in the catchment. For this purpose, the four land-use maps from the years 1990, 2000, 2008, and 2016 (Figure 2-2), and the ArcGIS – ArcMap Geographic Information System (GIS) software by ESRI were used.

Using the ArcGIS-ArcMap software, the land-use information inside the LU maps was standardized according to the land-use classification of the Ecuadorian Ministry of the Environment (e.g. Forest, Agriculture, etc). After that, the land-use maps were intersected using spatial analysis tools, inside the ArcGIS-ArcMap software, Then, the land-use information derived from the intersected land-use maps were subsequently subjected to a cross-tabulation process, obtaining the area of the transitions that occurred between the different land use coverages (Figure 1-5).

2.3.2.- Markov Chain Model

Markov chain is a stochastic model that predicts the probability of LU change from one state to another state by taking into account the past LU change trend at different spatio-temporal scales. In other ways, the Markov chain model is just a series of random values whose probabilities at a time interval depending on the value of the number at the previous time (Surabuddin Mondal et al. 2013). The output of this model is based on the probability of transition (Adhikari and Southworth 2012). The transition probability matrix of LU changes from time one to time two, which will be the basis for projecting to later periods (Surabuddin Mondal et al. 2013).

The probability matrix is a set of conditional probabilities for the cells in the model to go to a particular new state (Akin, Aliffi, and Sunar 2014). This model can be used as a basis to predict how a particular LUC over time (Fan, Y. Wang, and Z. Wang 2008; Hyandye and Martz 2017; Iacono et al. 2015; P. Subedi, K. Subedi, and Thapa 2013; Mandal 2014). Currently, several studies are using the Markov analysis to simulate LUC over different types of landscapes (Halmy et al. 2015; Mango et al. 2011).

The Markov model predicts the quantities of each LU type or the dynamic changes of LU pattern, but it is not strong at dealing with the spatial pattern of landscape change (S. H. Li et al. 2015), because it does not provide the spatial distribution of the change, which is highly imperative for understanding the potential impact of the projected changes (Halmy et al. 2015). The basic principle of the Markov chain model is that LU in the future ($t + 1$) can be determined as a function of the current LU (t) (Iacono et al. 2015). (Coppedge, Engle, and Fuhlendorf) in 2007

reported that the LUC for any particular location may not be random, but it depends upon previous or current LU situations.

The Markov chain model is very powerful to determine the possibility of LUC between two time periods. However, it cannot provide the spatial distribution of occurrences of LUC (Araya and Cabral 2010).

2.3.3.- Cellular Automata Model (CA)

The CA-based model can represent non-linear, spatial, and stochastic processes (C. He et al. 2006). Furthermore, the CA model is capable to model and control complex spatially distributed processes and provide clear insights into local behaviors and global patterns of Land-use/cover change. Moreover, the spatial and temporal complexities of LUC can be well represented and simulated using suitable transition rules in the CA model. However, the most important concern in the CA model is defining appropriate transition rules based on training data that controls the model (Al-shalabi et al. 2007). It is worth mentioning that the CA model is affected by neighborhood type, neighborhood size, and cell size parameters; these parameters should be considered to get optimum simulation results (Wang et al. 2012).

A cellular automata (CA) is a model that can change and control complex spatially distributed processes. The model provides clear insights into local and global patterns of LU dynamics that relate the new state to its previous state and those of its neighbors (Mango et al. 2011; Al-sharif and B. Pradhan 2014). The CA model has a strong capability in simulating the spatiotemporal characteristics of complex systems (X. Yang, X.-Q. Zheng, and R. Chen 2014). That is why it has been extensively used as a spatially dynamic model in LU research (Adhikari and Southworth 2012; Omar et al. 2014). This model can be understood as a dynamic and relatively simple spatial system, in which the state of each cell of the matrix depends on the previous state of the cells enclosed inside a defined neighborhood, following a set of transition rules (Rocha and Ferreira 2007).

Therefore, the CA model is capable enough to predict the spatial distribution of the LU pattern and its dynamics because it adds the spatial properties of LU. This model does not only use the information of the previous state of a LU as done by a Markov model but also uses the state of neighboring cells for its transition rules (Adhikari and Southworth 2012). The CA model serves as an analytical engine that enables dynamic modeling within GIS (Ye and Bai 2008) and remote sensing environment. Despite its advantages, the CA has some problems in the definition of transition rules, and model structure (Rocha and Ferreira 2007). As a result, it cannot predict LU dynamics. This shortcoming of the technique can be overcome through the integration with other different dynamic and empirical models (Halmy et al. 2015) such as CA_Markov.

2.3.4.- The CA_Markov Chain Model

The integrated CA-Markov model is a robust technique in terms of quantity estimation, as well as spatial and temporal dynamic modeling of LUC because remote sensing data and GIS can be proficiently incorporated. Additionally, the integrated CA-Markov model can translate the results of the Markov chain model using a CA function to spatially explicit outcomes that are required for urban planning and design (Guan et al. 2011; Arsanjani, Kainz, and Mousivand 2011). However, integration of dynamic simulation models with statistical and empirical models results in models that can overcome the shortcoming of a single model, since the integrated used models

will complement each other. Additionally, those integrated models using combined modeling approaches will provide a better understanding and improved LUC modeling (Guan et al. 2011).

The cellular automata (CA) and Markov chain model is a dynamic model in time and state. This model is robust in predicting the transitions or spatial and temporal dynamics among several LU types. The CA_Markov model has been extensively used in many scientific studies to predict the future LU because it integrates the advantage of cellular automata and the Markov chain element of spatial contiguity as well as knowledge of the likely spatial distribution of transitions (Arsanjani, Kainz, and Mousivand 2011; Eastman 2003; S. H. Li et al. 2015; Mango et al. 2011; Mas, J.F y Sandoval, F. 2011). That is why the CA and the Markov chain models depend on each other (Omar et al. 2014) to predict the future LU effectively. This model is capable of generating a better spatiotemporal pattern of the LUC (Sayemuzzaman and Jha 2014). This study, therefore, applied the CA_Markov model to assess the transition matrix among the 2000–2008, 2008–2016, and 2000–2016 LU dynamics and the probabilities of change, and to predict accurately the future likelihood of LU dynamics in both the spatial and temporal domains.

Also, in this study, the CA_Markov model was used to simulate the long-term dynamics of LU (2016–2036) based on the past LU maps supported by the driving force both in temporal changes and spatial distribution using the IDRISI-TerrSet Geospatial Monitoring and Modeling System software (Eastman 2003, 2012). The prediction of future LULC using the CA_Markov model was supported by the transition probabilities controlled by local rules. To run the model appropriately, the CA_Markov requires three types of data sets like the base land cover image (e.g., LU map of 2016), Markov transition areas file generated by the Markov chain model, and the transition suitability images collection, which was prepared using the Multi-criteria evaluation (MCE) module of TerrSet (Eastman 2012).

Likewise, a standard contiguity filter of 5×5 (Figure 2-7) was used to define the neighborhoods of each cell and to create spatially explicit contiguous weighing factors. The pixels that are far from the existing LU class have lower suitability than the pixels that are near (P. Subedi, K. Subedi, and Thapa 2013).

Figure 2-7: Standard 5 x 5-pixel contiguity filter.

0	0	1	0	0
0	1	1	1	0
1	1	1	1	1
0	1	1	1	0
0	0	1	0	0

2.3.5.- CA_Markov parameter selection and modeling procedure

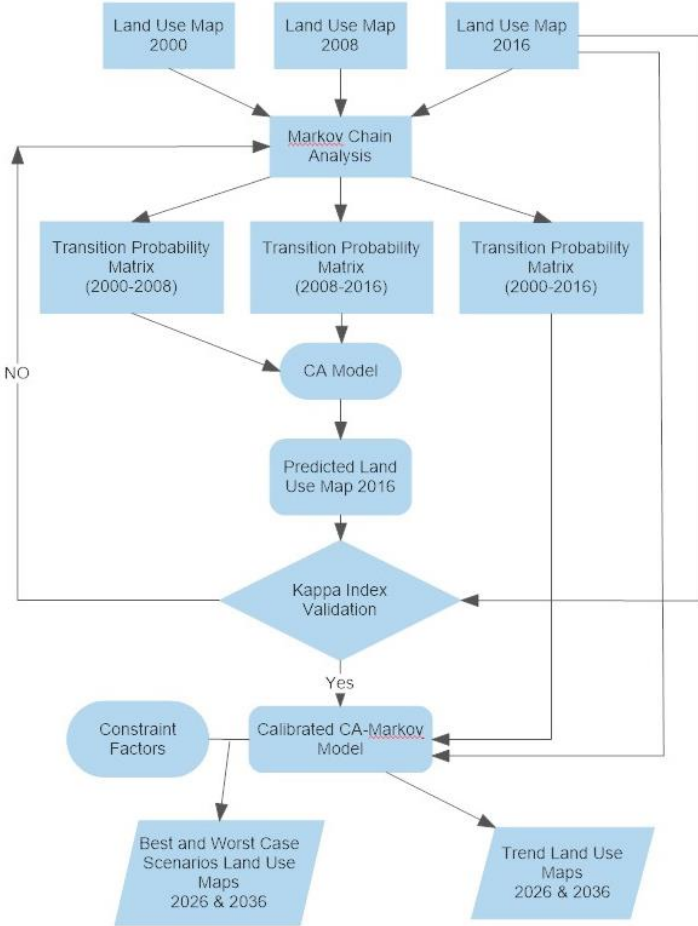
The CA_Markov model assumes that each parameter or factor of Land-use dynamics will be persistent to operate as before. (Eastman 2012) reported that one of the basic factors that can trigger the dynamics of Land-use / Land-use Change (LULC) events is proximity (e.g., Proximity to roads, rivers, etc...). The physical closeness to an existing LU class is likely to be a driver of change to this class in the future (Halmy et al. 2015; Mango et al. 2011). Proximity to major roads is thus one of the best indicators of LU dynamics because the population residing along

the road can expand their settlements, and/or clear forests, pasture areas, or bushes in time and space at various scales, either to enlarge their agricultural areas or fuelwood collection.

Mango et al. (2011) and Halmy et al. (2015) reported that LUC drivers often include an increase in population, distance to roads, and other factors. Therefore, this study considered the major physical and socio-economic parameters such as population density, elevation, rainfall, slope, LU type, proximity to roads and rivers (Table 2-1) to prepare the transition suitability map. The CA_Markov factors can be selected based on existing literature, analysis, or expert knowledge (Lopez-Morrero 2011; Hadi, Shafri, and Mahir 2014). The main reason is that there is no consistent standard for defining the suitability level of each LU factor.

For instance, the slope gradient was computed from the DEM 30 m × 30 m spatial resolution and then reclassified in ArcGIS software. Similarly, the population density was analyzed from the total population in the study area. The ultimate reason to consider population density as a factor was because highly populated and denser areas can increase the food demand. Moreover, the Euclidean distance function was applied to estimate the proximity from the roads and rivers based on the closest cell, and then each layer was reclassified in ArcGIS software.

Figure 2-8: CA-Markov Model Flowchart.



The two extreme values such as low and high were analyzed from the Euclidean distance to use as input for the fuzzy set membership analysis. Omar et al. (2014) and Rocha and Ferreira (2007) reported that the distance values should then standardized to the continuous suitability scale (0–255) through a fuzzy approach both in linear and sigmoidal functions.

Accordingly, this study standardized the values of each factor and constraint (like water bodies) using the fuzzy standardization in IDRISITerrSet Geospatial Modeling and Monitoring System software developed by Clark Labs at Clark University for the analysis of geospatial information (Eastman 2012). Afterward, the CA–Markov model was applied to simulate and predict future LUC in the study area as shown in the flowchart presented in Figure 2-9. Mainly the modeling procedure consisted of the following steps: (a) land-cover maps of 2000, 2008, and 2016 were assessed, (b) the transition area matrix was calculated using the Markov process, (c) transition suitability maps were prepared using multi-criteria evaluation (MCE), analytic hierarchy process (AHP) models and fuzzy membership functions in IDRISITerrSet and applied in CA–Markov (d) the actual and predicted map of the year 2016 were evaluated, and finally (e) the LU maps for the year 2026 and 2036 were simulated using the CA–Markov Model.

Table 2-4: Transition area probability matrix (2000 - 2008 – 2016).

Years	LU	Urban	Agriculture	Forest	Pasture	Paramo	Barren Soil
2000–2008	Urban	0.8832	0.1144	0.0000	0.0008	0.0008	0.0000
	Agriculture	0.0434	0.8407	0.0159	0.0253	0.0473	0.0143
	Forest	0.0052	0.0957	0.8335	0.0516	0.0093	0.0007
	Pasture	0.0032	0.0485	0.0947	0.7405	0.0825	0.0292
	Paramo	0.0014	0.0325	0.0065	0.0122	0.8065	0.1355
	Barren Soil	0.0226	0.0190	0.0000	0.0032	0.0656	0.5138
2008–2016	Urban	0.8864	0.0598	0.0115	0.0152	0.0196	0.0002
	Agriculture	0.0901	0.8640	0.0100	0.0122	0.0132	0.0062
	Forest	0.0101	0.0381	0.8790	0.0502	0.0214	0.0000
	Pasture	0.0270	0.1440	0.0821	0.7104	0.0224	0.0137
	Paramo	0.0107	0.0377	0.0056	0.0118	0.7506	0.1834
	Barren Soil	0.0416	0.0289	0.0005	0.0074	0.0103	0.6473
2000–2016	Urban	0.8915	0.1069	0.0000	0.0015	0.0000	0.0000
	Agriculture	0.0858	0.8167	0.0170	0.0182	0.0406	0.0150
	Forest	0.0142	0.0778	0.8288	0.0643	0.0141	0.0002
	Pasture	0.0063	0.0489	0.1475	0.6834	0.0733	0.0395
	Paramo	0.0040	0.0329	0.0065	0.0183	0.7696	0.1657
	Barren Soil	0.0289	0.0182	0.0019	0.0054	0.0055	0.5585

The transition matrix file was created and applied to the model for the specified time of 16 years (2000 – 2016). Then, to determine CA filters, the standard 5 x 5 pixels contiguity filter (Figure 2-7) was used in the modeling process (Figure 2-8) as the neighborhood definition. The LU map of 2016 was used as a base map to simulate LU trend maps for the years 2026 and 2036. This procedure was conducted by calculating the transition probability area matrix (Table 2-4) of 2000-2008, 2008-2016, and 2000-2016 to show how each land type was projected to change.

Data elements lying on the diagonal of the matrix indicate that a phenomenon will probably remain constant over time, while off-diagonal data indicate that various phenomena are likely to be converted to one of the other phenomena (Mekonnen et al. 2018; Mango et al. 2011; Eastman 2012).

For example, the transition probability matrix shows that the probability of future loss of Agriculture land to Urban areas from 2000 to 2008 was 4.3%. This probability of change increased reasonably to 9% in 2016. Table 2-4 shows that, for both periods, agricultural land possessed the highest likelihood of transforming into urban areas. Moreover, urban, agriculture, and forest were more likely to remain stable in the second period (2008–2016) compared to the first one (2000–2008).

GIS algorithms, MCE (multi-criteria evaluation), and fuzzy membership functions were applied to extract the transition potential maps of LU types; This step determined the status of the change. Transition potential maps represent the ability of a pixel to change to a new category or remain unchanged in each transition based on driving factors (Eastman 2003, 2012; Gidey et al. 2017). In this study, rainfall, slope, proximity to roads, rivers, forest, agricultural lands, pasture areas, barren soils, páramo, and distance to urban areas were set as driving factors.

Fuzzy membership functions (e.g., J-shaped monotonic decrease functions) were used to standardize the criterion scores or to rescale the factors into 0–255 in byte or (0.0 to 1.0) in real, where 0 represents unsuitable (or less suitable) and 255 signifies the most suitable (Mishra, Rai, and Mohan 2014; Omar et al. 2014; Keshtkar and Voigt 2016). AHP (analytic hierarchy process) was then run to determine the weight of the driving factors using pairwise evaluation. The weighting parameters and suitability level for each driving factor were chosen based on expert opinions, knowledge of the researcher, and literature of similar studies e.g., (Hamad, Balzter, and Kolo 2018; Rimal et al. 2017; Nath et al. 2020; Yirsaw et al. 2017; Yuanyuan Yang et al. 2015). The individual weights are listed in Table 2-5.

Table 2-5: Weights of each factor based on AHP and Fuzzy standardization.

No.	Factor	Weight
1	Slope (%)	0.0467
2	Elevation (m)	0.0175
3	Rainfall (mm)	0.0506
4	Population Density (Ppl/sqr Km)	0.3875
5	Proximity to Roads (m)	0.0658
6	Proximity to Rivers (m)	0.0291
7	Proximity to Pasture (m)	0.0544
8	Proximity to Agricultural (m)	0.0669
9	Proximity to Barren Soils (m)	0.0575
10	Proximity to Urban Areas (m)	0.0694
11	Proximity to Páramo (m)	0.0423
12	Proximity to Forests (m)	0.0578

Also in this study, I wanted to evaluate future impacts of LUC on the hydrological components inside the watershed using projected LU maps that consider different scenarios; Trend, “Best Case”, and “Worst Case”. The Trend scenario maintains the probabilities of change in land use that were predicted for the years 2026 and 2036. The “Best-case” scenario addresses the probabilities of change in LU towards a balanced scenario between conservation of natural ecosystems and productive activities within the basin by the years 2026 and 2036.

The “Worst-case” scenario addresses the probabilities of change in LU towards a scenario where extractive activities prevail and the productive areas in the watershed increase by the years 2026 and 2036. For this purpose, I added into the LUC analysis for the Best-Case and Worst-Case scenarios the following constraint factors and suitability levels (Table 2-6) based on the criteria of the Ecuadorian Ministry of the Environment and the Development and Territorial planning guidelines (GADs 2015) of the study area.

Table 2-6: Constraint Factors and suitability levels for LUC scenario analysis.

No.	Factor	Scenario	Suitability Level
1	Proximity to Conservation Areas, Natural Cover areas (Forest, Páramo), and water bodies.	Best-case	0-1000 m No suitability 1000 – 5000 m Increasing suitability >5000 m Highest suitability
		Worst-case	0-100 m Increasing suitability 100-500 m Highest suitability
2	Proximity to Riparian Areas.	Best-case	0-500 m No suitability 500-1000 m Increasing suitability >1000 m Highest suitability
		Worst-case	0-25 m Increasing suitability 25 -100 m Highest suitability
3	Slopes	Best-case	0% Highest suitability 0-15% Decreasing suitability >15% No suitability
		Worst-case	0-15% Highest suitability 15-25% Decreasing suitability
4	Proximity to Main Roads	Best-case	0-500 m Highest suitability 500-5000 m Decreasing suitability >5000 m No suitability
		Worst-case	0-2500 m Highest suitability 2500-5000 m Decreasing suitability

2.3.6.- Land-use modeling evaluation

The model evaluation was executed by comparing the agreement between the predicted Land-use map of 2016 with the real Land-use map of 2016 (Figure 1-3) based on the Kappa variation/statistic index (Congalton 1991) which is inside the validation tool in IDRISITerrSet (Eastman 2012).

An accuracy higher than 80% infers confidence in the simulation (Keshtkar and Voigt 2016; Araya and Cabral 2010). The Kappa statistic index is widely applied to validate the actual and predicted LU map of an area, this helps to determine how well does a pair of maps agree with the number of cells and their location in each category (Keshtkar and Voigt 2016; P. H. Verburg et al. 2002; G. R. Pontius and Malanson 2005; Peter H. Verburg et al. 2006).

The overall accuracy of the prediction based on the CA-Markov model was obtained from the Kno index, which is the standard Kappa index of agreement. The index also validates the simulation to predict the location. All these indexes of agreement results are shown in Table 3-2 (Chapter 3.1).

After the validation procedure, the future LU map predictions for the Trend scenarios, the Best-case scenarios, and the Worst-case scenarios for the years 2026 and 2036 were modeled using the CA_Markov model. The different LU maps of each scenario were used as input data during in hydrological modeling process (see Chapter 2.4) of the future scenarios in the study area.

2.4.- Methods for analyzing and modeling hydrological processes and creating scenarios

Within the Integrated Water Resources Management (IWRM) framework, the water resources behavior in a watershed should be studied taking into account the combined effects of land-use and climate changes (Juckem et al. 2008). In the Ecuadorian Andes, a large number of studies have been conducted to investigate various aspects of climate change impacts on water resources (Vuille et al. 2003; Espinoza Villar et al. 2009; Urrutia and Vuille

2009; Buytaert et al. 2010; D. Mora et al. 2014). Although progress has been made in assessing the impacts of land-use change (LUC) and climate change on the Ecuador watershed's hydrology, only a few studies have attempted to assess the attribution of changes in the water balance to LUC. However, much less attention has been paid to LUC impacts concerning water availability for hydropower potential, which is important because hydropower has become the principal source of energy in most of the Andean countries (Bradley et al. 2006; Nolivos et al. 2015).

Hydrological modeling of watersheds is one of the main water resource planning and management tools that can be used to understand the processes that control the water movement at different spatial and temporal scales. It may be used to estimate water availability, to predict short and mid-term streamflows, and to analyze the hydrological response of a watershed due to changes in Land-use cover (dos R. Pereira et al. 2016b). Therefore, a quantitative hydrological model with the ability to estimate with good accuracy the water regime of the catchment in a fast, economical, and safe way is important to support the development of better planning and management of water resources (dos R. Pereira et al. 2016a; K. Abbaspour et al. 2015; Beven and Binley 1992; Tuo et al. 2016).

The relations of hydrological components and land-use have been researched around the world and used to predict the impacts of future land-use change on hydrology and water resources. Typical methodologies used in these studies included observations from experimental catchments, time-series analysis for characteristic variables (e.g., runoff, evapotranspiration), and simulation studies using different hydrological models (B. Lin et al. 2015).

During recent decades, several distributed hydrological models have been developed to simulate hydrological processes in basins, such as the Soil and Water Assessment Tool (SWAT) (J. G. Arnold et al. 1998), the European Hydrological System (SHE) (Abbott et al. 1986), the Topography-based Hydrological Model (TOPMODEL) (Beven and Kirkby 1979), and others like HEC, VIC, IHDM, and WATFLOOD, are capable of simulating temporal-spatial variations in hydrological process and assisting in understanding the mechanisms of influence behind land-use impacts (B. Lin et al. 2015), because they allow for an approximate characterization of the spatial variability of a basin by use of data and parameters in a point-grid network (Wang et al. 2012).

Among the models mentioned above, the SWAT has excelled because previous studies have demonstrated the ability of SWAT in detecting the impacts of land-use and climate change on hydrological components in different areas (Nie et al. 2011; Guo 2008; P. W. Gassman et al. 2010; P. W. Gassman et al. 2007). SWAT has been applied to investigate the influence on water resources by simulating annual water yield for different periods that differed in land-use (Nie et al. 2011; B. Lin et al. 2015).

Streamflow (m^3/s) is the main variable that determines the sustainability of hydropower production in a hydro-electrical plant, and Surface Runoff (mm) is directly related to it (Winchell et al. 2013). In that sense, those two variables will be the main variables to be analyzed in the study area using the SWAT model to provide multitemporal information of water resources availability, concerning land-use changes in the catchment, that would lead to having a stronger IWRM process in the study area in the future.

The SWAT model was chosen for this study because it is widely used to assess hydrology in small and large catchments around the world. SWAT is a continuous in time, semi-distributed, process-based model (J. G. Arnold et al. 1998; P. W. Gassman et al. 2007; P. W. Gassman et al. 2010) that has been applied to agricultural basins where quantitative and qualitative drainage aspects and erosion processes are to be studied, in addition to enabling

the assessment of the hydrological behavior of basins facing changes in land-use cover. For an extensive overview of the SWAT model see Chapter 2.4.1, also see the SWAT model literature database(http://www.card.iastate.edu/swat_articles/).

As mentioned before in Chapter 2.3, this study also analyses the medium–long term (years 2026 and 2036) responses of streamflow to changes in land use (LUC) in the study area using the SWAT model. To accomplish that goal, it is necessary to assess the medium-long term trends of rainfall and streamflow in the catchment, as they are the key driving forces that can modify the watershed’s hydrology and water availability (Mekonnen et al. 2018; Abe et al. 2018).

2.4.1.- Time series trend analysis methods

The analysis of historical trends of rainfall and streamflow can help to reveal the effect of climate change or variability on water resources (Guo 2008). We analyzed the trends in annual rainfall and monthly streamflow time-series using the Mann–Kendall [MK] (Mann 1945; Kendall 1970) and Pettitt’s (Pettitt 1979) tests. The MK trend and Pettitt’s homogeneity tests have been widely applied to detect monotonic and homogeneous trends, respectively, to determine change points in long-term hydro-climatic time-series data (Mekonnen et al. 2018). These tests were selected because of their robustness concerning missing and tied values and to non-normality, which are common in hydroclimatic time series; moreover, they have the same power as their parametric counterparts such as the T-test (Wang et al. 2012; Mekonnen et al. 2018). All the trend results in this study have been evaluated at the 5% level of significance to ensure the effective exploration of the trend.

Also in this study, the Change Point Test was used, in this case, the Pettitt test is used to identify whether or not there is a point change or jump in the data series (Pettitt 1979). This method detects one unknown change point by considering a sequence of random variables $(X_t) = X_1, X_2, \dots, X_N, X_{N+1}, \dots, X_T$ that may have a change point at N , if the X_T variable for $t = 1, 2, \dots, N$ time step has a common distribution function, $F_1(x)$, and X_t for $t = N + 1, \dots, T$ time step has a common distribution function, $F_2(x)$, where $F_1(x) \neq F_2(x)$.

The trend magnitude is estimated using a non-parametric median-based slope estimator (Eq. 1) proposed by (Sen 1968), as it is not greatly affected by gross data errors or outliers and can be computed when data are missing. The slope estimation is given by

Equation 1: Trend magnitude / slope estimation equation (Sen 1968).

$$\beta = \text{Median} \left[\frac{X_j - X_k}{j - k} \right] \text{ for all } k < j,$$

where X_j and X_k are the sequential data values, and n is the number of the recorded data. $1 < k < j < n$, and β is considered as the median of all possible combinations of pairs for the whole data set. A positive value of β indicates an upward (increasing) trend, and a negative value indicates a downward (decreasing) trend in the time series. All MK trend tests, Pettitt change-point detections, and Sen’s slope analyses were conducted using the XLSTAT add-in tool from Excel (<https://www.xlstat.com/>).

2.4.2- The SWAT model

The Soil and Water Assessment Tool (SWAT) (J. G. Arnold et al. 1998; Neitsch et al. 2011) was applied in this study to model the impacts of LUC on the hydrologic regime of the upper Coca River watershed. The method we

used is divided into two parts: (1) hydrological modeling to simulate hydrological components for each land-use map of the years 1990, 2000, 2008, and 2016 (Figure 2-2); (2) hydrological modeling to simulate future impacts of LUC on the hydrological components using projected LUC maps (Figures 3-2, 3-3, and 3-4) that consider three different scenarios: Trend, “Best Case”, and “Worst Case”.

The Trend scenario maintains the probabilities of change in Land-use that were predicted for the years 2026 and 2036. The “Best-case” scenario addresses the probabilities of change in Land-use towards a balanced scenario between conservation of natural ecosystems and productive activities within the basin by the years 2026 and 2036. Also, different land management practices were incorporated into the “Best-case” scenario simulations. The “Worst-case” scenario addresses the probabilities of change in Land-use towards a scenario where extractive activities prevail and the productive areas in the basin increase by the years 2026 and 2036.

The SWAT model is a process-oriented, spatially semi-distributed, and time-continuous river basin model (J. G. Arnold et al. 1998; Alemayehu et al. 2017) that operates on different time steps (Leta et al. 2016), created by the United States Department of Agriculture (USDA) (J. G. Arnold et al. 1998). The model was developed to assess the impact of human activities, land-use change, and climate change on hydrological components, soil erosion/sediment transport, pollution transport, and nutrient cycles in agricultural watersheds (Neitsch et al. 2011; Lee et al. 2018; Nie et al. 2011; Leta et al. 2016; Alemayehu et al. 2017; Mango et al. 2011; van Griensven et al. 2012, 2012; P. W. Gassman et al. 2007; van Griensven et al. 2012). SWAT has been used in many studies in tropical areas around the world to investigate watershed hydrology (Alemayehu et al. 2017) as well as to study the hydrological impacts of land-use change (Mango et al. 2011; P. W. Gassman et al. 2007; P. W. Gassman et al. 2010).

For modeling purposes, SWAT simulates the hydrologic cycle based on the water balance equation (Eq. 2) (Neitsch 2005).

Equation 2: SWAT Model water balance equation.

$$SW_t = SW_0 + \sum_{i=1}^t (R_{day\ i} - Q_{surf\ i} - E_{a\ i} - w_{seep\ i} - Q_{gw\ i})$$

Where **SW_t** is the soil water content at the end of the day, **SW₀** shows the initial amount of soil water content, **t** represents time in days, **R_t** gives the amount of rainfall, **Q_t** gives the amount of surface runoff, **ET_t** gives the amount of evapotranspiration, **P_t** gives the percolation and **QR_t** gives the amount of return flow. All components are given in mm.

The surface runoff is estimated using a modification of the SCS (Soil Conservation Service, now the Natural Resources Conservation Resource) curve number method (USDA 1972) with daily rainfall amounts. The curve number values are based on soil type, land-use maps, and land management conditions, then, the values are adjusted according to soil moisture conditions. Percolation is calculated using the combination of a storage routing technique and a crack-flow model (Nie et al. 2011; J. G. Arnold et al. 1998). The lateral flow is estimated simultaneously with percolation using a kinematic storage model (Sloan et al. 1983). The groundwater flow (Baseflow) into the channel is calculated based on the hydraulic conductivity of the shallow aquifer, distance from

subbasin to the main channel, and water table height (Nie et al. 2011; Neitsch et al. 2011; J. G. Arnold et al. 1998). For more details about the theory behind the SWAT model, see (Neitsch et al. 2011).

In the SWAT model, a watershed is divided into subwatersheds or subbasins. Subbasins are further divided into a series of uniform hydrological response units (HRUs) based on soil, land-use/land-cover maps, and slopes. Hydrological components, sediment yield, and nutrient cycles are simulated for each HRU and then aggregated for the subbasins (Nie et al. 2011). Hydrological components simulated in the SWAT model include evapotranspiration (ET), surface runoff, percolation, lateral flow, groundwater flow (Baseflow), transmission losses, and ponds (J. G. Arnold et al. 1998). Evaporation and transpiration are simulated separately: evaporation is computed using exponential functions of soil depth and water content and transpiration is estimated using a linear function of potential evapotranspiration (PET) and leaf area index (Nie et al. 2011; Neitsch et al. 2011). In SWAT, three methods can be used to estimate PET: 1) Hargreaves method (Hargreaves 1985), 2) Priestley and Taylor method (Priestley and Taylor 1972), and 3) Penman and Monteith method (Monteith 1965). Since the meteorological information available for the catchment only contains precipitation and temperature (max-min) data, the Hargreaves method was chosen to calculate PET in this study.

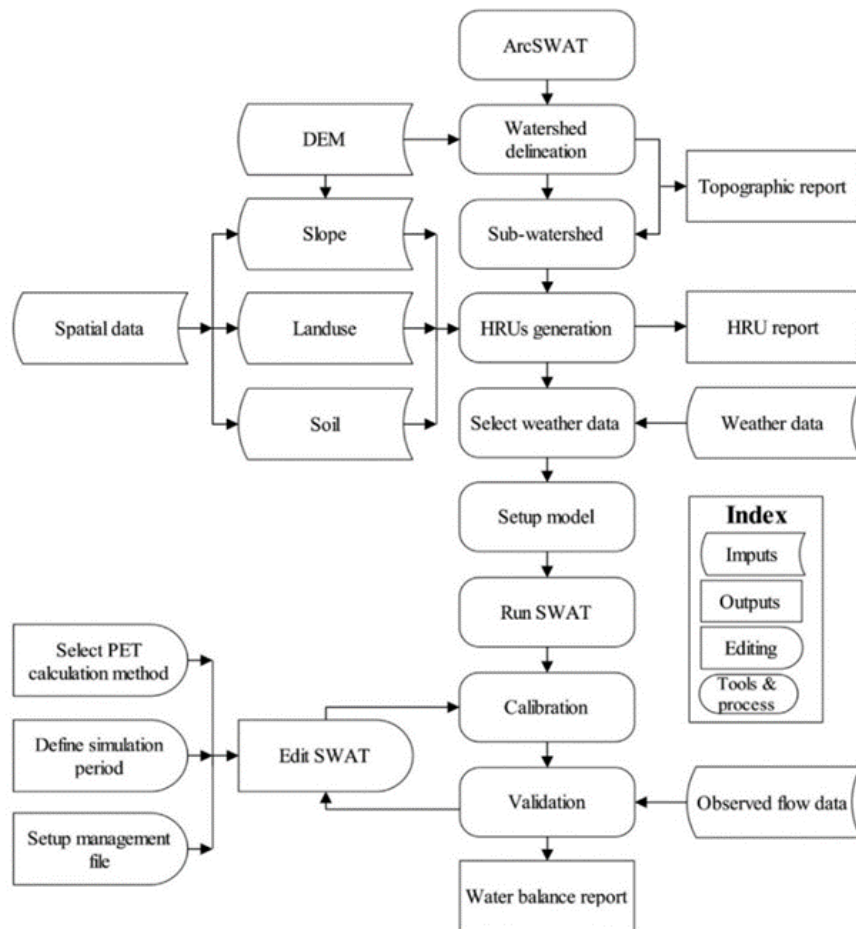
2.4.3.- SWAT model set-up for the study area

In this study, The ArcView GIS 10.4 interface for SWAT2012 (Winchell et al. 2013) was used to configure and parameterize the SWAT model for the study area (Upper Coca River watershed). The datasets used in the model are listed in Table 2-1. The model inputs included a 30 x 30 meters spatial resolution digital elevation model (DEM) of the watershed (Figure 2-1 A), Soil data and soil map (Figure 2-1 B), Land-use data, and Land-use maps of four different years (1990, 2000, 2008, and 2016) (Figure 2-2), and daily time series of precipitation and minimum-maximum temperature from 1980 to 2016 derived from four meteorological stations inside the watershed (Figure 2-3).

The SWAT model was built up based on the geospatial data (DEM, land-use, and soil maps) and the meteorological data. For a more comprehensive view of the process see (Figure 2-9).

The basin delineation depends on the DEM for the watershed and stream network delineation, analyzing the drainage patterns of the basin surface. The model fills all of the non-draining zones to create a flow direction and superimposes the digitized stream network into the DEM to define the location of stream networks. The model proposes the minimum, maximum, and suggested size of the sub-watershed area in hectares (Ha) to define the minimum drainage area. Generally, the smaller the threshold area, the more detailed the drainage networks and the number of sub-basins and HRUs (Leta et al. 2016). In addition, more processing time and space are needed. In this study, a smaller area (2500 ha) is provided to get all sub-basins of the study area. As a result, there are 83 sub-basins of the Coca river basin for this study. Later, the sub-basins were sub-divided into 1300 hydrological response units (HRUs), based on *zero threshold values* for Land-use, soil type, and slope class of the watershed. The *zero threshold value* means that at the time when the minimum size - in Ha's - of the HRUs can be defined, based on the Land-use, soil, and topography of the area, we will not assign any value; In this way, we will obtain the highest possible number of HRUs in the watershed.

Figure 2-9: SWAT Model set-up process and model inputs.



Adopted from (Kundu, Khare, and Mondal 2017)

The distribution of Land-use, soil, and slope characteristics within each HRU has the greatest impact on the predicted streamflow (J. Arnold et al. 2012; Berihun et al. 2019). As the percentage of Land-use, slope, and soil threshold increases, the actual evapotranspiration decreases due to eliminated land-use classes (Vilaysane et al. 2015; Leta et al. 2016). Besides, the use of zero threshold value for HRUs classification facilitates a better assessment of the effect of land-use change on the water balance components, which requires high-resolution land-use representation and it is critical in assessing river basin management practice studies (Leta et al. 2016). Therefore, the characteristics of HRUs are the key factors affecting streamflow.

Once the HRUs are created, the meteorological data is included in the model, then the model is set up and ready to run. Nevertheless, according to (Jing Yang et al. 2012), in SWAT, simulations should consider the knowledge of hydrological processes inside the watershed. Thus, key hydrological parameters, such as the Inicial Soil Water Storage / Field Capacity Water Content (FFCB), should be adjusted before the first run of the model, using a manual calibration procedure guided by expert knowledge and initial values derived from the literature (Michael Strauch and Martin Volk 2013; Memarian et al. 2012; Abe et al. 2018; Andrianaki et al. 2019; Bäse 2016). Therefore, the SWAT model for the Coca river basin was set up and the FFCB initial values for the catchment were changed (from 0 to 0.9) according to the previous knowledge of the study area.

The SWAT model has limitations in simulating the seasonal growth cycles for trees and perennial vegetation in the tropics using their default plant growth processes values, where rainfall rather than temperature is the dominant plant growth controlling factor (van Griensven et al. 2012; Alemayehu et al. 2017). In that sense, (J. Arnold et al. 2012) underscored the need for a realistic representation of the local and regional plant growth processes to reliably simulate the water balance, erosion, and nutrient yields using SWAT in tropic watersheds.

With that being said, the crop parameters/plant growth information (such as leaf area index, canopy height, biomass, or crop yields) and vegetation data of the watershed (Table 2-7) for the modeling procedures using SWAT were obtained from the National Forest Inventory of Ecuador <https://www.ambiente.gob.ec/evaluacion-nacional-forestal-del-ecuador-enf/>, and studies from the Catholic University of Ecuador (MT. Camacho 2010; Valero, Padilla, and Cruz 2012; Urrutia and Vuille 2009). With those new values, the land-use databases inside the SWAT model of the catchment were updated. Because there is no vegetation present in land covers like Barren Soils and Urban settlements inside the catchment, we used the default values present in the SWAT model for those land-use covers.

Table 2-7: Crop parameters /plant growth information and vegetation of the study area.

Land-use	SWAT CODE	BLAI	CHTMX	BIO_E	T_BASE	T_OP	OV_N	USLE_C
		DV/CV	DV/CV	DV/CV	DV/CV	DV/CV	DV/CV	DV/CV
Agriculture	AGRL	3 / 5	1 / 2	33.5 / 56.7	7 / 11	18 / 25	0.09 / 0.14	0.02 / 0.045
Forest	FRST	5 / 8	6 / 10	15 / 45.3	3 / 10	20 / 23	0.05 / 0.1	0.001 / 0.005
Pasture	PAST	4 / 6	0.5 / 2	35 / 41	10 / 12	15 / 25	0.08 / 0.15	0.003 / 0.065
Páramo	FESC	1 / 1	1.5 / 2.5	30 / 35.8	1 / 2	12 / 15	0.05 / 0.12	0.003 / 0.005

DV: Default value; **CV:** Changed value

BLAI: Leaf area index; **CHTMX:** Max canopy height; **BIO_E:** Biomass/Energy Ratio; **T_BASE:** Min temperature plant growth (°C); **T_OP:** Optimal temperature for plant growth (°C); **OV_N:** Manning's "n" value for overland flow; **USLE_C:** Value of USLE C factor applicable to the land cover/plant.

Precipitation is a major driving force of hydrological processes, sediment and chemical fluxes (Tuo et al. 2016; Worku, Khare, and Tripathi 2017; Yusuf, Biswajeet Pradhan, and Idrees 2014), and therefore reliable precipitation data are important inputs for SWAT (Galván et al. 2014; Monteiro et al. 2016; M. Volk, Lorz, and M. Strauch 2012) and other hydrological models (M. Volk 2016; Mekonnen et al. 2018; Nie et al. 2011; van Griensven et al. 2012). Therefore, an accurate representation of the temporal and spatial variability of precipitation is of importance to achieve an accurate river basin model. In other words, physically-based hydrological models such as SWAT cannot generate accurate predictions of hydrological processes without adequate representations of the regional precipitation distribution. Subsequently, without an accurate simulation of hydrological processes, reliable predictions of other relevant behaviors such as water quality and erosion cannot be achieved (Chaplot, Saleh, and Jaynes 2005).

The sparse and heterogeneous spatial distribution of rain gauges often results in inaccurate precipitation inputs for SWAT, especially when modeling large river basin or basins with complex heterogeneous terrains like mountainous regions (e.g. Andes catchments) where the assumption of spatially uniform rainfall is not valid (dos R. Pereira et al. 2016b; Ficklin et al. 2009; Galván et al. 2014). Furthermore, the current method of representing precipitation in the SWAT model is simplistic, since it only uses data from one precipitation gauging station that is nearest to the centroid of each subbasin (Galván et al. 2014). Therefore, improved precipitation inputs that consider regional spatial variations are crucial for achieving reliable modeling results with SWAT (Ficklin et al.

2009; Fan, Y. Wang, and Z. Wang 2008). SWAT utilizes elevation bands to simulate precipitation variability in a subbasin due to orographic effects (Neitsch et al. 2011).

To consider the orographic effects on precipitation and temperature in mountainous areas, SWAT uses the elevation bands method which allows for up to ten elevation bands in each subbasin. In this work, five elevation bands have been applied to all the 83 sub-basins in the study area for the SWAT model.

- Band 1: From 640 to 1663 m.a.s.l
- Band 2: From 1663 to 2683 m.a.s.l
- Band 3: From 2683 to 3709 m.a.s.l
- Band 4: From 3709 to 4732 m.a.s.l
- Band 5: From 4732 to 5759 m.a.s.l

Equation 3: SWAT Model elevation bands method equation.

$$R_{band} = R_{day} + (EL_{band} - EL_{gauge}) \cdot \frac{plaps}{days_{pcp,yr} \cdot 1000}, R_{day} > 0.01$$

$$R_{day} = \sum_{bnd=1}^b R_{band} \cdot fr_{bnd}$$

As shown in Eq. 3, the method modifies the regional precipitation by weighting the elevation difference between the band of the rain gauge and the other bands where **Rband** is the precipitation in the elevation band (mm), **Rday** is the precipitation recorded at the rain gauge (mm), **ELband** is the mean elevation at the elevation band (m), **ELgauge** is the elevation at the recording gauge (m), **plaps** is the precipitation lapse rate (mm/km) and **dayspcp,yr** is the average number of days of precipitation in the subbasin in a year, **frbnd** is the fraction of the sub-basin area within the elevation band, and **b** is the total number of elevation bands in the sub-basin.

Notice that in addition to Eq. 3, SWAT imposes the following condition: if **Rband** < 0, then **Rband** = 0. This condition prevents the elevation band method from being a constant adjustment of the input precipitation data. This method has been proven to be useful in several watersheds with complex heterogeneous terrains like mountainous regions (K. Abbaspour et al. 2007; Al-sharif and B. Pradhan 2014; Čerkasova 2019).

After the accomplishment of all SWAT model set-up steps for the study area, the first simulation, of the Coca River basin, was performed for a period of 37 years (1980 – 2016) using the land-use map corresponding to the year 1990. Also, for this simulation and all the subsequent simulations, a warm-up period of two years was established, allowing the model to make the hydrologic cycle fully functional and stabilize some initial model parameters (P. W. Gassman et al. 2007; P. W. Gassman et al. 2010). After that, calibration and validation procedures were executed (see Figure 2-9) using monthly discharge data series from 1980 to 2016 (Figure 2-5).

2.4.4.- Model Calibration, evaluation, and uncertainty procedures

Calibration of watershed models is not an easy process because models include many uncertainty types like input, model structure, parameters, and output uncertainties. Input uncertainty is a result of errors in input data such as

rainfall, and more importantly, extension of point data to large areas in distributed models. Parameter uncertainty is usually caused as a result of inherent non-uniqueness of parameters in inverse modeling. Parameters represent processes, and the fact that processes can compensate for each other gives rise to many sets of parameters that produce the same output signal (K. Abbaspour 2012; K. Abbaspour, Johnson, and van Genuchten 2004).

Reporting the uncertainty is a necessity because, without it, calibration is meaningless and misleading. Any analysis with a calibrated model must include the uncertainty in the result by propagating the parameter uncertainties. Also, as explained in Chapter 2.2, hydrologic models frequently contain many parameters that cannot be measured as they are time-consuming, costly, and sometimes hard to access. In that sense, Inverse Modeling (K. Abbaspour et al. 2007; Beven and Binley 1992; J. Refsgaard et al. 2005) has become a popular method for hydrologic calibration and uncertainty analysis purposes, because of its ability to handle parameter correlation and high computational efficiency (Beven and Binley 1992; K. Abbaspour et al. 2007).

In this study, uncertainty in parameters of the modeling process will be reported using the Sequential Uncertainty Fitting Method version 2 (SUFI-2) (K. Abbaspour et al. 1997; K. Abbaspour 2012) algorithm, which is a multi-site, semi-automated, inverse modeling procedure (K. Abbaspour et al. 2015), based on a Bayesian framework, and it is available in SWAT-CUP (Calibration and Uncertainty Program) which was used for the calibration and validation process of the Coca River basin SWAT simulations. SWAT-CUP is a software package, developed by the Swiss Federal Institute of Aquatic Science and Technology (EAWAG) in 2009. It is a public domain program, and as such may be used and copied freely. It enables sensitivity analysis, calibration, validation, and uncertainty analysis of SWAT models. For more details about SWAT-CUP, please refer to (K. Abbaspour 2012).

In SUFI-2, uncertainty in parameters, expressed as ranges (uniform distributions), accounts for all sources of uncertainties such as uncertainty in driving variables (e.g., rainfall), conceptual model, parameters, and observed data (K. Abbaspour 2012; Vilaysane et al. 2015). Propagation of the uncertainties in the parameters leads to uncertainties in the model output variables, which are expressed as probability distributions (certain parameter ranges), calculated using Latin hypercube sampling (K. Abbaspour et al. 1997; K. Abbaspour 2012).

SUFI-2 is based on a stochastic procedure for drawing independent parameter sets using Latin Hypercube Sampling (LHS). The simulation uncertainty is quantified by the 95% prediction uncertainty (95PPU). The 95PPU is calculated at the 2.5% and 97.5% levels of the cumulative distribution of an output variable obtained through LHS, disallowing 5% of the very bad simulations. Because SUFI-2 is a stochastic procedure, the application of the traditional R² and Nash-Sutcliffe (NSE) statistics is not an option to compare the two signals. For this reason, Abbaspour et al. suggest using two measures, referred to as the P-factor and the R-factor (K. Abbaspour et al. 1997; K. Abbaspour et al. 2007; K. Abbaspour 2012; K. Abbaspour et al. 2015).

The P-factor is the percentage of the measured data bracketed by the 95PPU band. This index provides a measure of the model's ability to capture uncertainties. As all the "true" processes are reflected in the measurements, the degree to which the 95PPU does not bracket the measured data indicates the prediction error. Ideally, the P-factor should have a value of 1, indicating 100% bracketing of the measured data, hence capturing or accounting for all the correct processes (Jing Yang et al. 2012; K. Abbaspour et al. 2015; K. Abbaspour et al. 1997; J. G. Arnold et al. 1998).

The R-factor, on the other hand, is a measure of the quality of the calibration and indicates the average thickness of the 95PPU band divided by the standard deviation of the measured data/variable. Its value should ideally be near zero, hence coinciding with the measured data. However, because of measurement errors and model uncertainties, the ideal values will generally not be achieved, and a desirable value would be less than 1.

Theoretically, the value of the P factor ranges between 0 and 100% while that of the R-factor ranges between 0 and infinity. A P-factor of 1 and an R-factor of zero is a simulation that exactly corresponds to the measured data. SUFI-2 hence seeks to bracket most of the measured data with the smallest possible uncertainty band. The combination of the P-factor and R-factor together indicates the strength of the model calibration and uncertainty assessment, as these are intimately linked (J. Arnold et al. 2012; K. Abbaspour et al. 2015; K. Abbaspour et al. 1997). For a more detailed explanation about SUFI-2, refer to (K. Abbaspour, Johnson, and van Genuchten 2004; K. Abbaspour et al. 2007).

2.4.5.- Calibration, Validation, Sensitivity, and Uncertainty analysis

In this study, to carry out the calibration and validation processes, we used the SWAT-CUP software (K. Abbaspour 2012; K. Abbaspour et al. 2015).

Table 2-8: Hydrological parameters considered for sensitivity analysis.

Parameter Name	t-Stat	P-Value	Rank
1:R__CN2.mgt	8.436100904	0.000000000	1
9:V__ALPHA_BNK.rte	7.028901677	0.000000001	2
20:V__LAT_TTIME.hru	-6.255784616	0.000000021	3
7:V__CH_N2.rte	-5.582768734	0.000000340	4
8:V__CH_K2.rte	-4.323736244	0.000045423	5
16:V__SOL_K(..).sol	1.982287479	0.051014920	6
14:V__REVAPMN.gw	-1.765384554	0.081463749	7
11:V__ESCO.hru	1.749787625	0.084138919	8
2:V__ALPHA_BF.gw	-1.723032027	0.088896632	9
13:V__RCHRG_DP.gw	1.416502921	0.160661296	10
5:R__SOL_AWC(..).sol	-1.338129048	0.184792674	11
17:R__SOL_BD(..).sol	-1.139020063	0.258225978	12
12:V__EPCO.hru	0.916195642	0.362424853	13
6:V__GW_REVAP.gw	-0.704651404	0.483153119	14
10:V__SURLAG.bsn	-0.656102035	0.513714322	15
18:V__SFTMP.bsn	0.618997664	0.537744980	16
21:V__CH_N1.sub	-0.493112157	0.623336747	17
4:V__GWQMN.gw	-0.484527822	0.629386770	18
19:V__OV_N.hru	-0.431462681	0.667337623	19
15:R__SHALLST.gw	0.293550090	0.769891476	20
22:V__CANMX.hru	0.134141914	0.893640355	21
3:V__GW_DELAY.gw	-0.020898762	0.983380475	22

("a_", "v_" and "r_" means an absolute increase, a replacement, and a relative change to the initial parameter values, respectively).

SWAT-CUP is a package used to carry out sensitivity analysis, calibration, and validation of the SWAT model. In this study, we followed the calibration and validation approach of Klemes and Gan (Klemes 1986; Gan 1997) that consists of equally splitting the available data, when the record is sufficiently long, to represent different climatic conditions (e.g. wet, moderate, dry years) in the study area (Odusanya et al. 2019).

In that sense, the hydrometeorological data of the catchment (37 years) was split into three segments, which considers a warming-up period (1980 – 1981) to initialize the state variables of the system (e.g initial soil moisture content) with the SWAT model simulations, a calibration period (1982 – 2000), and a validation period (2001 – 2016). Calibration and validation were executed in SWAT-CUP. Before calibration, a sensitivity analysis was performed, using the Latin Hypercube global sensitivity analysis (LHS) technique based on the multiple regression method (K. Abbaspour et al. 2015) implemented in SUFI-2 / SWAT-CUP, to identify the most sensitive parameters in the watershed. Over-parameterization of a complex model often leads to complications of parametric nonuniqueness and equifinality in hydrological models, particularly for distributed models, which may negatively impact prediction uncertainties (Schoups, van de Giesen, and Savenije 2008).

Therefore, a sensitivity analysis was conducted to lessen the number of parameters for the efficient use of the model (van Griensven et al. 2012). With the sensitivity analysis, we obtain the most sensitive parameters by examining the resulting P-value and the t-stat value. The P-value determines the significance of the sensitivity (a value close to zero has more significance) and the t-stat value provides a measure of parameter sensitivity (a larger absolute value is more sensitive) (Odusanya et al. 2019).

After this procedure, the parameters were ranked (Table 2-8) from the most sensitive to the least sensitive. According to the literature (Neitsch et al. 2011; K. Abbaspour 2012; K. Abbaspour, Johnson, and van Genuchten 2004), and based on the sensitivity analysis, 6 of the most sensitive parameters were selected for this study (Table 2-9) and altered during the calibration process using SUFI-2. The other 16 parameters remained constant for the SWAT model simulations because they showed a lower sensitivity to change while all other parameters are kept constant at some value.

In Table 2-8, we found the common hydrological parameters used for calibration of hydrological models recommended in the literature (K. Abbaspour, Johnson, and van Genuchten 2004; K. Abbaspour et al. 2015; Buytaert et al. 2010; Čerkasova 2019; dos R. Pereira et al. 2016a; dos R. Pereira et al. 2016b; P. W. Gassman et al. 2010; Hamad, Balzter, and Kolo 2018; Sharad K. Jain et al. 2017; Khalid et al. 2016; Khoi and Thom 2015; Mekonnen et al. 2018; Worku, Khare, and Tripathi 2017).

In Table 2-9, we find the parameters used for the calibration and uncertainty analysis procedure using the SUFI-2 optimization algorithm. Also, we find the initial parameter ranges that are based on the SWAT-CUP official documentation (Neitsch et al. 2011; Neitsch 2005, 2002; K. Abbaspour 2012). With these initial ranges, the model was calibrated with four iterations, for each iteration, 1500 simulations were run as suggested in the literature (K. Abbaspour 2012; Neitsch et al. 2011; Tuo et al. 2016). After each iteration, the ranges of the parameters were modified (normally narrowed down) according to both the new parameters suggested by the program

(K. Abbaspour, Johnson, and van Genuchten 2004; K. Abbaspour et al. 2007; K. Abbaspour 2012) and their reasonable physical limitations.

Table 2-9: Parameter description and ranges for calibration procedures with the model.

Parameter Description	Parameter Symbol	Sensitivity Ranking	Initial Range
SCS runoff curve number.	CN2.mgt	1	-0.30 – 0.30
Lateral flow travel time.	LAT_TTIME.hru	2	0 – 180
Baseflow alpha factor for bank storage.	ALPHA_BNK.rte	3	0 - 1
Manning's "n" value for the main channel.	CH_N2.rte	4	0.01 – 0.3
Effective hydraulic conductivity in main channel alluvium.	CH_K2.rte	5	0.025 - 500
Saturated hydraulic conductivity	SOL_K().sol	6	0 - 2000

To evaluate the goodness of the calibration and validation procedures, we used The Nash–Sutcliffe coefficient (NSE), the Root mean squared error (RSR), and the coefficient of determination (R²) for streamflow simulations. NSE measures the quantity difference between the predictions and the observed data, with NSE = 1 being the optimal value. RSR optimal value would be 0, which indicates zero residual variation and therefore perfect model simulation. The lower RSR, the better the model simulation. R² ranges from 0 to 1 and represents the trend similarity between the observed data and the simulated ones, with higher R² values indicating better model performance. The model performance has been classified using the NSE value according to the work of (D. N. Moriasi 2007).

These coefficients are recommended in the literature to analyze monthly outputs and median objective functions, sign test, autocorrelation, and crosscorrelation for assessing daily output based on comparisons of SWAT model results with measured streamflow (Neitsch et al. 2011; Olenin; Qi et al. 2018; J. Refsgaard et al. 2005; Worku, Khare, and Tripathi 2017; van Griensven et al. 2012; Githui et al. 2009; Kundu, Khare, and Mondal 2017; M. Volk 2016; Mekonnen et al. 2018; J. Arnold et al. 2012).

Table 2-10: General performance ratings for NSE and RSR statistics (monthly time step).

Performance Rating	NSE	RSR
Very good	$0.75 < \text{NSE} \leq 1.00$	$0.00 < \text{RSR} < 0.50$
Good	$0.65 < \text{NSE} \leq 0.75$	$0.50 < \text{RSR} < 0.60$
Satisfactory	$0.50 < \text{NSE} \leq 0.65$	$0.60 < \text{RSR} < 0.70$
Unsatisfactory	$\text{NSE} \leq 0.50$	$\text{RSR} > 0.70$

Data Source: ((D. N. Moriasi 2007)

In Table 2-10, the general performance ratings for NSE and RSR statistics for a monthly time step for SWAT calibration and validation procedures are shown according to (D. N. Moriasi 2007). For the uncertainty analysis evaluation, the P-values and R-values were used as mentioned before in this chapter. When the calibration, validation, and uncertainty analysis procedures were completed, we used the final calibration ranges values, of the 6 chosen parameters (Table 2-9), into the SWAT model simulations of the study area. The first simulations were performed using the Land-use maps of the years 1990, 2000, 2008, and 2016. Then, the simulations with the

SWAT model for the medium-long term scenarios were performed using the projected Land-use maps scenarios (Trend, Best-case, and Worst-case) of the years 2026 and 2036, and the meteorological projections of the study area (Chapter 2.4.1 and 3.2.1).

CHAPTER 3.- Results and Discussion

3.1.- Land-use change (LUC) analysis and scenarios of socioeconomic aspects

The actual Land-use of 2016 was compared with the simulated 2016 land-use (Figure 3-1) based on the CA-Markov model. Table 3-1 shows the chi-square (χ^2) test result for the validation of the model. We hypothesized that the area statistics of the actual and the simulated image were equal. As we can see in Table 3-1, no statistically significant differences can be found to reject the hypothesis.

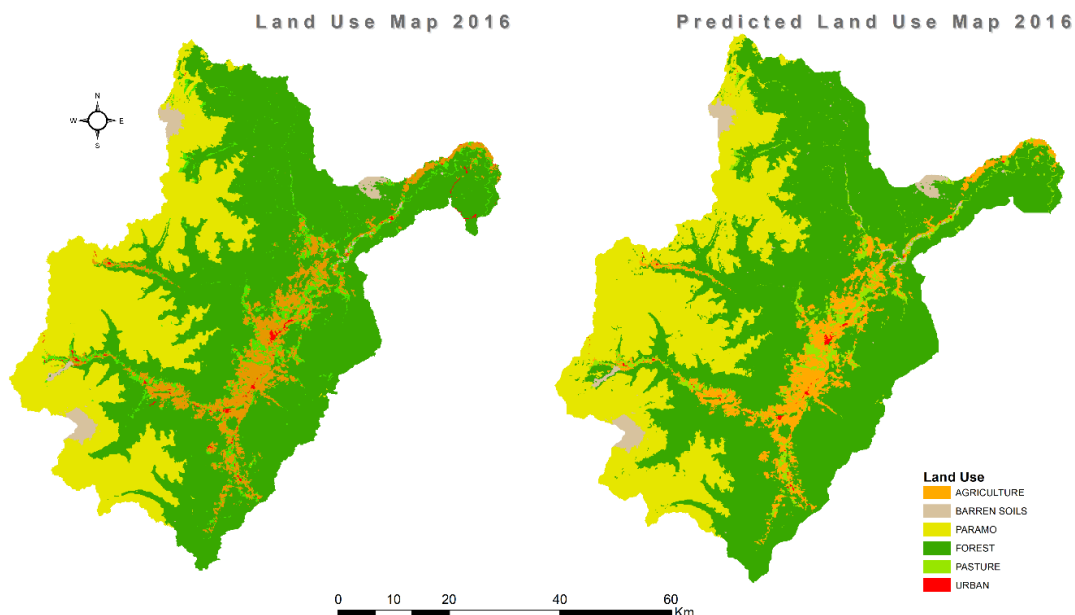
Table 3-1: Validation of the simulated Land-use (LU) map of 2016 based on the actual LU map of 2016.

Chi-Square Test			
Land-use Classes	Land-use 2016 (%) [A]	Simulated LU 2016 (%) [B]	$(B - A)^2 / A$
Agriculture	7.23	6.99	0.0080
Forest	57.12	58.04	0.0149
Pasture	3.51	3.24	0.0215
Páramo	30.36	29.99	0.0045
Barren soil	1.50	1.57	0.0028
Urban	0.28	0.17	0.0397
Total	100	100	0.0914

Note: $\chi^2 = \sum(B - A)^2 / A = 0.0914$. A and B represent the percentage of each LU cover in the maps.

However, this does not necessarily validate the agreement on the spatial distribution of the LULC classes of the study site. To solve this problem, we performed a more sophisticated Kappa index of agreement between the two images. Moreover, the Kappa coefficient value was measured using the following set of conditions: < 0 = less than chance agreement, $0.01-0.40$ = poor agreement, $0.41-0.60$ = moderate agreement, $0.61-0.80$ = substantial agreement, and $0.81-1.00$ = very good agreement. According to (Mukherjee et al. 2009), these statistics measure the goodness of fit between the model predictions and reality, which is corrected for accuracy by chance.

Figure 3-1: Land-use map of 2016 vs. Predicted Land-use map of 2016.



The results of the model evaluation performed by the IDRISITerrSet Geospatial Modeling and Monitoring System software represents a validation analysis of the agreement/disagreement components (Table 3-2), which is further partitioned into 0.0364 (error due to quantity / DisagreeQuantity) and 0.0865 (error due to allocation/DisagreeGridcell). Therefore, the data table inferred that the main disagreement between the two maps was due to an allocation error rather than quantity errors between the simulated and actual 2016 LU maps.

Moreover, the overall accuracy of the prediction based on the CA-Markov model could be obtained from the Kno index. The Klocation index validates the simulation to predict the location. All these indexes of agreement results are shown in Table 3-2, and Table 3-3, and the average value is found to be 0.9033, which means that the LULC categories of the actual and simulated Land-use maps of 2016 were 90% similar.

These results indicate that the CA-Markov model was effective in simulating LU in 2016. Thus, the CA-Markov model can be reliable in predicting future LUC maps of the study area with the assumption that an unvarying rate of change (Trend scenarios 2026 - 2036) will occur in the future.

Table 3-2: Validation analysis of the actual and simulated LU maps of 2016.

Agreement / Disagreement	Value	Value %
Agreement Chance	0.1279	12.79
Agreement Quantity	0.1035	10.35
Agreement Gridcell	0.6457	64.57
Disagreement Gridcell	0.0865	8.65
Disagreement Quantity	0.0364	3.64

Table 3-3: Accuracy assessment of the simulated Land-use map of 2016.

Index	Value
Kno	0.9020
Klocation	0.9153
KlocationStrata	0.9154
Kstandard	0.8754

Data Source: Values calculated by the CA-Markov model of IDRISITerrSet software.

The Trend scenario maintains the probabilities of change in Land-use that were predicted for the years 2026 and 2036 (see Figure 3-2 and Table 3-4). The “Best-case” scenario addresses the probabilities of change in LU towards a balanced scenario between the conservation of natural ecosystems and productive activities within the basin by the years 2026 and 2036 (see Figure 3-3 and Table 3-5). The “Worst-case” scenario addresses the probabilities of change in LU towards a scenario where extractive activities prevail and the productive areas in the watershed increase by the years 2026 and 2036 (see Figure 3-4 and Table 3-6). For this purpose, we added into the LUC analysis for the Best-Case and Worst-Case scenarios the constraint factors and suitability levels showed in Table 2-6 because the rate of change will vary about the Trend scenario.

About 0.28% of the total study area was urban in 2016 and is predicted to reach 0.47% and 0.68% by 2026 and 2036, respectively (Table 3-4). Also, agricultural areas will increase from 7.90% to 8.61% by 2036. In contrast, forest cover is predicted to decrease from 57.12% to 56.25% by 2036, and pasture cover will decline from 3.51% in 2016 to 3.02% and 2.60% by 2026 and 2036, respectively.

Table 3-4: LU cover area (%) of Trend Scenarios (2026 – 2036) and gain/loss (%) estimation.

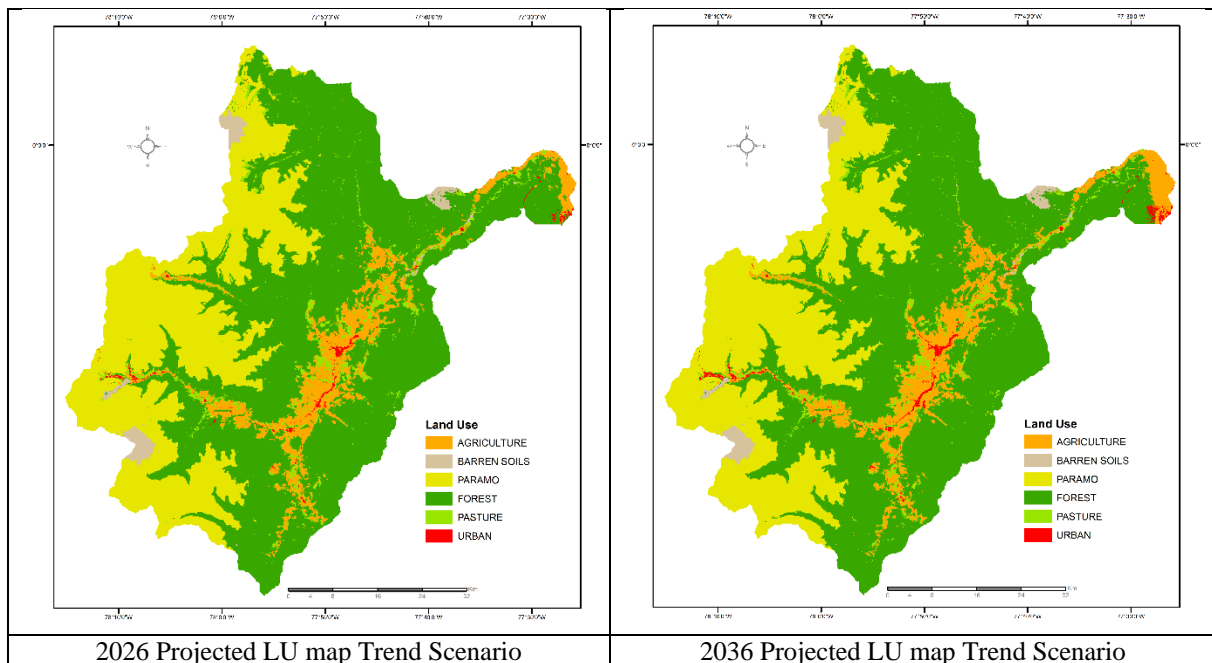
LU Cover	LU 2016 (%)	LU 2026 (%)	LU 2036 (%)	2016-2026	2026-2036	2016-2036
Agriculture	7.23	7.90	8.61	0.67	0.72	1.39
Barren Soils	1.50	1.50	1.50	0.00	0.00	0.00
Paramo	30.36	30.36	30.36	0.00	0.00	0.00
Forest	57.12	56.75	56.25	-0.37	-0.50	-0.87
Pasture	3.51	3.02	2.60	-0.49	-0.42	-0.92
Urban	0.28	0.47	0.68	0.19	0.21	0.40
Total	100	100	100			

Note: Positive values refer to projected gain (%) and negative values refer to projected loss (%).

The predicted urban development across the basin valley can be explained as a result of the migration processes to the catchment because of the Hydropower plant (HPP) construction. In 2008 the construction of the Coca Codo Sinclair HPP begins, and a process of migration to the study area is initiated from Ecuadorians inside the catchment, from other cities, and foreigners who start working in the HPP construction and associated sectors like restaurants, commerce, hotels, security, and transportation. (Sierra 2013; SENPLADES 2014).

The number of people dedicated to agricultural activities decreases, but agricultural areas increases. According to the National Planning Secretariat (SENPLADES 2014), there are 3000 new workers in the catchment, by the year 2014, and the central government assumes that 20% of these workers will stay in the area after the conclusion of the HPP in 2016. These workers also will bring their families, which implies that we will have an average of 4 people per household for every single worker that will stay in the study area.

Figure 3-2: Predicted LU maps of 2026 and 2036 Trend Scenario



More people implies more food needed and this carries agricultural areas expansion processes, which would explain the increase in the agricultural areas and the decrease in forest cover by 2026 and 2036. Since 2015, the local authorities inside the study area promote technology transfer for agroproduction activities and improvement programs for agricultural and livestock production. These programs lead to higher production in fewer areas

(GADs 2015), a process that can explain the decrease in Pasture areas by the years 2026 and 2036. Also, the authorities inside the catchment promote management programs, like environmental payments and environmental education, with the people to maintain and recover natural ecosystems in the watershed (Andean moorland/páramo and natural forest cover).

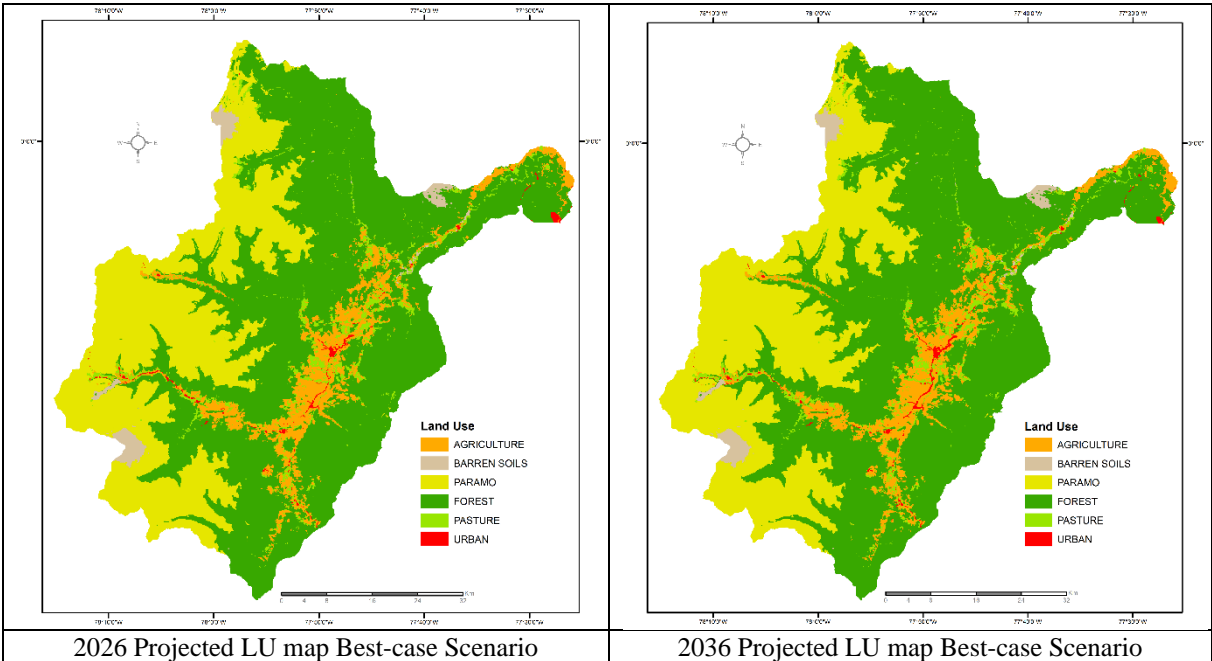
Table 3-5: LU cover area (%) of Best-Case Scenarios (2026 – 2036) and gain/loss (%) estimation.

LU Cover	LU 2016 (%)	LU BC 2026 (%)	LU BC 2036 (%)	2016-2026	2026-2036	2016-2036
Agriculture	7.23	7.31	7.44	0.08	0.14	0.22
Barren Soils	1.50	1.50	1.38	0.00	-0.12	-0.12
Paramo	30.36	30.45	30.47	0.09	0.03	0.11
Forest	57.12	56.98	56.90	-0.14	-0.08	-0.22
Pasture	3.51	3.30	3.33	-0.22	0.03	-0.18
Urban	0.28	0.46	0.48	0.19	0.01	0.20
Total	100	100	100			

Note: Positive values refer to projected gain (%) and negative values refer to projected loss (%).

As we said before, the “Best-case” scenario addresses the probabilities of change in LU towards a balanced scenario between the conservation of natural ecosystems and productive activities within the basin by the year 2026 and 2036 (see Figure 3-3 and Table 3-5). In that sense, the results show that by the year 2036 -Best-case scenario- we can expect an increase of 0.22% (1224 Ha) in agricultural areas in relation to the year 2016. Increase that can be explained due to the reduction of the barren soil area (-0.12%) by the year 2036 in the catchment. Having this in mind, we can argue that the agroproduction improvement programs would succeed in obtain higher production in fewer areas. That also can be seen in the pasture areas projections, where about 3.51% of the catchment area was pasture cover and is predicted to have a decrease of 0.22% and 0.18% by 2026 and 2036, respectively.

Figure 3-3: Predicted LU maps of 2026 and 2036 Best-case Scenario



For the natural covers/ecosystems in the catchment (Andean Páramo/Moorland and Natural Forest), the projections of the Best-case scenario show a relative state of preservation by the year 2036 in relation to the year 2016; with an increment of 0.11% for Paramo areas and a decrease of 0.22% in Forests areas in the catchment, projections that could be explained because of the successful implementation of the environmental payment programs and environmental education programs (GADs 2015) by the authorities inside the study area.

On the other hand, urban expansion processes in the catchment are predicted to reach 0.48% by the year 2036, which is less than 805 Ha in comparison with the Trend Scenario. To explain these projections, we can refer to the Territorial planning and urban expansion plans that the central government launched in 2015 (GADs 2015; SENPLADES 2014), with the main objectives of consolidation of the human settlements system, improvement of transportation infrastructure, and connectivity services.

The “Worst-case” scenario addresses the probabilities of change in LU towards a scenario where extractive activities prevail and the productive areas in the watershed increase by the year 2026 and 2036 (See Figure 3-4). Projection results of the Worst-case scenario (Table 3-6) reveal that the Urban areas will reach 0.46% and 0.67% in the study area by 2026 and 2036, respectively. This means that the Urban areas in the catchment will have an increase of 1571 Ha by 2036 in relation to the year 2016. Besides, Agricultural areas will increase from 29103 Ha (7.23%) to 44912 Ha (11.15%) by 2036; this could be explained in the sense that some of the Pasture areas turned into Agricultural lands and some into Urban areas and the agricultural areas expansion process in the catchment turned areas of Natural Forest into new Agricultural cover. In that sense, is expected that in this scenario, Forest areas in the catchment will have a decrease of 3.33% (-13407 Ha) by 2036, in relation to 2016.

Table 3-6: LU cover area (%) of Worst-Case Scenarios (2026 – 2036) and gain/loss (%) estimation.

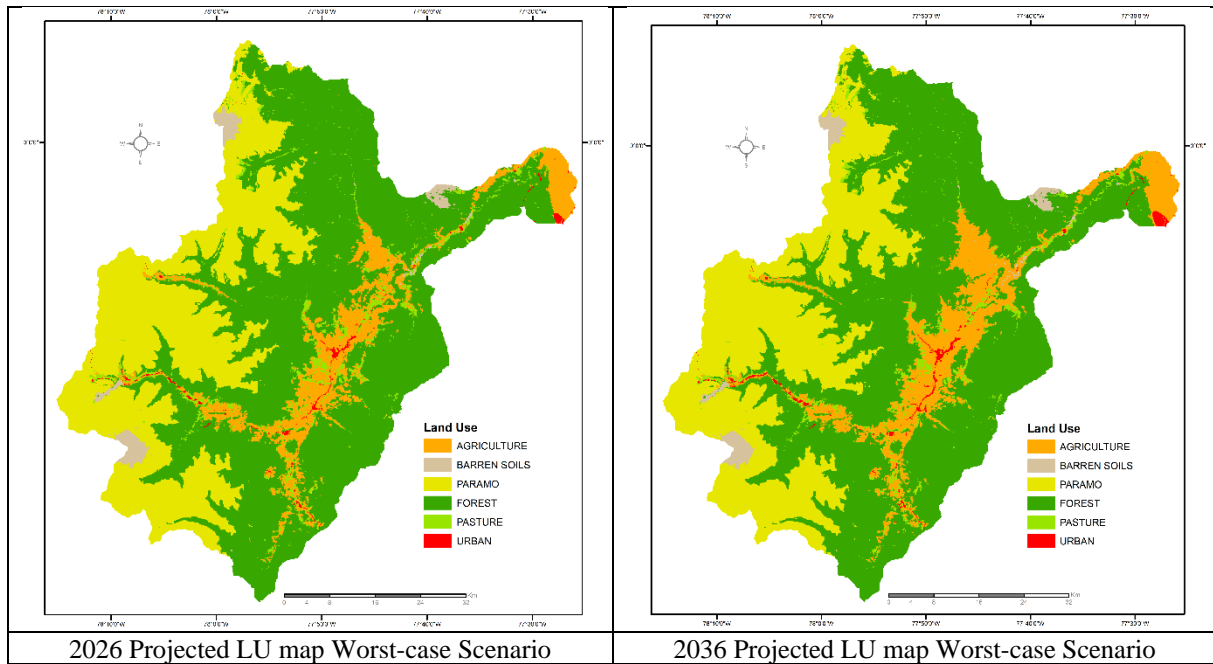
LU Cover	LU 2016 (%)	LU WC 2026 (%)	LU WC 2036 (%)	2016-2026	2026-2036	2016-2036
Agriculture	7.23	9.11	11.15	1.89	2.04	3.93
Barren Soils	1.50	1.50	1.50	0.00	0.00	0.00
Paramo	30.36	30.36	30.37	0.00	0.01	0.01
Forest	57.12	55.61	53.79	-1.51	-1.82	-3.33
Pasture	3.51	2.95	2.52	-0.56	-0.43	-0.99
Urban	0.28	0.46	0.67	0.19	0.20	0.39
Total	100	100	100			

Note: Positive values refer to projected gain (%) and negative values refer to projected loss (%).

Since the Andean Páramo/Moorland cover is not near to the agricultural or urban areas, we can expect that this land cover won't be reduced because of known socio-economic factors in the catchment, and the natural regeneration processes of this ecosystem will allow an area increment of 1.34% by 2036 in relation to 2016.

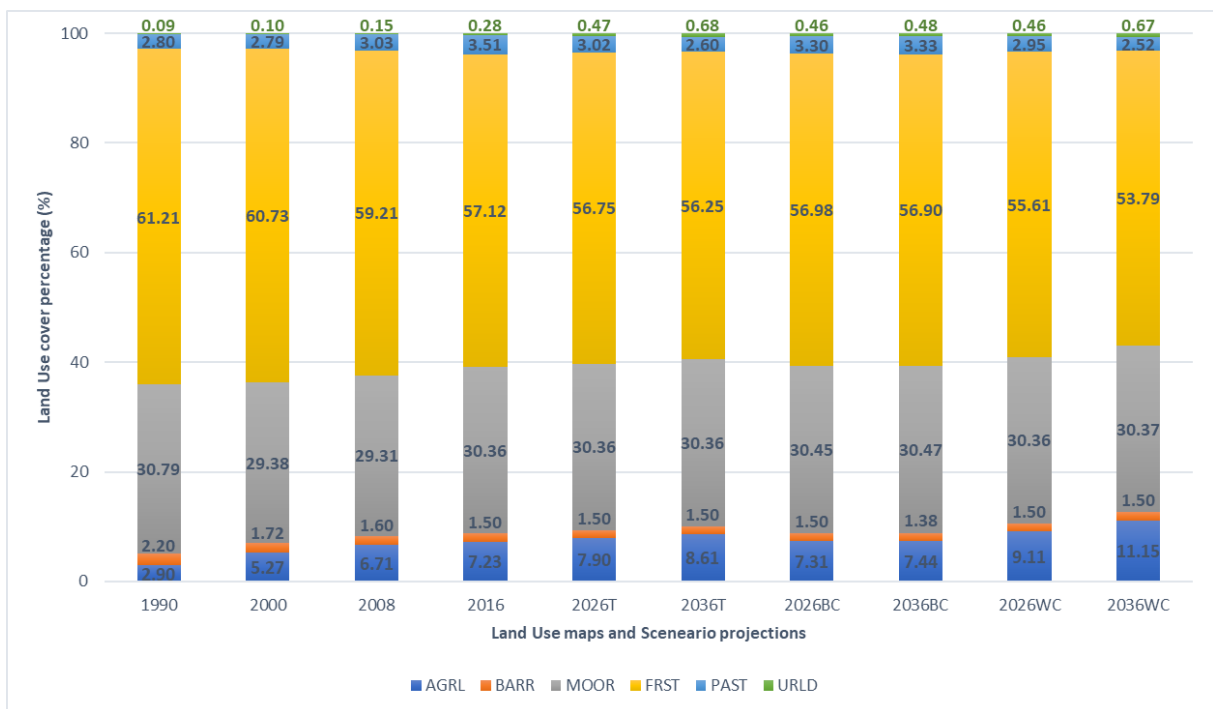
The worst-case scenario is an example of what could happen if all proposed Plans and Projects presented by the Government and local authorities (SENPLADES 2014; Sierra 2013; GADs 2015) of the study area fail in their implementation due to the uncertainties related to political will, anthropogenic pressures, conflicting interests among stakeholders and decision-makers, and population acceptance in the catchment.

Figure 3-4: Predicted LU maps of 2026 and 2036 Worst-case Scenario.



In Figure 3-5 the results show that over the years and LUC projected scenarios, the different LU cover percentages have been changed. The most significant changes are related to the Agricultural cover (AGRL) which has increased from 2.9% in 1990 to 7.23% in 2016. Also, for the LUC Trend scenarios, AGRL has increased its percentages in the study area from 7.9% to 8.61% for the years 2026 and 2036 respectively. For the Best-case scenarios of 2026 and 2036, the percentages show 7.31% and 7.44%. Finally, for the Worst-case scenarios the percentages have changed to 9.1% in 2026, and 11.15% in 2036.

Figure 3-5: Land-use coverage percentage according to the different LU maps and scenarios



Agriculture (AGRL), Barren soils (BARR), Andean Páramo – Moorland (MOOR), Natural Forest cover (FRST), Pasture areas (PAST), Urban areas (URLD). Trend Scenario (T), Best-case Scenario (BC), Worst-case Scenario (WC)

For the Forest cover in the catchment (FRST), the most significant changes are related to the Worst-case scenarios, where FRST decreases from 55.61% in 2026 to 53.79% in 2036, in relation to the total area of the catchment, which is 402736 hectares.

3.2.- Hydrological analysis and scenarios

3.2.1.- Trend analysis

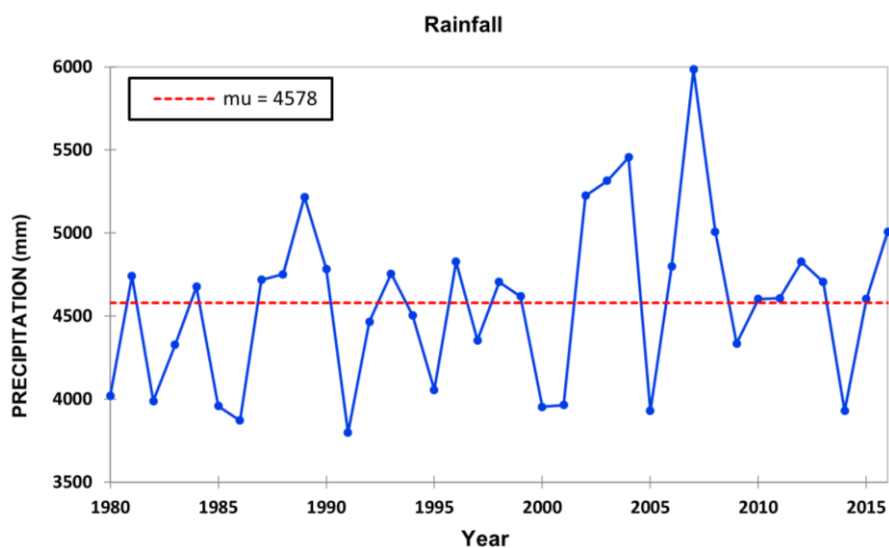
The Mann-Kendall (MK) (Mann 1945; Kendall 1970) trend test results, of the catchment station's time series, revealed No statistically significant Trends in the series. The computed probability value (p -value) was greater than the significance level ($\alpha = 0.05$). This means that No Trend existed in the precipitation and streamflow measurements in the study area, which agrees with the results obtained by Duque and Vazquez (2015), and Chunchu (2019).

The change-point analysis was carried out using the Pettitt tests. The tests showed that the magnitudes of trends are not statistically significant, as explained by the values of Sen's slope. In that regard, the Pettitt test could not detect any jump point in the data series. Therefore, it can be said that the analyses performed on the data sets of the study area have reported that there are no statistically significant trends, and no jump points have been identified in the data series. See Table 3-7 and Figure 3-6.

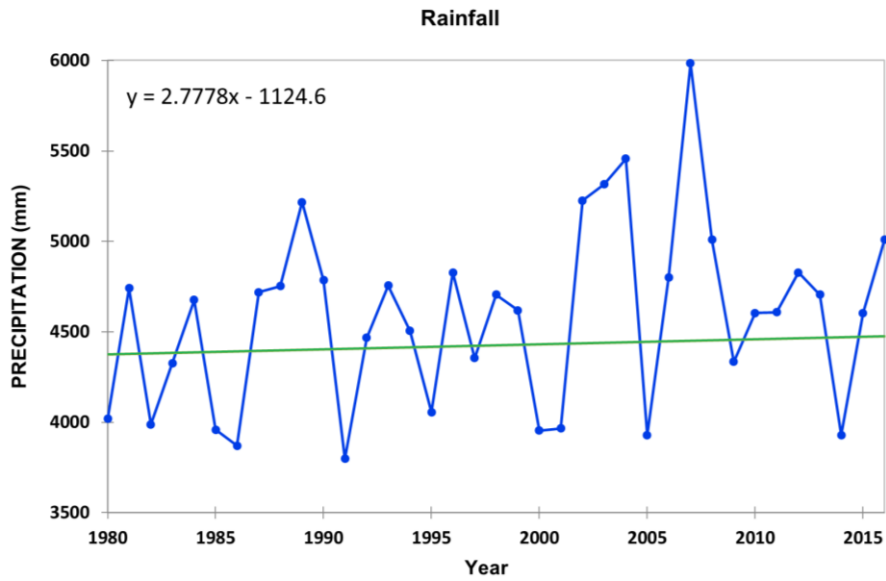
Table 3-7: MK and Pettitt tests for the study area's rainfall and streamflow data.

Variable	Time Scale	Mann-Kendall (MK)		Pettitt Test		Sen's slope
		Significance level (α)	p-value	Changepoint	Result	
Rainfall	Annual	0.05	0.143	No	No Change	10.01
Streamflow	Annual	0.05	0.258	No	No Change	12.12

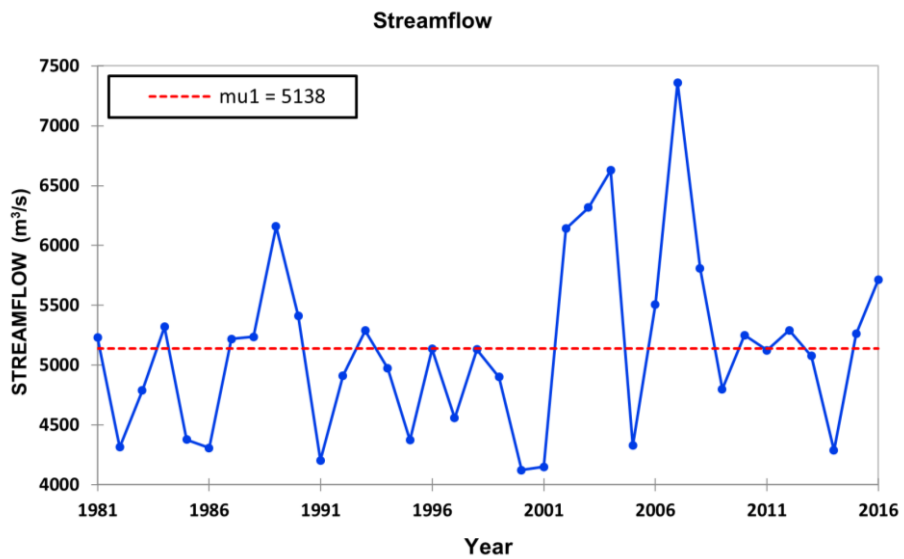
Figure 3-6: Pettitt homogeneity tests of hydrometeorological variables



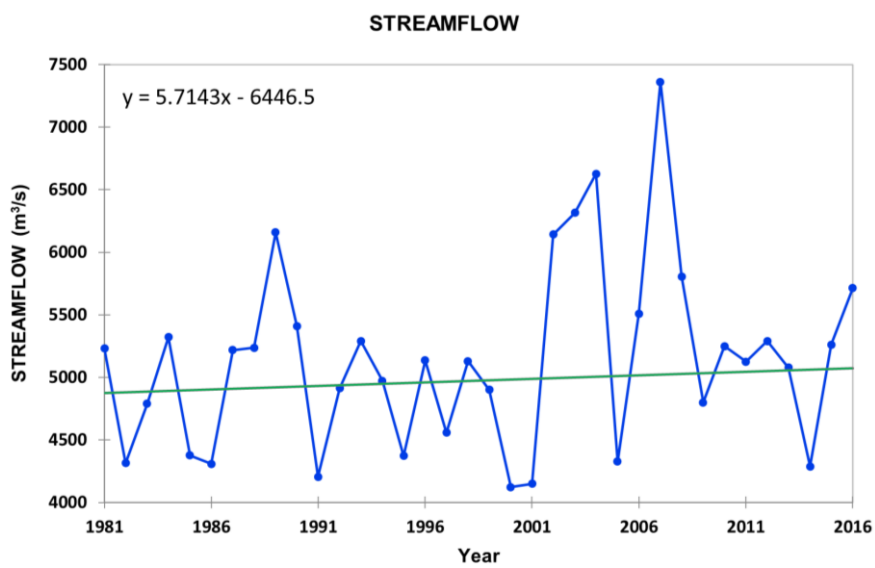
A)



B)



C)



D)

A) Annual rainfall, B) Annual streamflow, C) Linear trend of mean annual rainfall, D) Linear trend of mean annual streamflow.
Where μ is the mean annual precipitation (mm), and μ_1 is the mean annual flow (m³/s).

With these results in mind, we proceed to generate a new set of precipitation values for the 4 meteorological stations in the study area from 2017 to 2036 using an aleatory approach. This approach consists of select random years of daily precipitation values from the available data series (1980-2016) and uses them as new sets of daily precipitation values to fulfill the data of the new precipitation dataset (2017-2036); as an example, we randomly choose the year 2002 (all the daily values) and copy them as the values that correspond to the year 2017, then, we choose another year of daily precipitation values and copy them for the year 2018; we repeated that process until we completed the new precipitation dataset from 2017 to 2036. Once we had this new dataset, we incorporated this information inside the SWAT model to execute the hydrological simulation of the study area according to the projected scenarios (see Chapters 3.1 and 3.2.2).

3.2.2.- Results of the SWAT modeling

Sensitivity analysis

The sensitivity analysis (Table 2-8) shows that, in general, CN2, LAT_TTIME, ALPHA_BNK, CH_N2, CH_K2, and SOL_K are the most sensitive and important parameters for the catchment, as they show larger absolute values of *t*-statistics and their *p*-values are significant at 5% level of significance.

The most sensitive parameter is the SCS curve number at moisture condition II (CN2), followed by the Lateral flow travel time (LAT_TTIME). The high sensitivity regarding CN2 was expected as it is the primary parameter that influences the amount of runoff generated from HRUs (K. Abbaspour 2012). The Saturated soil hydraulic conductivity (SOL K) that controls the lateral flow contribution to streamflow is also a sensitive parameter in the catchment.

This should be expected because the study area is dominated by forested Land-use and permeable soils with steep topography, and lateral flow contribution is high in the mountainous parts of the study area. The Baseflow alpha factor for bank storage (ALPHA_BNK), is identified as a parameter with a third sensitivity rank. This could be partly explained due to the presence of “swamps”, small lagoons, and shallow aquifers in the high altitude areas of the watershed, which is the specific characteristics of the Andean páramo ecosystem (Nolivos et al. 2015). The channel Manning’s roughness coefficient (CH_N2) and the Effective hydraulic conductivity in the main channel (CH_K2) are found to be the 4th and 5th ranked parameters, respectively. Such parameters could affect the surface runoff processes, evapotranspiration, and streamflow (Leta et al. 2016).

Calibration, Validation, and Uncertainties

Once our sensitivity analysis showed the most sensitive parameters for streamflow in the catchment (Table 3-8), those parameters were used for the calibration and uncertainty analysis procedure using the SUFI-2 optimization algorithm, which is available in SWAT-CUP for SWAT model calibration procedures, as explained in Chapter 2.4.3.

The model was calibrated with four iterations, for each iteration, 1500 simulations were run as suggested in the literature (K. Abbaspour 2012). After each iteration, the ranges of the parameters were modified (normally narrowed down) according to both the new parameters suggested by the program (K. Abbaspour 2012; K. Abbaspour et al. 1997) and their reasonable physical limitations.

Table 3-8: Streamflow most sensitive parameters and final ranges for model calibration.

Parameter Description	Parameter Symbol	Sensitivity Ranking	Initial Range	Calibration Range Value
SCS runoff curve number.	CN2.mgt	1	-0.30 – 0.30	0.038353 - 0.243233
Lateral flow travel time.	LAT_TTIME.hru	2	0 – 180	23.371927 - 63.164673
Baseflow alpha factor for bank storage.	ALPHA_BNK.rte	3	0 - 1	0.315327 - 0.820572
Manning's "n" value for the main channel.	CH_N2.rte	4	0.01 – 0.3	0.086359 - 0.129659
Effective hydraulic conductivity in main channel alluvium.	CH_K2.rte	5	0.025 - 500	133.988220 - 195.154755
Saturated hydraulic conductivity	SOL_K().sol	6	0 - 2000	377.537109 - 781.288269

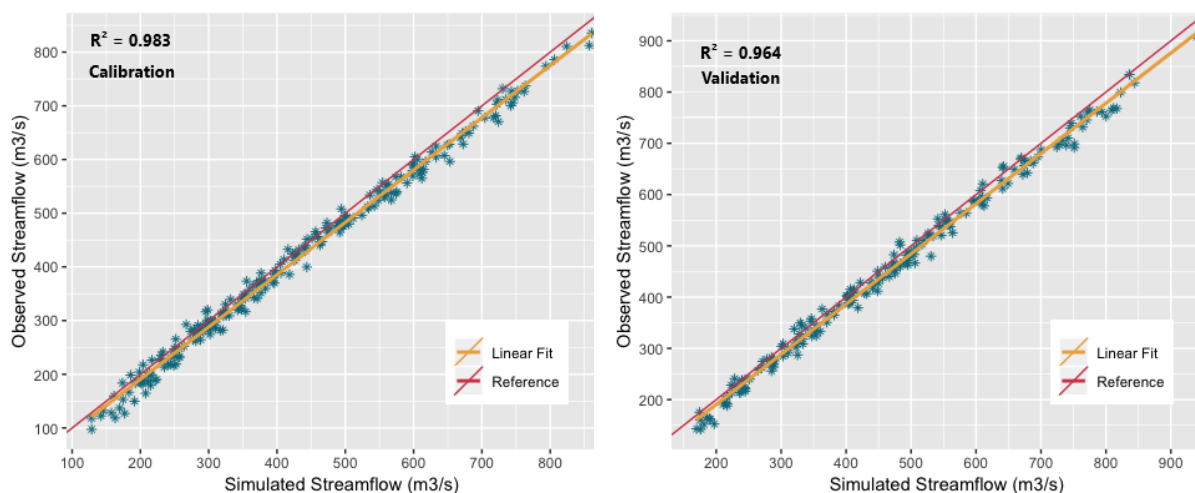
The final parameter ranges values for the model calibration can be found in Table 3-8. After that, the final ranges of the calibrated parameters were included in the validation analysis, and the model was validated with one iteration of 1500 simulations as suggested in the literature (K. Abbaspour 2012).

Table 3-9: Streamflow calibration, validation, and uncertainty analysis results.

Variable	Station	Procedure	Period	NSE	R ²	RSR	Performance	P-Factor	R-Factor
Streamflow	Low	Calibration	1982 - 2000	0.99	0.983	0.23	Very good	0.93	0.52
Streamflow	Low	Validation	2001 - 2016	0.98	0.964	0.27	Very good	0.91	0.55

The calibration procedure was executed using the monthly flow data measurements in the catchment of the Station Low from 1982 to 2000, and the validation procedure using the flow data from 2001 to 2016. Table 3-9 shows the summary of the performance and results for the monthly streamflow calibration, validation, and uncertainty analysis of the SWAT model in the catchment. Also, we find that the R² coefficient for calibration shows a value of 0.98 between the observed and simulated flow. The regression analysis of validation indicates an R² value of 0.96 between the observed and the simulated flow and it was executed with the data from 2001 to 2016. See Figure 3-7 for a graphical detail.

Figure 3-7: R² analysis of Observed vs. Simulated Flows (m³/s) for calibration and validation



The performance of the model for calibration and validation is rated according to (D. N. Moriasi 2007) for the NSE and RSR statistics (Table 2-9). For the calibration procedure, the NSE value shows 0.99, and the RSR value of 0.23. In that sense, the results showed that there was a very good agreement between the observed and simulated flows. The validation statistics also displayed a very good model performance with an NS value of 0.98 and an RSR value of 0.27.

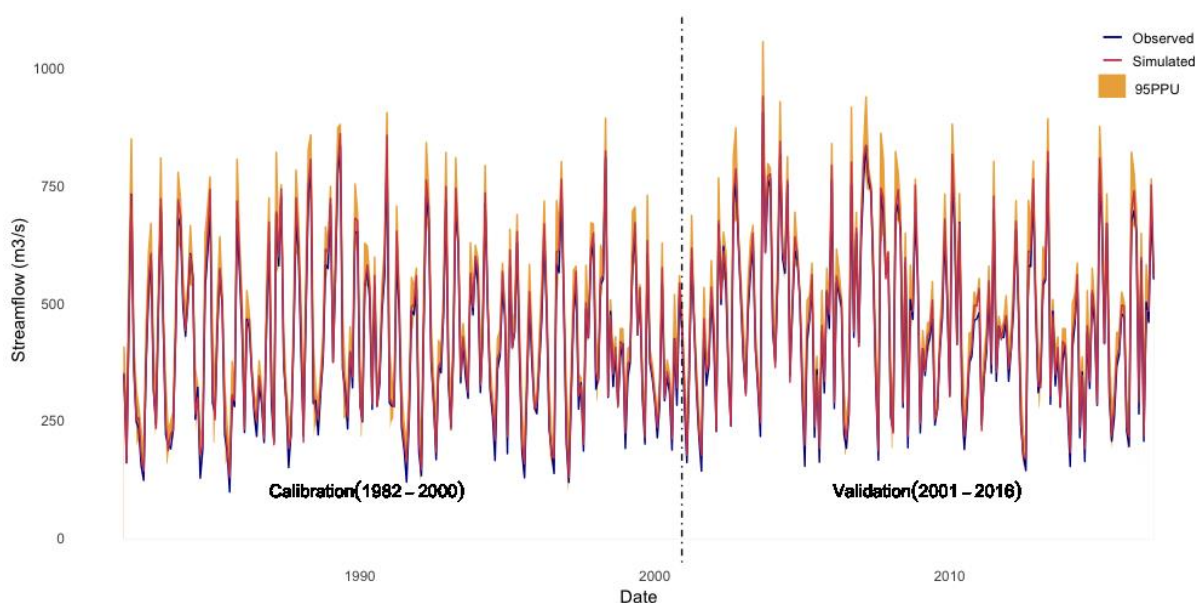
Also, during the calibration and validation procedures using the SUFI-2 optimization algorithm (Chapter 2.4.3), the uncertainty analysis was performed. The output uncertainty of the model, quantified by a 95% prediction uncertainty (95PPU, known as the *P*-factor) is calculated at the 2.5% and 97.5% levels of the cumulative distribution of an output variable (Jing Yang et al. 2012).

The *P*-factor ranges from 0 to 1. Another factor used to quantify the uncertainty analysis is the *R*-factor, which is the average width of the 95PPU band divided by the standard deviation of the observed values. The *R*-factor ranges from 0 to infinity. A *P*-factor of 1 and an *R*-factor of zero is a simulation that exactly corresponds to the measured data, which is an ideal but impossible case due to uncertainties from the measurements and other different sources (Abbas 2016).

SUFI-2 hence seeks to bracket most of the measured data with the smallest possible uncertainty band. A higher value of the *P*-factor can be attained at the cost of a higher *R*-factor. Thus, a balance must be achieved between the two factors, which will result in decreasing parameter uncertainty. When satisfactory values of these factors are attained, the reduced parameter uncertainty ranges are the preferred ones (K. Abbaspour 2012).

The uncertainty analyses with SUFI-2 for both the calibration and validation periods are shown in Figure 3-8. The blue line represents the Observed streamflow values, the red line represents the Simulated streamflow values, and the orange region is the 95% prediction band interval (95PPU) for the parameter set of the best estimation, and it covers most of the flows during the calibration and validation periods.

Figure 3-8: Uncertainty analysis with SUFI-2 algorithm for calibration and validation of streamflow

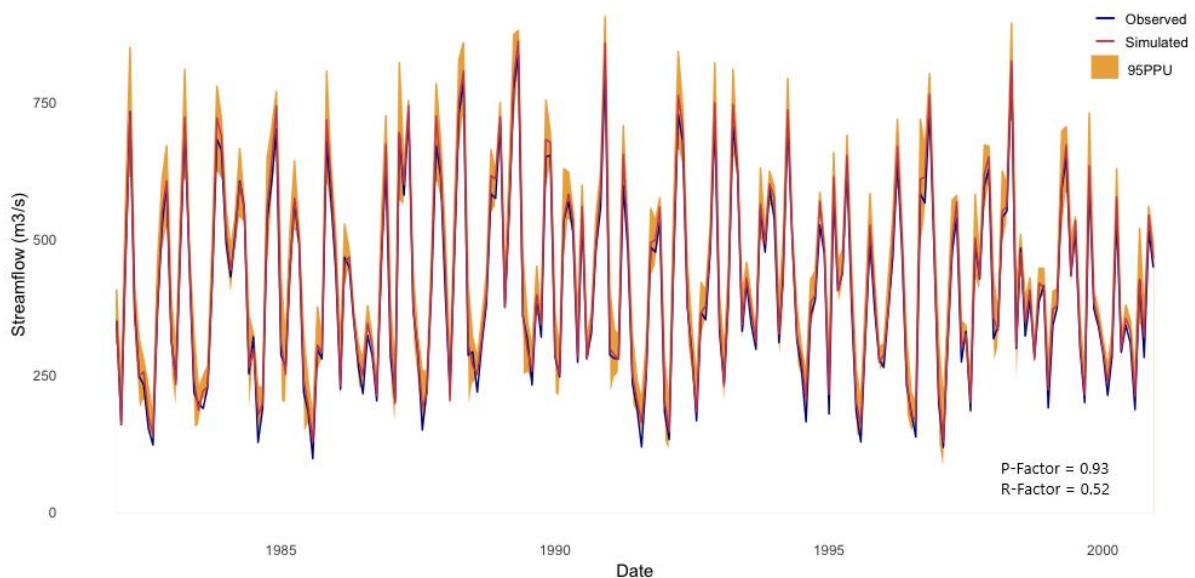


Parameter uncertainties also contribute to the prediction uncertainties of the models (K. Abbaspour et al. 2015). The prediction uncertainties discussed here only refer to the prediction uncertainties of streamflow, which are reflected by the values of the P-factor and R-factor of the model (Figures 3-9 and 3-10). As we can see in Table 3-9, in the final calibration procedure the model obtained a good prediction of uncertainties according to (K. Abbaspour 2012), capturing 93% of the observations, and having a 95PPU band narrower than 1 (R-factor of 0.52). For the validation procedure, the model shows also a good prediction of uncertainties, capturing 91% of the observed flows with an R-factor of 0.55.

The parameters that were used for the streamflow calibration are the most sensitive parameters after the sensitivity analysis (Table 3-8), those parameters are mainly the parameters that govern the surface runoff response, the subsurface response, and the response of the basin. Based on previous studies and literature (Mekonnen et al. 2018; Vilaysane et al. 2015; K. Abbaspour 2012), the performance of the model for the study area was very good during the calibration and validation procedures.

The sensitivity analysis indicates that the parameters of SCS runoff curve number (CN2), Lateral flow travel time (LAT_TTime), Baseflow alpha factor for bank storage (ALPHA_BNK), Effective hydraulic conductivity in main channel alluvium (CH_K2), Manning's "n" value for the main channel (CH_N2), and Saturated hydraulic conductivity (SOL_K) play important roles in the calibration and validation procedures of the model. P. Luo et al. (2011) report that CH_K2 and ALPHA_BNK parameters have a significant impact on the calibration procedure, and the sampling size of the validation iteration procedure (1500 simulations) with the SUFI-2 algorithm may also affect the model sensitivity, and with that some uncertainties.

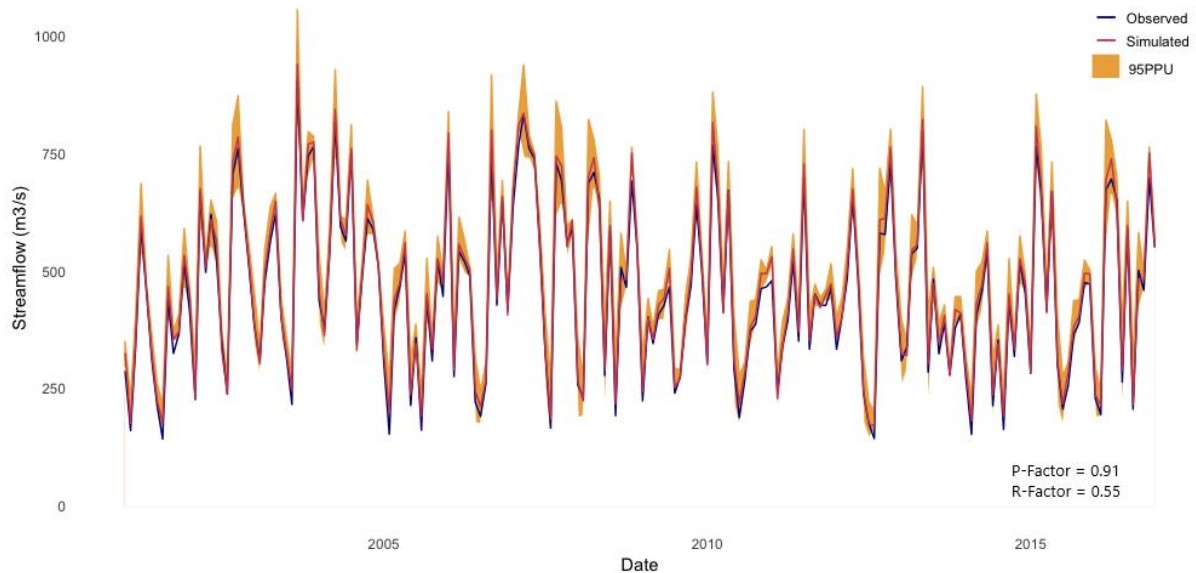
Figure 3-9: Calibration of the model and Uncertainty analysis of monthly streamflow (m³/s)



In Figures 3-9 and 3-10, we observe that there is a slight overestimation in some of the base flow values in our model, although these values were captured by the corresponding 95PPU band. That slight overestimation could be associated due to the uncertainties within the calibrated range values of our parameters like CN2 and SOL_K (K. Abbaspour et al. 2015; K. Abbaspour et al. 1997), and the rainfall variability inside the catchment (J. G. Arnold et al. 1998). The reduction in P-factor from 93% to 91% during validation was a clear indication of the uncertainties

from the different input variables, such as rainfall. The precipitation and streamflow data series used in this study may have involved some possible uncertainties like human and instrumental errors. Nevertheless, the overall result demonstrated that the model was able to simulate the hydrological characteristics of the catchment very well.

Figure 3-10: Validation of the model and Uncertainty analysis of monthly streamflow (m³/s).



With that being said, after the calibration and validation procedures, the model performs consistently well in reaching desirable uncertainties with satisfactory values of P-factor and R-factor. Considering the entire period (1982 to 2016), a good parameter uncertainty ranges prediction was achieved by using the SUFI-2 method for the model of the catchment.

3.2.3.- Effect of the different LUC scenarios on streamflow and water balance components

The calibrated and validated SWAT model, for the future scenario simulations, and its parameter settings for the study area was forced by weather data from the 2017 – 2036 period, keeping the DEM and soil data constant while changing only the projected LU maps from 2026, and 2036 for the Trend, “Best-Case”, and “Worst-Case” scenarios, as suggested by Hassaballah et al. (2017) and Mekonnen et al. (2018).

The simulation results of the calibrated and validated SWAT model reflect the effect of LUC (Trend, “Best-Case”, and “Worst-Case” scenarios) on streamflow and the water balance components in the study area for the years 2026 and 2036, see Table 3-10, Figure 3-11, and Figure 3-12.

The results from Table 3-10 indicated that SurQ/WYLD ratio changed from 62.6% to 64% and 65% for the LU Trend scenario 2026 and 2036 respectively. For the Best-case scenario, the ratio changed to 60.8% in 2026 and 60.5% in 2036, while for the Worst-case scenario, the ratio changed to 68.6% and 69.4% for the years 2026 and 2036 respectively. On the other hand, the GWQ/WYLD ratio changed from 20.9% to 20% and 19.4% for the Trend scenario (2026 – 2036), to 22.1% and 22.8% for the Best-case scenario (2026 – 2036), and, to 17.4% and 16.8% for the Worst-case scenario (2026 – 2036).

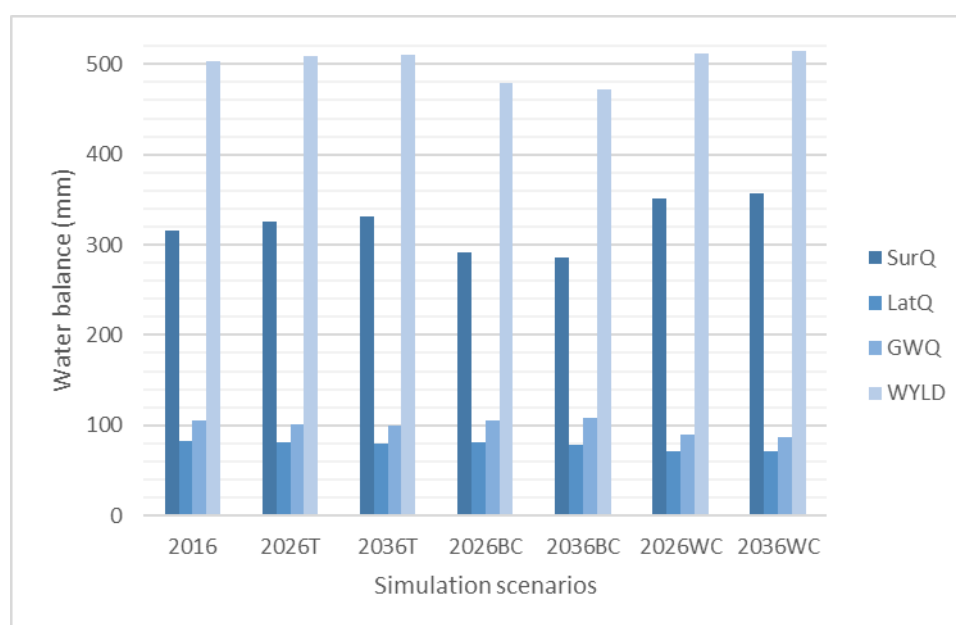
Table 3-10: Mean annual water-balance results, according to the different scenario simulations.

Variable	Units	Simulation / LU scenario						
		2016	2026T	2036T	2026BC	2036BC	2026WC	2036WC
SurQ	mm	315.2	325.7	332.0	291.1	286.0	351.7	357.0
LatQ	mm	83.2	81.3	79.3	81.8	78.9	71.2	70.6
GWQ	mm	105.1	101.6	99.3	105.7	107.7	89.4	86.5
WYLD	mm	503.5	508.6	510.6	478.7	472.6	512.3	514.1
ET	mm	90.8	88.7	88.5	91.1	93.3	86.5	87.3
SurQ / WYLD	%	62.6	64.0	65.0	60.8	60.5	68.6	69.4
LatQ / WYLD	%	16.5	16.0	15.5	17.1	16.7	13.9	13.7
GWQ / WYLD	%	20.9	20.0	19.4	22.1	22.8	17.4	16.8

Trend Scenario (T), Best-case Scenario (BC), Worst-case Scenario (WC). Surface runoff (SurQ), Lateral flow (LatQ), Baseflow (GWQ), Water yield (WYLD), Evapotranspiration (ET). WYLD = SurQ + LatQ + GWQ. WYLD (mm) is the total amount of water leaving the HRUs and entering the main channel.

The increment in SurQ/WYLD ratio and the reduction in the GWQ/WYLD ratio over the different scenarios could be attributed to the reduction in the natural forest coverage and the increment in agricultural lands in the catchment (Figure 3-5), especially in the Trend and Worst-case scenarios LU maps, relative to the 2016 LU map. Furthermore, deforestation may reduce the canopy's interception of the rainfall, decrease soil infiltration by increasing raindrop impacts, and reducing plant transpiration, which can significantly increase surface runoff, reducing the base flow (Huang, P. Wu, and Zhao 2013). As the results show in Table 3-10, the evapotranspiration change caused by the LUC is minimal, in that sense, the incidence of changes in evapotranspiration are not significant to explain surface runoff and baseflow changes in these simulations.

Figure 3-11: Mean annual water-balance of the study area with different LU simulation scenarios.



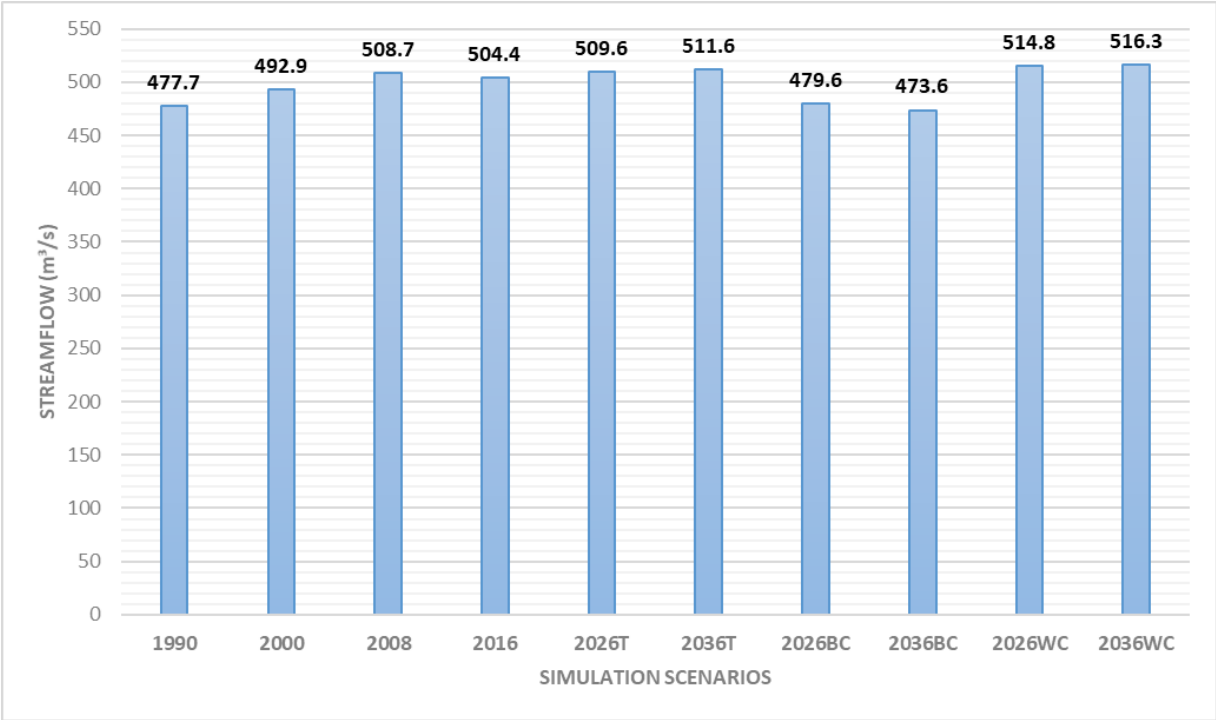
Trend Scenario (T), Best-case Scenario (BC), Worst-case Scenario (WC). Surface runoff (SurQ), Lateral flow (LatQ), Baseflow (GWQ), Water yield (WYLD).

Concerning the year 2016, the Best-case scenario results of 2026 and 2036 show a decreasing Surface runoff (SurQ / WYLD) ratio from 62.6% to 60.8% and 60.5% respectively, and an increasing base flow ratio (GWQ/WYLD) from 20.9% to 22.1% in 2026 and 22.8% in 2036. Those ratios could be explained because of the soil and water conservation measures established by the central and local government entities in the catchment that were

implemented during the Best-case LUC maps generation in Chapter 3.1. Measures like environmental payment programs for natural cover conservation, reforestation, regeneration, and agroforestry arrangements in pasture lands and agricultural areas in steep slopes all around the study area valley. As a result of those measures, the Natural Forest cover decreased by just 0.25% in 2026, and 0.39% in 2036, relative to 2016 (Figure 3-5). On the other hand, Agricultural areas increased by 1.1% in 2026, and 2.9% in 2023 in the catchment for the Best-case scenario.

The results in Figure 3-12 and Figure 3-13 indicate that streamflow is affected by LUC in the study area. The effect of LUC on the streamflow shows an increment in the Trend and “Worst-case” scenarios, and a decrement for the Best-case scenarios. In that sense for the Trend scenarios, the streamflow changed 1.04% in 2026, and 1.45% in 2036, relative to 2016. The Worst-case scenarios present changes in 1.02% for 2026, and 0.91% for 2036, in relation to the average daily streamflow of the Trend scenario. For the Best-Case scenarios, the streamflow changed to -5.89% and -7.4% in 2026 and 2036 respectively, in relation to the average daily streamflow of the Trend scenario.

Figure 3-12: Average daily streamflow (m³/s) that reaches the HPP at the catchment outlet by scenario.



Trend Scenario (T), Best-case Scenario (BC), Worst-case Scenario (WC)

The decrease in streamflow could be a result of Andean Páramo and Natural Forest cover maintenance or regeneration in the Best-case scenarios, and a small increment in agricultural lands (Figure 3-5). The study area Natural Forest cover and the Andean Páramo ecosystem have soils with high water retention capacity and high porosity, which delayed the release of water to the catchment outlet (Podwojewski and Poulénard 2000).

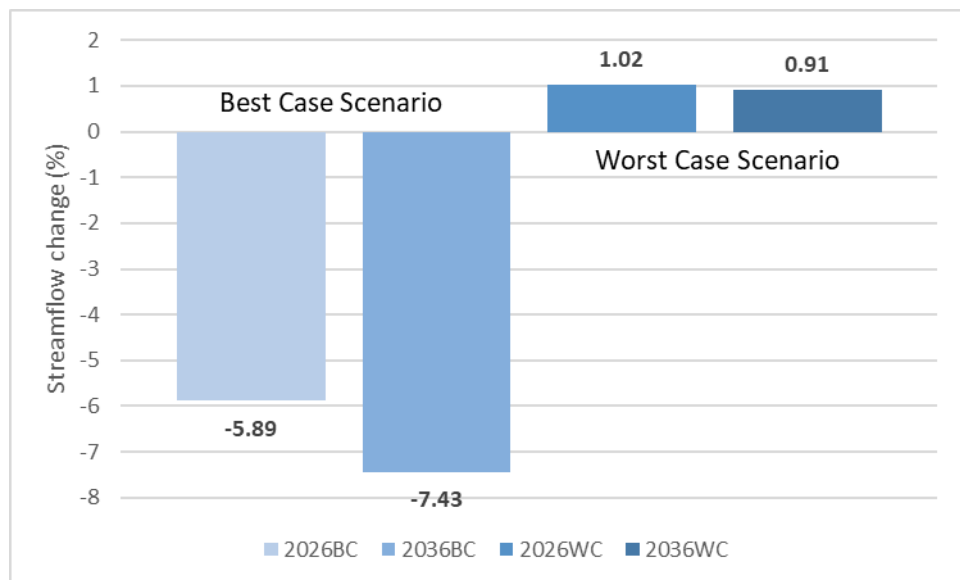
However, forest removal or degradation implies less infiltration due to a decrease in soil permeability, less interception of rainfall by the tree canopies, and thus more surface runoff and high flow peaks (Hassaballah et al. 2017; Mekonnen et al. 2018). In addition to the decreasing Forest cover for the Trend and Worst-case scenarios,

increases in Pasture areas in steep slopes decrease water infiltration due to soil compaction caused by grazing, which produces higher runoff and an increase in annual streamflow (Hassaballah et al. 2017).

Also, high runoff and streamflow values in the study area could be associated with the soil saturation and high moisture conditions of the soils of the catchment, where the average precipitation ranges are between 3500 to 6000 mm/year, the mean annual temperature - over space - is 19°C, the mean evaporation is 1200 mm/year, and the average annual relative humidity value in the catchment is 90% (ENTRIX S.A. 2009).

In the end, the results show (Figure 3-12 and Figure 3-13) that the average daily streamflow for the different simulation scenarios would be more than the 375 m³/s, which is the necessary daily flow for hydropower generation at the outlet of the watershed. With that being said, LUC in the study area would affect the average daily streamflow that reaches the watershed outlet under the proposed different scenarios by the years 2026 and 2036, but these changes in streamflow would not be a factor that could affect the electricity production of the Coca Codo Sinclair hydropower plant (CCS-HPP) in the study area in the future according to our results.

Figure 3-13: Changes on streamflow (%) by scenarios, relative to Trend Scenario 2026 and 2036



Best-case Scenario (BC), Worst-case Scenario (WC)

Nevertheless, bigger soil loss rates from agricultural areas and an increasing amount of sediments that reach the HPP at the catchment outlet would be factors that could affect Hydropower production in the future. LUC in watersheds would have a significant impact on soil losses, especially in agricultural areas (Buytaert, Iñiguez, and Bièvre 2007).

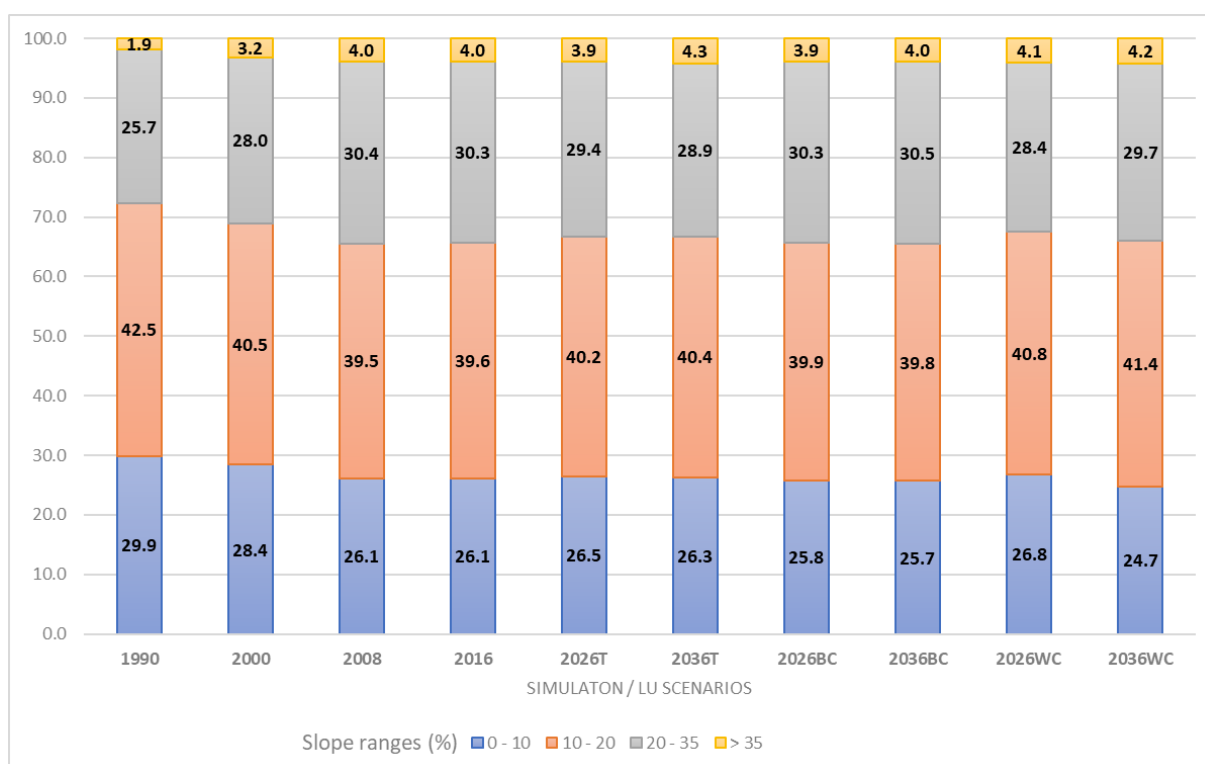
Natural forest cover converted into agricultural and pasture lands with steep slopes, and combined with high surface runoff rates are factors that trigger erosion processes with high soil losses rates in tropics (Huang, P. Wu, and Zhao 2013; Worku, Khare, and Tripathi 2017; Nie et al. 2011). In addition to the natural erosion processes, soil losses associated with surface runoff can be accelerated by human practices like agriculture, deforestation, and urban development (El-Swaify, Dangler, and Armstrong 1982).

Table 3-11: Agricultural areas (Ha and %) vs. Slope ranges, according to the LU scenario simulations.

SLOPE	AGR L 90	AGR L 00	AGR L 08	AGR L 16	AGR L 26T	AGRL 26BC	AGRL 26WC	AGR L 36T	AGRL 36BC	AGRL 36WC
0 - 10	3483	6029	7057	7606	8412	7595	9819	9130	7572	11097
10 - 20	4954	8594	10668	11526	12780	11752	14970	14026	11742	18577
20 - 35	2994	5939	8228	8821	9358	8917	10415	10043	8975	13360
> 35	225	671	1079	1150	1251	1161	1502	1496	1178	1881
Total	11656	21233	27032	29103	31802	29425	36706	34695	29467	44915
SLOPE	AGR L 90	AGR L 00	AGR L 08	AGR L 16	AGR L 26T	AGRL 26BC	AGRL 26WC	AGR L 36T	AGRL 36BC	AGRL 36WC
0 - 10	29.9	28.4	26.1	26.1	26.5	25.8	26.8	26.3	25.7	24.7
10 - 20	42.5	40.5	39.5	39.6	40.2	39.9	40.8	40.4	39.8	41.4
20 - 35	25.7	28.0	30.4	30.3	29.4	30.3	28.4	28.9	30.5	29.7
> 35	1.9	3.2	4.0	4.0	3.9	3.9	4.1	4.3	4.0	4.2
Total	100.0									

Agricultural areas (AGRL), Trend Scenario (T), Best-case Scenario (BC), Worst-case Scenario (WC)

Figure 3-14: Agricultural areas (%) vs. Slope ranges in the catchment by scenario simulations.



Trend Scenario (T), Best-case Scenario (BC), Worst-case Scenario (WC)

In Table 3-11 and Figure 3-14, it can be seen that agricultural areas have increased over the different years and scenario simulations, both in their total number, as well as in the percentage within each slope range in the watershed. From 1990 to 2016, agricultural areas increased by 150%. A fact that must be taken into account when planning actions and measures for the proper management of the basin resources is that the amount of hectares on slopes greater than 20% and 35% has been gradually increasing. In 1990 the percentage of agricultural areas in slopes between 20 – 35% was 25.7% while in 2016 this percentage changed to 30.3%, which represents an

increment of 5800Ha. The same case can be seen in agriculture areas on slopes greater than 35%, with an increment of 925 Ha by the year 2016 in relation to 1990.

The results show increments in agricultural areas for every LU map and scenario simulation and slope range in the catchment, in relation to 1990. In the particular case of the Best-case scenarios (2026 – 2036), increments in agriculture areas, in total and according to the different slope ranges, are not that substantial as the increments that can be expected at the Trend or the Worst-case scenarios.

Table 3-12: Agricultural area's changes (%) vs. Slope ranges, regarding 2016 by scenario simulations.

SLOPE	2026 T	2026 BC	2026 WC	2036 T	2036 BC	2036 WC
0 - 10	10.6	-0.1	29.1	20.0	-0.4	45.9
10 - 20	10.9	2.0	29.9	21.7	1.9	61.2
20 - 35	6.1	1.1	18.1	13.8	1.7	51.5
> 35	8.8	1.0	30.5	30.0	2.4	63.5
Total Change	9.3	1.1	26.1	19.2	1.2	54.3

Trend Scenario (T), Best-case Scenario (BC), Worst-case Scenario (WC)

In Table 3-12, it can be seen that for the Best-case scenarios, the expected change in the total of agricultural lands in relation to 2016 is 1.1% for 2026 and 1.2% for 2036. On the other hand, for the Worst-case scenarios, agricultural areas increased from 26.1% in 2026 to 54.3% in 2036, in relation to 2016. Here the situation becomes worrying because increases in agricultural areas in slopes greater than 35% reach 30.5% (1500 Ha) in 2026 and 63.5% (1900 Ha) in 2036, in relation to 2016. For the Trend scenarios, the results show a total increase of 9.3% and 19.2% for the years 2026 and 2036 respectively, in relation to 2016.

As already indicated in Tables 3-11 and 3-12, and Figures 3-5 and 3-14, agricultural land and urban areas were continuously increasing at the expense of other LUC covers (Forest, Páramo, and Barren soils) during 1990 – 2016, and in our LUC projection scenarios. Inside Table 3-13, it can be seen the average annual Soil Loss [SL] (T/Ha) and Surface runoff [SurQ] (mm) in the agriculture areas of the catchment with the different slope ranges. Also, it is shown the Regression analysis (R^2) results of the correlation between SurQ and SL.

The LUC between all the years and scenario simulations from forest, barren soils, and Andean Páramo into Agricultural lands, has contributed to increasing the surface runoff (SurQ) and Soil losses (SL) as shown in Table 3-13. Between 1990 and 2016, an increase in both SL (from 23.7 to 31.6 T/Ha/year) and SurQ (from 161.3 to 171.3 mm/year) could be explained by the decrease of natural forest areas into agricultural lands. During this period, land redistribution policies of the Ecuadorian Amazon region required the farmer to prove that the land was being used and producing to legalize land ownership (Sierra 2013), in that sense, farmers transform forest areas inside their properties into agricultural and pasture lands. The year 2008 was atypical in terms of rainfall within the basin, reaching 8000 mm, exceeding by almost 2000mm the average annual rainfall in the basin; generating a significant increase in the SL rates and SurQ in agricultural lands all over the catchment.

According to the LUC simulations, for the Trend scenario, could be expected a slight increment in SL and SurQ in 2036 in relation to 2016, behavior that could be explained due to the actual watershed management active programs in the study area, such as reforestation and soil conservation programs, and forestry arrangements in steep slopes agricultural areas. For the Best-case scenarios, it could be expected that SL and SurQ may have a

reduction in 2026 and 2036. The results show that in 2026 agricultural areas would have SL of 20.7 T/Ha with an average SurQ of 163.5 mm. In 2036 SL in agricultural areas would reach 22.1 T/Ha and an average SurQ of 160mm. These changes could be explained because of the watershed management measures and programs implemented in the catchment by the Central and local government entities, where forest cover has been preserved, and the agricultural lands had a minimum increment in relation to 2016 (Table 3-12).

Table 3-13: Soil Loss -SL- (T/Ha), Surface runoff -SurQ- (mm), and Regression analysis correlation (R²).

	1990			2000		
<i>SLOPE</i>	<i>SL (T/Ha)</i>	<i>SurQ (mm)</i>	<i>R²</i>	<i>SL (T/Ha)</i>	<i>SurQ (mm)</i>	<i>R²</i>
0-10	8.3	161.2	0.95	10.1	163.6	0.87
10-20	18.2	163.1	0.94	23.6	165.6	0.91
20-35	27.4	162.2	0.85	35.5	164.3	0.94
> 35	40.7	159.8	0.9	47.5	161.3	0.89
<i>Av. Total</i>	23.7	161.6		29.2	163.7	
Year	2008			2016		
<i>SLOPE</i>	<i>SL (T/Ha)</i>	<i>SurQ (mm)</i>	<i>R²</i>	<i>SL (T/Ha)</i>	<i>SurQ (mm)</i>	<i>R²</i>
0-10	13.4	192.1	0.91	11.0	171.3	0.90
10-20	29.1	191.1	0.91	24.4	175.1	0.89
20-35	45.2	195.0	0.87	36.9	171.5	0.92
> 35	70.0	194.2	0.95	54.1	167.3	0.95
<i>Av. Total</i>	39.4	193.1		31.6	171.3	
	2026 Trend			2036 Trend		
<i>SLOPE</i>	<i>SL (T/Ha)</i>	<i>SurQ (mm)</i>	<i>R²</i>	<i>SL (T/Ha)</i>	<i>SurQ (mm)</i>	<i>R²</i>
0-10	10.5	174.2	0.91	12.4	176.4	0.95
10-20	20.7	178.1	0.93	22.7	178.7	0.89
20-35	33.1	172.9	0.87	37.4	175.5	0.90
> 35	51.3	169.8	0.85	54.0	171.6	0.90
<i>Av. Total</i>	28.9	173.8		31.6	175.5	
	2026 BC			2036 BC		
<i>SLOPE</i>	<i>SL (T/Ha)</i>	<i>SurQ (mm)</i>	<i>R²</i>	<i>SL (T/Ha)</i>	<i>SurQ (mm)</i>	<i>R²</i>
0-10	10.4	165.9	0.9	8.7	161.4	0.86
10-20	23.3	163.0	0.89	19.0	162.9	0.92
20-35	34.6	168.5	0.87	28.7	159.8	0.90
> 35	42.3	156.6	0.94	32.1	155.9	0.89
<i>Av. Total</i>	27.7	163.5		22.1	160.0	
	2026 WC			2036 WC		
<i>SLOPE</i>	<i>SL (T/Ha)</i>	<i>SurQ (mm)</i>	<i>R²</i>	<i>SL (T/Ha)</i>	<i>SurQ (mm)</i>	<i>R²</i>
0-10	11.6	186.2	0.91	14.5	190.3	0.87
10-20	23.5	183.1	0.91	29.5	193.1	0.89
20-35	35.9	189.5	0.9	48.2	195.5	0.91
> 35	54.4	183.8	0.92	73.8	194.3	0.90
<i>Av. Total</i>	31.3	185.7		41.5	193.3	

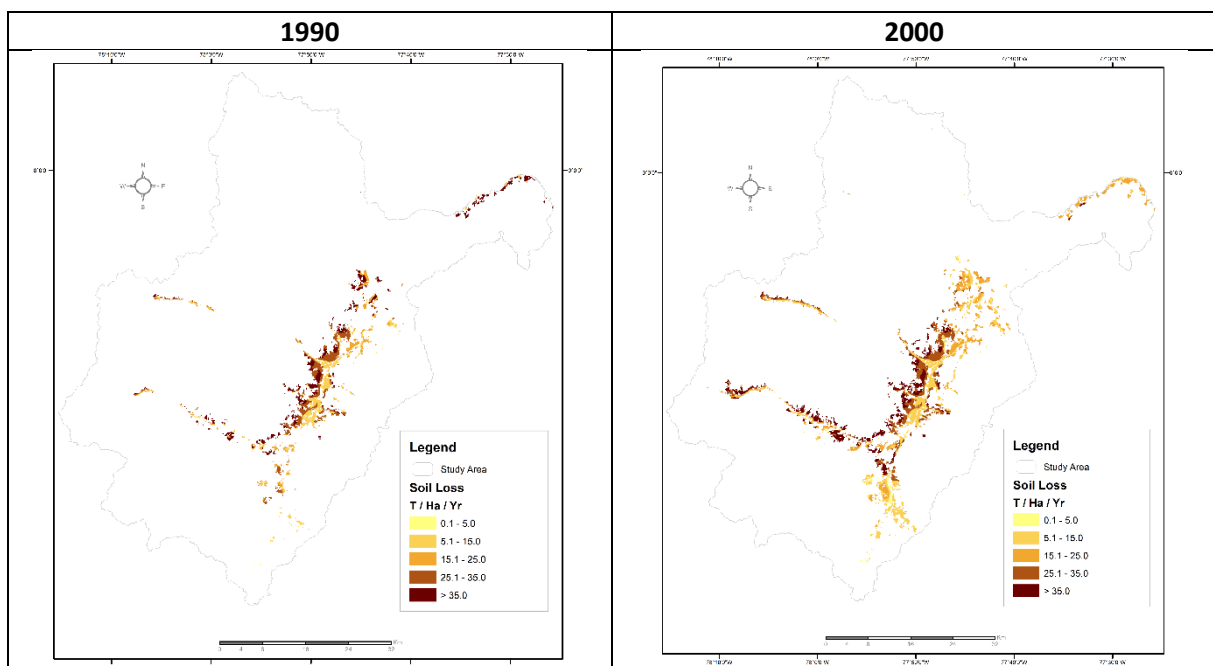
Note: Significance level $p < 0.001$. Trend Scenario (T), Best-case Scenario (BC), Worst-case Scenario (WC)

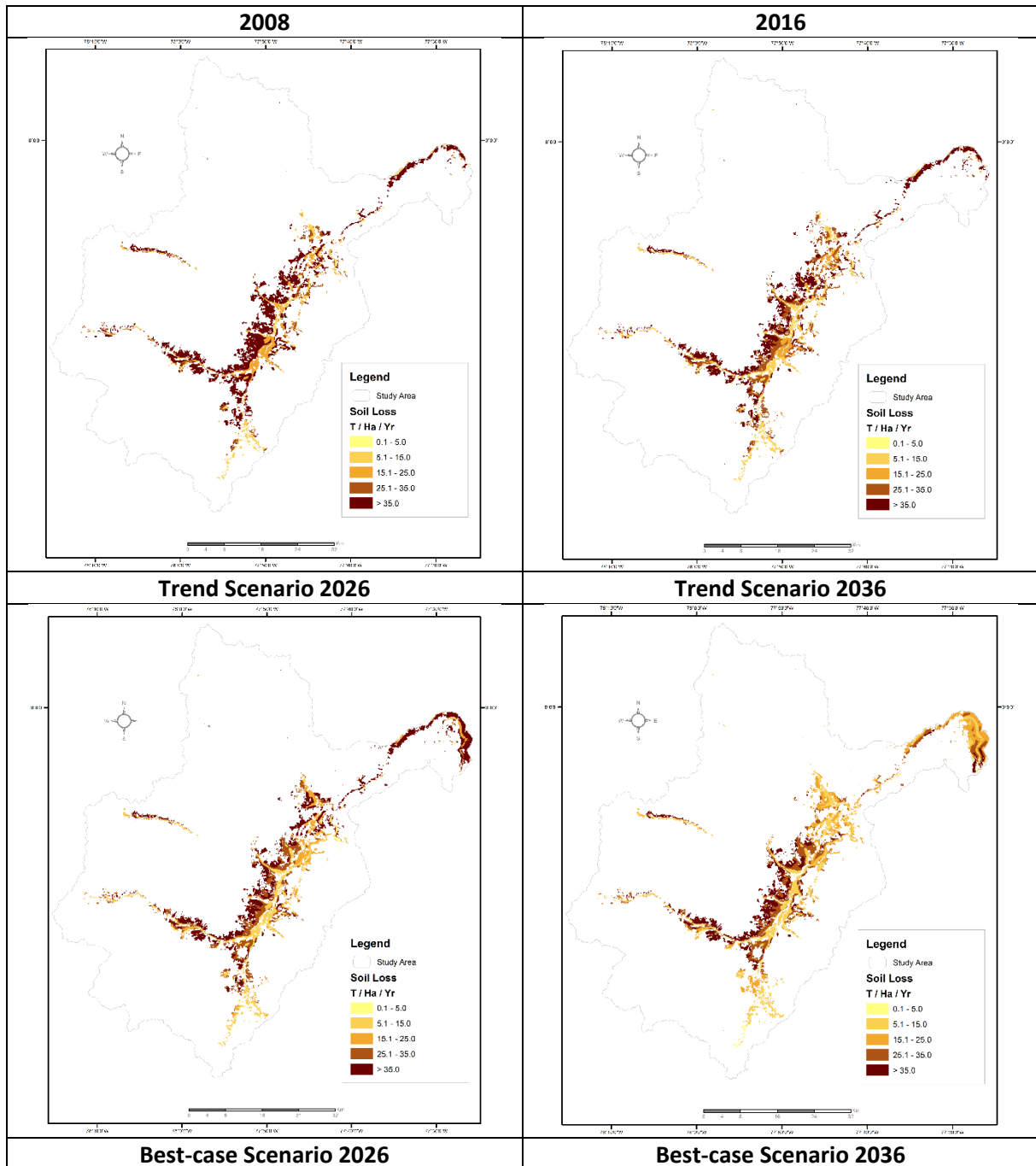
At the Worst-case scenario simulation results, it can be seen that SL and SurQ have a considerable increment in agricultural areas, both in total and according to the slope ranges in relation to 2016 in the catchment. In that regard, under the WC scenario 2026, the amount of SL would reach an average of 31.3 T/Ha with a SurQ of 185.7 mm. By 2036, the average SL would reach 41.5 T/Ha with a SurQ of 193.3. Those increments could be explained because of the progressive expansion of the agricultural areas. The conversion of forest land into agricultural lands can cause increases in surface runoff and sediment yields under different slope conditions (Nie et al. 2011; Nath et al. 2020).

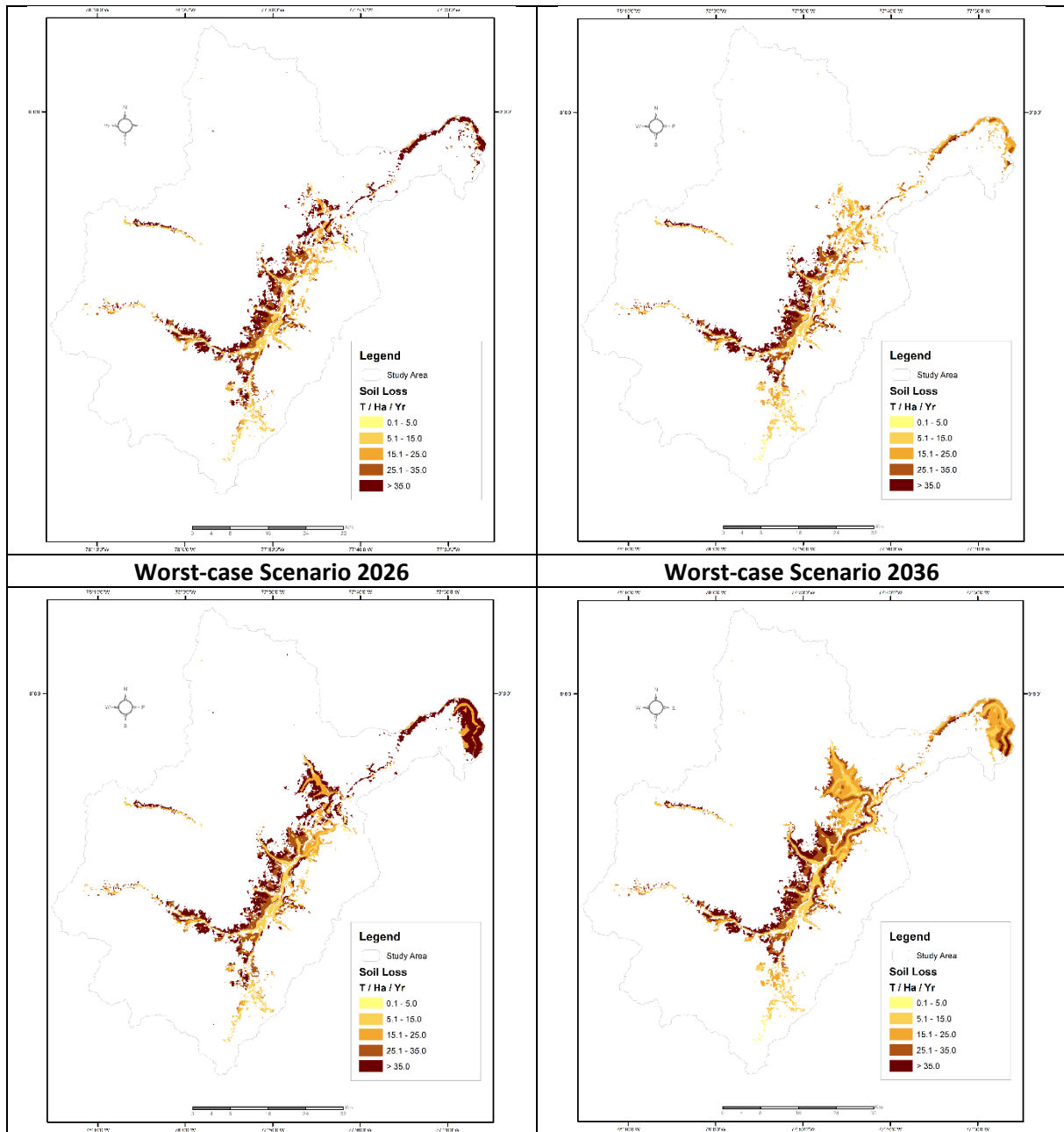
Therefore, it can be concluded that the spatial and temporal distribution of LU cover governs runoff amount in the catchment, as well as contribute to the change in the soil losses and sediment yield. In the end, the results indicate that surface runoff and soil losses are sensitive to LUC in the catchment. To demonstrate that, positive correlations between surface runoff and soil losses were found in the agricultural areas of the catchment. The correlations were determined for all simulations including the LUC projections information and the slope ranges of the agricultural areas. In that sense, the results (Table 3-13) show that Soil Losses in the agricultural areas of the catchment increases when Surface Runoff is increased. Also, the SWAT model results of the study area presented Soil Loss values that agree with the values from (Laraque et al. 2004), where the author reports specific Soil Losses of 12.69 T/Ha/year at the Coca River watershed from 2001 to 2002.

Nevertheless, as a matter of principle, it would be desirable to avoid soil erosion under any circumstances. In reality, however, a certain degree of soil loss must be accepted as normal, for example, by the natural forces of geological erosion in undisturbed lands (El-Swaify, Dangler, and Armstrong 1982). In addition to the natural erosion processes, anthropogenic factors such as changes in Land-use can accelerate soil loss rates in a catchment (Huang, P. Wu, and Zhao 2013). In setting tolerable limits for soil loss, several factors have been considered (such as soil regeneration rates, weather, topography, among others) to establish tolerance limits of soil loss in agricultural lands in the tropics (El-Swaify, Dangler, and Armstrong 1982). In that regard, Nunes et al. (2012) calculated tolerable soil loss limits ranging from 15 – 25 Tm/ha/yr for agricultural lands in the tropics.

Figure 3-15: Soil Loss (T/Ha/Yr) in agricultural areas according to the scenario simulations.







Results in Table 3-13 and Figure 3-15 show that the average soil loss rates in agricultural lands of the catchment with a slope range between 0 -20%, are inside the tolerable soil loss limits for tropics. Also, agricultural areas with slope ranges above 20% exceed the tolerable soil loss rates ranges, this means that these rates could lead to the reduction of the fertility of the soils of the agricultural areas (Lambin and Geist 2006; Juckem et al. 2008). Thus, a greater agricultural area is required to produce the same amount as before, in this way, LUC processes are intensified, in particular, changes from natural forest cover to agricultural and pasture areas in steep slopes (C. He et al. 2006), and with that, the natural balance of the watershed would be affected as we have seen at the study area's SWAT model results for the different land-use scenarios.

CHAPTER 4.- Summary, Conclusions, and Recommendations

This study provides a better understanding and substantial information about how land-use changes could affect streamflow and water-balance components separately and jointly, which is useful for basin-wide integrated water resources management. However, in this study, it should be considered that during the different analyses there are some limitations related to uncertainties driven by processes not accounted for by the model, and processes unknown to the modeler.

In that sense, the available land use and soil maps used in this study could have contributed to some degree to uncertainties in the results during the modeling procedures, because the scale of the maps might be too coarse. Likewise, the upper Coca River basin is a tropical watershed and is exposed to high spatial variability in rainfall distribution that cannot be captured entirely using only 4 meteorological stations, that limitation could have also contributed to some degree to uncertainties during the hydrological analysis. Also, the presence of an active volcano (The Reventador) inside the basin could contribute to some degree to uncertainties during the hydrological modeling procedures; landslides can produce large amounts of sediments, especially landslides triggered by volcanic activity.

To reduce this kind of uncertainties that came from our study limitations, land use, and soil optimization studies that can improve the accuracy of the land-use change projections and hydrologic simulations are necessary. Likewise, soil erosion processes research and sediment transport measurements that can reduce uncertainties during the hydrological analysis are recommended in the basin. Also, it is necessary the implementation of a representative meteorologic station network inside the basin, to overcome the rainfall spatial variability distribution limitations.

The objective of this study was to understand how the future changes in land use of the study area, under different projected scenarios, would affect the hydrological components of the catchment from an Integrated Water Resources Management (IWRM) point of view, and in particular on the streamflow that reaches the outlet of the watershed with hydropower generation purposes. To complete this objective, the combined Markov and Cellular Automata model (CA-Markov, available in TerrSet software) was used for the Land-use change dynamics analysis and scenario projections of the catchment. To understand the long-term variations of rainfall and streamflow in the catchment the MK and Pettitt tests statistical techniques were used. Finally, to assess the effects of the different LUC scenarios on the hydrology of the catchment, the semi-distributed Soil and Water Assessment Tool (SWAT model) was used.

For assessing the future changes in land cover of the study area, three Land-use maps were used as base maps (2000, 2008, and 2016); After the validation of the model, the accuracy assessment shows that the results are reliable. With that information, future land-use change scenarios (Trend, Best-case, and Worst-case) were projected for the years 2026 and 2036 using the CA-Markov model. The projected land-use maps of the study area showed that the dominant processes between all scenarios are a decrease in natural forest cover and an increase in agricultural and urban areas.

Relatively to the year 2016, the forest cover decreased by 0.6% (2026) and 1.5% (2036) for the Trend scenario. The Best-case scenario results show that the forest cover decreased by 0.2% and 0.4% in 2026 and 2036 respectively. For the Worst-case scenario, forest cover decreased by 2.6% in 2026 and 5.8% in 2036. Increases in

agricultural areas are expected by 9.3% in 2026, and 19.2% in 2036 for the Trend scenario; 1.1% in 2026, and 3% in 2036 for the Best-case scenario; and 26.1% in 2026, and 54.3% in 2036 for the Worst-case scenario. Urban areas increments for the Trend scenario are expected by 69% in 2026, and 143.5% in 2036; 67.3% in 2026, and 71.6% in 2036 for the Best-case scenario; and for the Worst-case scenario, increments are expected by 67.3% in 2026, and 140% in 2036. Forest cover reductions are probably related to agricultural and urban areas expansion due to socio-economical processes between the different future scenarios. Urban areas expansion occurred mostly near road networks at the catchment valley.

The MK and Pettitt tests showed no statistically significant change in the annual rainfall over the study area between 1980 and 2016. At the same time, both tests showed no statistically significant trend of monthly runoff values during those 37 years. With these results, we proceed to generate a new set of precipitation values for the 4 meteorological stations in the study area from 2017 to 2036 using an aleatory approach. This approach consists of select random years of daily precipitation values from the available data series (1980-2016) and uses them as new sets of daily precipitation values to fulfill the data of the new precipitation dataset from 2017 to 2036.

The SWAT model was used to analyze the future effects of the different Land-use projected scenarios on the average daily streamflow at the watershed outlet. The SWAT model for the study area was successfully calibrated and validated for streamflow. Multi-objective function statistics: coefficient of determination (R²), Nash–Sutcliffe efficiency (NSE), and root-mean-square error observations (RSR) for monthly streamflow are obtained as 0.98, 0.99, and 0.23 during the calibration period, respectively, whereas corresponding values during validation periods were 0.96, 0.98, and 0.27, respectively.

At the final calibration procedure, the model obtained a good prediction of uncertainties according to (K. Abbaspour 2012), capturing 93% of the observations, and having a 95PPU band narrower than 1 (R-factor of 0.52). For the validation procedure, the model shows also a good prediction of uncertainties, capturing 91% of the observed flows with an R-factor of 0.55. However, the reduction of the P-factor from 93% to 91% during the validation procedure, indicated uncertainties that can be related to a slight overestimation in some of the base flow values in our model, associated with uncertainties within the calibrated range values of our parameters like CN2 and SOL_K (K. Abbaspour et al. 2015; K. Abbaspour et al. 1997) and the rainfall variability inside the catchment (J. G. Arnold et al. 1998). Nevertheless, the overall result demonstrated that the SWAT model produced good results with reasonably good parameter uncertainty ranges, meaning this model can be used for further analysis of streamflow in the study area.

The results showed that the effects of the Land-use change (LUC) for the Trend scenario, increased the average daily streamflow by 1.04% in 2026 and 1.45% in 2036, in relation to 2016. For the Worst-case scenario, the average daily streamflow increased by 2.08% in 2026 and 2.37% in 2036, in relation to 2016. Finally, the average daily streamflow for the Best-case scenarios shows a decrease of 4.91% in 2026, and 6.1% in 2036, in relation to the 2016 streamflow values in the catchment.

Also, the results (Table 3-11 and Figure 3-11) show that surface runoff (SurQ) is increasing for the Trend and Worst-case scenarios, while the base flow (GWQ) is decreasing due to the expansion of agricultural lands and reduction of natural forest cover as compared to the baseline-period 2016 Land-use map. In general, natural forest

cover reductions and agricultural area increments for the Trend and Worst-case scenarios led to an average daily streamflow increment from 2016 to 2026 and 2036.

The SWAT model results show that the average daily streamflow for the different projected scenarios would be more than the 375 m³/s in any case, which is the necessary daily flow for hydropower generation at the outlet of the watershed. On the other hand, increments in soil loss rates from agricultural areas and an increasing amount of sediments that reach the HPP at the catchment outlet would be factors that could affect Hydropower production in the future.

Natural forest cover converted into agricultural lands with steep slopes, and combined with high surface runoff rates are factors that trigger erosion processes with high soil loss rates. Our results show that agricultural areas have increased over the different years and scenario simulations, both in their total number, as well as in the percentage within each slope range in the watershed. From 1990 to 2016, agricultural areas increased by 150%, and the amount of hectares on slopes greater than 20% and 35% has been gradually increasing between all scenario projections.

The LUC between all the years and scenario simulations from forest cover into agricultural lands has contributed to increasing the surface runoff (SurQ), and with that Soil losses (SL) rates in the catchment as shown in Table 3-13. Also, the results show (Figure 3-15) that agricultural areas with slope ranges above 20% exceed the tolerable soil loss rates ranges in tropics (15-25 T/Ha/Yr), which means that these rates could lead to the reduction of the fertility of the soils of the agricultural lands, affecting negatively the socio-economic development of the study area. Thus, more agricultural areas are required to produce the same amount as before; LUC processes are intensified, in particular, changes from forest cover into agricultural areas in steep slopes, affecting the natural balance of the watershed.

Therefore, it can be concluded that the spatial and temporal distribution of LU cover governs the surface runoff amount in the catchment, as well as contribute to the change in soil losses and sediments that reach the catchment outlet. In other words, the results indicate that surface runoff and soil losses are sensitive to LUC in the study area. According to the results, streamflow changes – over the future scenarios - would not be a factor that could affect the electricity production of the study area's hydropower plant in the future; however, protecting and conserving the natural forest cover and expanding soil-and-water conservation activities is highly recommended, not only to maintain the streamflow for hydropower production but also to reduce soil erosion in the catchment. Also, sustainable, site-specific, demand-driven, and integrated watershed conservation measures should be considered by the decision-makers to reduce and mitigate the LUC dynamic consequences in the upper Coca River watershed. Some of the activities and measures recommended to be implemented in the future as part of an adequate IWRM process in the basin include:

- Natural cover conservation and restoration programs implementation.
- Environmental services payment programs.
- Soil conservation practices, especially in agricultural areas with steep slopes.
- Agroforestry and silvopastoral systems implementation.
- Technology transfer programs for agricultural production efficiency.
- Spatial and urban planning at basin level.

Hydropower projects are generally very large scale and complex, and as one type of renewable energy resource, hydropower development brings in some benefits such as the flexibility of electricity production and supply. However, sustainability issues associated with hydropower developments should not be neglected; and to be able to ensure sustainable development in the CRB (which comprises the long-term hydropower production, ecosystems conservation, and the socio-economic well-being of the population in the basin), other variables and processes that were not covered in this study must be analyzed in further work within an IWRM framework.

In that regard, some additional aspects to be considered in future work include (i) Impacts of construction activities on the terrestrial and aquatic environment and species, (ii) Downstream hydrology and environmental flows, (iii) Sediment transport and erosion processes, (iv) Rare endangered species, (v) Movement of species and connectivity, (vi) Pest species within the reservoir (flora & fauna), (vii) Air and water quality, (viii) Waste management, (ix) Impacts of displacement on individuals and communities, (x) Community acceptance, (xi) Equitable distribution of the benefits of the project, (xii) Protection of cultural heritage, (xiii) Public health, (xiv) Capital cost and recurrent cost, and (xv) Green House gasses emissions.

Hydropower development in the Amazon has countless hydrological, ecological and social impacts, and critical questions about its overall sustainability remain unanswered at a variety of scales. Considering the numerous impacts of hydropower expansion in the Amazon, the reduction of this expansion should be accounted as an economic, social, and ecological investment for the future since the loss of ecological services will affect South America and the planet; however, with strong political and economic pressure to harness the Amazon's hydropower potential, this is likely unfeasible. Nevertheless, an alternative to building new generation capacity would be to implement "demand-side" energy policy solutions, such as energy conservation. Taking steps to reduce the environmental impacts of dams could be considered the "next-best" practice, including optimizing dam operations to reduce hydrologic regime alterations and improving our understanding of the links between altered hydrology and impacts on ecological and social systems.

This study was proposed to contribute to the solution of the general problems exposed at the beginning of this document, which in general, are the result of land-use changes -induced by the presence of hydropower plants- within inadequate IWRM processes, or the lack of them, in the Amazon basin. Thus, this study contributes to the analysis of Land-use change effects on the hydrology of the upper Coca River basin, towards an adequate IWRM process in the future. Where the results of this study will help the decision-makers to ensure long-term hydropower production, the conservation of natural resources, the economic development of the population, and the wellbeing of the basin ecosystems. Furthermore, is an opportunity to enhance the communication and articulation between science and policy through the analysis and design of scientifically founded solutions for two main working lines in water resources management. Finally, the combination of tools and methods used in this study represents a useful and replicable methodology to support decision processes within an IWRM framework. Especially in countries where information is scarce or not easily accessible.

Bibliography

- Abbas, T. 2016. "Uncertainty Analysis of Runoff and Sedimentation in a Forested Watershed Using Sequential Uncertainty Fitting Method." 8 (4).
- Abbaspour, K. 2012. *SWAT-CUP Calibration and Uncertainty Programs*. With the assistance of EAWAG. <https://swat.tamu.edu/software/swat-cup/>.
- Abbaspour, K., H. Johnson, and M. van Genuchten. 2004. "Estimating Uncertain Flow and Transport Parameters Using a Sequential Uncertainty Fitting Procedure." *Vadose Zone Journal* 3 (4): 1340–52. <https://doi.org/10.2113/3.4.1340>.
- Abbaspour, K., E. Rouholahnejad, S. Vaghefi, R. Srinivasan, H. Yang, and B. Kløve. 2015. "A Continental-Scale Hydrology and Water Quality Model for Europe: Calibration and Uncertainty of a High-Resolution Large-Scale SWAT Model." *Journal of Hydrology* 524:733–52. <https://doi.org/10.1016/j.jhydrol.2015.03.027>.
- Abbaspour, K., M. van Genuchten, R. Schulin, and E. Schla. 1997. "A Sequential Uncertainty Domain Inverse Procedure for Estimating Subsurface Flow and Transport Parameters." 33 (8): 1879–92.
- Abbaspour, K., J. Yang, I. Maximov, R. Siber, K. Bogner, J. Mieleitner, J. Zobrist, and R. Srinivasan. 2007. "Modelling Hydrology and Water Quality in the Pre-Alpine/alpine Thur Watershed Using SWAT." *Journal of Hydrology* 333 (2-4): 413–30. <https://doi.org/10.1016/j.jhydrol.2006.09.014>.
- Abbott, M. B., J. C. Bathurst, J. A. Cunge, P. E. O'Connell, and J. Rasmussen. 1986. "An Introduction to the European Hydrological System — Systeme Hydrologique Europeen, "SHE", 2: Structure of a Physically-Based, Distributed Modelling System." *Journal of Hydrology* 87 (1-2): 61–77. [https://doi.org/10.1016/0022-1694\(86\)90115-0](https://doi.org/10.1016/0022-1694(86)90115-0).
- Abe, C., F. Lobo, Y. Dibike, M. Costa, V. Dos Santos, and E. Novo. 2018. "Modelling the Effects of Historical and Future Land Cover Changes on the Hydrology of an Amazonian Basin." *Water* 10 (7): 932. <https://doi.org/10.3390/w10070932>.
- Adhikari, S., and J. Southworth. 2012. "Simulating Forest Cover Changes of Bannerghatta National Park Based on a CA-Markov Model: A Remote Sensing Approach." *Remote Sensing* 4 (10): 3215–43. <https://doi.org/10.3390/rs4103215>.
- Akin, A., S. Aliffi, and F. Sunar. 2014. "Spatio-Temporal Urban Change Analysis and the Ecological Threats Concerning the Third Bridge in Istanbul City." *Int. Arch. Photogramm. Remote Sens. Spatial Inf. Sci.* XL-7:9–14. <https://doi.org/10.5194/isprsarchives-XL-7-9-2014>.
- Alemayehu, T., A. van Griensven, B. Woldegiorgis, and W. Bauwens. 2017. "An Improved SWAT Vegetation Growth Module and Its Evaluation for Four Tropical Ecosystems." *Hydrol. Earth Syst. Sci.* 21 (9): 4449–67. <https://doi.org/10.5194/hess-21-4449-2017>.
- Alho, Cleber J. R., Roberto E. Reis, and Pedro P. U. Aquino. 2015. "Amazonian Freshwater Habitats Experiencing Environmental and Socioeconomic Threats Affecting Subsistence Fisheries." *Ambio* 44 (5): 412–25. <https://doi.org/10.1007/s13280-014-0610-z>.
- Almeida Prado, Fernando, Simone Athayde, Joann Mossa, Stephanie Bohlman, Flavia Leite, and Anthony Oliver-Smith. 2016. "How Much Is Enough? An Integrated Examination of Energy Security, Economic Growth and Climate Change Related to Hydropower Expansion in Brazil." *Renewable and Sustainable Energy Reviews* 53:1132–36. <https://doi.org/10.1016/j.rser.2015.09.050>.
- Al-shalabi, M., L. Billa, B. Pradhan, S. Mansor, and A. Al-sharif. 2007. "Modelling Urban Growth Evolution and Land-Use Changes Using GIS Based Cellular Automata and SLEUTH Models: The Case of Sana'a Metropolitan City, Yemen." *Environmental Earth Sciences* 70 (1): 425–37. https://www.academia.edu/10033879/Modelling_urban_growth_evolution_and_land_use_changes_using_GIS_based_cellular_automata_and_SLEUTH_models_the_case_of_Sana_a_metropolitan_city_Yemen.
- Al-sharif, A., and B. Pradhan. 2013. "Urban Sprawl Analysis of Tripoli Metropolitan City (Libya) Using Remote Sensing Data and Multivariate Logistic Regression Model." *Journal of the Indian Society of Remote Sensing* 42 (1). https://www.researchgate.net/publication/260057944_Urban_Sprawl_Analysis_of_Tripoli_Metropolitan_City_Libya_Using_Remote_Sensing_Data_and_Multivariate_Logistic_Regression_Model.

- Al-sharif, A., and B. Pradhan. 2014. "Monitoring and Predicting Land Use Change in Tripoli Metropolitan City Using an Integrated Markov Chain and Cellular Automata Models in GIS." *Arab J Geosci* 7 (10): 4291–4301. <https://doi.org/10.1007/s12517-013-1119-7>.
- Anderson, Elizabeth P., Clinton N. Jenkins, Sebastian Heilpern, Javier A. Maldonado-Ocampo, Fernando M. Carvajal-Vallejos, Andrea C. Encalada, Juan Francisco Rivadeneira et al. 2018. "Fragmentation of Andes-to-Amazon Connectivity by Hydropower Dams." *Science Advances* 4 (1): eaao1642. <https://doi.org/10.1126/sciadv.aao1642>.
- Andrade, André de Lima, and Marco Aurélio dos Santos. 2015. "Hydroelectric Plants Environmental Viability: Strategic Environmental Assessment Application in Brazil." *Renewable and Sustainable Energy Reviews* 52:1413–23. <https://doi.org/10.1016/j.rser.2015.07.152>.
- Andrianaki, M., J. Shrestha, F. Kobierska, N. Nikolaidis, and S. Bernasconi. 2019. "Assessment of SWAT Spatial and Temporal Transferability for a High-Altitude Glacierized Catchment." *Hydrol. Earth Syst. Sci.* 23 (8): 3219–32. <https://doi.org/10.5194/hess-23-3219-2019>.
- Ansar, Atif, Bent Flyvbjerg, Alexander Budzier, and Daniel Lunn. 2014. "Should We Build More Large Dams? The Actual Costs of Hydropower Megaproject Development." *Energy Policy* 69:43–56. <https://doi.org/10.1016/j.enpol.2013.10.069>.
- Arantes, Daniel B. Fitzgerald, David J. Hoeninghaus, and Kirk O. Winemiller. 2019. "Impacts of Hydroelectric Dams on Fishes and Fisheries in Tropical Rivers Through the Lens of Functional Traits." *Current Opinion in Environmental Sustainability* 37:28–40. <https://doi.org/10.1016/j.cosust.2019.04.009>.
- Araújo, C., and J. Wang. 2015. "The Dammed River Dolphins of Brazil: Impacts and Conservation." *Oryx* 49 (1): 17–24. <https://doi.org/10.1017/S0030605314000362>.
- Araya, Y., and P. Cabral. 2010. "Analysis and Modeling of Urban Land Cover Change in Setúbal and Sesimbra, Portugal." *Remote Sensing* 2 (6): 1549–63. <https://doi.org/10.3390/rs2061549>.
- Arnold, J., D. Moriasi, P. Gassman, K. Abbaspour, M. White, R. Srinivasan, C. Santhi, and R. Harmel. 2012. "SWAT: Model Use, Calibration, and Validation." 55: 1491–1508.
- Arnold, J. G., R. Srinivasan, R. S. Muttiah, and J. R. Williams. 1998. "LARGE AREA HYDROLOGIC MODELING and ASSESSMENT PART I: MODEL DEVELOPMENT." *J Am Water Resources Assoc* 34 (1): 73–89. <https://doi.org/10.1111/j.1752-1688.1998.tb05961.x>.
- Arsanjani, J., W. Kainz, and A. Mousivand. 2011. "Tracking Dynamic Land-Use Change Using Spatially Explicit Markov Chain Based on Cellular Automata: The Case of Tehran." *International Journal of Image and Data Fusion* 2 (4): 329–45. <https://doi.org/10.1080/19479832.2011.605397>.
- Athayde, Simone, Mason Mathews, Stephanie Bohlman, Walterlina Brasil, Carolina R. C. Doria, Jynessa Dutka-Gianelli, Philip M. Fearnside et al. 2019. "Mapping Research on Hydropower and Sustainability in the Brazilian Amazon: Advances, Gaps in Knowledge and Future Directions." *Current Opinion in Environmental Sustainability* 37:50–69. <https://doi.org/10.1016/j.cosust.2019.06.004>.
- Bäse, F. 2016. "Interception Loss of Changing Land Covers in the Humid Tropical Lowland of Latin America: A Synthesis of Experimental and Modeling Approaches." Cumulative dissertation, Institute of Earth and Environmental Sciences, Faculty of Mathematics and Natural Sciences at The University of Potsdam, Germany.
- Berihun, Mulatu Liyew, Atsushi Tsunekawa, Nigussie Haregeweyn, Derege Tsegaye Meshesha, Enyew Adgo, Mitsuru Tsubo, Tsugiyuki Masunaga et al. 2019. "Hydrological Responses to Land Use/land Cover Change and Climate Variability in Contrasting Agro-Ecological Environments of the Upper Blue Nile Basin, Ethiopia." *The Science of the total environment* 689:347–65. <https://doi.org/10.1016/j.scitotenv.2019.06.338>.
- Beven, K., and A. Binley. 1992. "The Future of Distributed Models: Model Calibration and Uncertainty Prediction." *Hydrol. Process.* 6 (3): 279–98. <https://doi.org/10.1002/hyp.3360060305>.
- Beven, K., and M. Kirkby. 1979. "A Physically Based, Variable Contributing Area Model of Basin Hydrology / Un Modèle À Base Physique De Zone D'appel Variable De L'hydrologie Du Bassin Versant." *Hydrological Sciences Bulletin* 24 (1): 43–69. <https://doi.org/10.1080/02626667909491834>.
- Bradley, R., M. Vuille, H. Diaz, and W. Vergara. 2006. "Climate Change. Threats to Water Supplies in the Tropical Andes." *Science (New York, N.Y.)* 312 (5781): 1755–56. <https://doi.org/10.1126/science.1128087>.
- Brouwer, R. 2005. "Uncertainties in the Economic Analysis of the European Water Framework Directive: Harmonized Techniques and Representative River Basin Data for Assessment and Use of Uncertainty Information in Integrated Water Management." E05-03.

- Brown, J. 2004. "Knowledge, Uncertainty and Physical Geography: Towards the Development of Methodologies for Questioning Belief." *Transactions of the Institute of British Geographers, New Series* 29: 367–81. <https://www.jstor.org/stable/3804497>.
- Brown, R., A. Colotelo, Brett D. Pflugrath, Craig A. Boys, Lee J. Baumgartner, Z. Daniel Deng, Luiz G. M. Silva et al. 2014. "Understanding Barotrauma in Fish Passing Hydro Structures: A Global Strategy for Sustainable Development of Water Resources." *Fisheries* 39 (3): 108–22. <https://doi.org/10.1080/03632415.2014.883570>.
- Buytaert, W., V. Iñiguez, and B. Bièvre. 2007. "The Effects of Afforestation and Cultivation on Water Yield in the Andean Páramo." *Forest Ecology and Management* 251 (1-2): 22–30. <https://doi.org/10.1016/j.foreco.2007.06.035>.
- Buytaert, W., M. Vuille, A. Dewulf, R. Urrutia, A. Karmalkar, and R. Céleri. 2010. "Uncertainties in Climate Change Projections and Regional Downscaling in the Tropical Andes: Implications for Water Resources Management." *Hydrol. Earth Syst. Sci.* 14 (7): 1247–58. <https://doi.org/10.5194/hess-14-1247-2010>.
- Buytaert et al. 2006. "Human Impact on the Hydrology of the Andean Páramos." *Earth-Science Reviews* 79 (1-2): 53–72. <https://doi.org/10.1016/j.earscirev.2006.06.002>.
- Camacho, M., E. Molero, and M. Paegelow. 2010. "Modelos Geomáticos Aplicados a La Simulación De Cambios De Usos Del Suelo. Evaluación Del Potencial De Cambio." *Tecnologías de la Información Geográfica*, 658–78.
- Camacho, MT. 2010. "MODELOS GEOMÁTICOS APLICADOS a LA SIMULACIÓN DE CAMBIOS DE USOS DEL SUELO. EVALUACIÓN DEL POTENCIAL DE CAMBIO." 658–78.
- Castello, L., David G. McGrath, Laura L. Hess, Michael T. Coe, Paul A. Lefebvre, Paulo Petry, Marcia N. Macedo, Vivian F. Renó, and Caroline C. Arantes. 2013. "The Vulnerability of Amazon Freshwater Ecosystems." *Conservation Letters* 6 (4): 217–29. <https://doi.org/10.1111/conl.12008>.
- Čerkasova, N. 2019. "Assessing Climate Change Impacts on Streamflow, Sediment and Nutrient Loadings of the Minija River (Lithuania): A Hillslope Watershed Discretization Application with High-Resolution Spatial Inputs." *Water* 11 (4): 676. <https://doi.org/10.3390/w11040676>.
- Chaplot, V., A. Saleh, and D. Jaynes. 2005. "Effect of the Accuracy of Spatial Rainfall Information on the Modeling of Water, Sediment, and NO₃-N Loads at the Watershed Level." *Journal of Hydrology* 312 (1-4): 223–34. <https://doi.org/10.1016/j.jhydrol.2005.02.019>.
- Chuncho, C. 2019. "Páramos Del Ecuador, Importancia Y Afectaciones." 9 (2): 71–83.
- CONELEC. 2009. *Plan Maestro De Electrificación 2009-2020*. With the assistance of Consejo Nacional de Electricidad. Quito, Ecuador.
- Congalton, R. 1991. "A Review of Assessing the Accuracy of Classifications of Remotely Sensed Data." *Remote Sensing of Environment* 37 (1): 35–46. [https://doi.org/10.1016/0034-4257\(91\)90048-B](https://doi.org/10.1016/0034-4257(91)90048-B).
- Coppedge, B., D. Engle, and S. Fuhlendorf. 2007. "Markov Models of Land Cover Dynamics in a Southern Great Plains Grassland Region." *Landscape Ecology* 22 (9): 1383–93. https://www.academia.edu/21591709/Markov_models_of_land_cover_dynamics_in_a_southern_Great_Plains_grassland_region?auto=download.
- dos R. Pereira, D., M. Martinez, D. Da Silva, and F. Pruski. 2016a. "Hydrological Simulation in a Basin of Typical Tropical Climate and Soil Using the SWAT Model Part II: Simulation of Hydrological Variables and Soil Use Scenarios." *Journal of Hydrology: Regional Studies* 5:149–63. <https://doi.org/10.1016/j.ejrh.2015.11.008>.
- dos R. Pereira, D., A. Mauro, F. Pruski, and D. Da Silva. 2016b. "Hydrological Simulation in a Basin of Typical Tropical Climate and Soil Using the SWAT Model Part I: Calibration and Validation Tests." *Journal of Hydrology: Regional Studies* 7:14–37. <https://doi.org/10.1016/j.ejrh.2016.05.002>.
- Duque, L., and R. Vazquez. 2015. "Water Availability Modelling for a Tropical Mountain Catchment as a Funcion of Its Soil Cover." 7.
- Easterling, D, Meehl, G. 2000. "Climate Extremes: Observations, Modeling, and Impacts." 289: 2068–74.
- Eastman, R. 2003. "IDRISI Kilimanjaro: Guide to GIS and Image Processing." <https://www.mtholyoke.edu/courses/tmillet/couse/geog307/files/Kilimanjaro%20Manual.pdf>. Accessed August 20, 2020.
- Eastman, R. 2012. "IDRISI Selva Tutorial." http://uhulag.mendelu.cz/files/pagesdata/eng/gis/idrisi_selva_tutorial.pdf. Accessed August 20, 2020.

- El-Swaify, S., E. Dangler, and C. Armstrong. 1982. *Soil Erosion by Water in the Tropics* 24. Hawaii: College of tropical agriculture and human resources. Accessed January 08, 2021. <https://www.ctahr.hawaii.edu/oc/freepubs/pdf/RES-024.pdf>.
- ENTRIX S.A. 2009. *Estudio De Impacto Ambiental Proyecto Hidroelectrico Coca Codo Sinclair*. 1st ed. 12 vols. Ecuador.
- Escrig-Olmedo, Elena, María Ángeles Fernández-Izquierdo, Idoya Ferrero-Ferrero, Juana María Rivera-Lirio, and María Jesús Muñoz-Torres. 2019. "Rating the Raters: Evaluating How ESG Rating Agencies Integrate Sustainability Principles." *Sustainability* 11 (3): 915. <https://doi.org/10.3390/su11030915>.
- Espinoza Villar, J., J. Ronchail, J. Guyot, G. Cochonneau, W. Lavado, E. Oliveira, R. Pombosa, and P. Vauchel. 2009. "Spatio-Temporal Rainfall Variability in the Amazon Basin Countries (Brazil, Peru, Bolivia, Colombia, and Ecuador)." *Int. J. Climatol.* 29 (11): 1574–94. <https://doi.org/10.1002/joc.1791>.
- Fan, F., Y. Wang, and Z. Wang. 2008. "Temporal and Spatial Change Detecting (1998-2003) And Predicting of Land Use and Land Cover in Core Corridor of Pearl River Delta (China) By Using TM and ETM+ Images." *Environmental Monitoring and Assessment* 137 (1-3): 127–47. <https://doi.org/10.1007/s10661-007-9734-y>.
- Fearnside, Philip M. 1995. "Hydroelectric Dams in the Brazilian Amazon as Sources of 'Greenhouse' Gases." *Envir. Conserv.* 22 (1): 7–19. <https://doi.org/10.1017/S0376892900034020>.
- Fearnside, Philip M. 2013. *Decision Making on Amazon Dams: Politics Trumps Uncertainty in the Madeira River Sediments Controversy*. Manaus, Amazonas, Brazil: National Institute for Research in the Amazon (INPA). <http://www.water-alternatives.org/index.php/volume6/v6issue2/218-a6-2-15/file>.
- Fearnside, Philip M. 2014. "Impacts of Brazil's Madeira River Dams: Unlearned Lessons for Hydroelectric Development in Amazonia." *Environmental Science & Policy* 38:164–72. <https://doi.org/10.1016/j.envsci.2013.11.004>.
- Fearnside, Philip M. 2016. "Environmental and Social Impacts of Hydroelectric Dams in Brazilian Amazonia: Implications for the Aluminum Industry." *World Development* 77:48–65. <https://doi.org/10.1016/j.worlddev.2015.08.015>.
- Fearnside, Philip M., and Salvador Pueyo. 2012. "Greenhouse-Gas Emissions from Tropical Dams." *Nature Clim Change* 2 (6): 382–84. <https://doi.org/10.1038/nclimate1540>.
- Ferreira, Denise, Cunha, Priscilla P. Chaves, Darley C. L. Matos, and Pia Parolin. 2013. "Impacts of Hydroelectric Dams on Alluvial Riparian Plant Communities in Eastern Brazilian Amazonian." *Anais da Academia Brasileira de Ciencias* 85 (3): 1013–23. <https://doi.org/10.1590/S0001-37652013000300012>.
- Ficklin, D., Y. Luo, E. Luedeling, and M. Zhang. 2009. "Climate Change Sensitivity Assessment of a Highly Agricultural Watershed Using SWAT." *Journal of Hydrology* 374 (1-2): 16–29. <https://doi.org/10.1016/j.jhydrol.2009.05.016>.
- Finer, Matt, and Clinton N. Jenkins. 2012. "Proliferation of Hydroelectric Dams in the Andean Amazon and Implications for Andes-Amazon Connectivity." *PLOS ONE* 7 (4): e35126. <https://doi.org/10.1371/journal.pone.0035126>.
- Fontaine, T., J. Klassen, T. Cruickshank, and R Hotchkiss. 2001. "Hydrological Response to Climate Change in the Black Hills of South Dakota, USA." *Hydrological Sciences Journal* 46 (1): 27–40. <https://doi.org/10.1080/02626660109492798>.
- GADs. 2015. *Plan De Desarrollo Y Ordenamiento Territorial: 2014-2019*. 2nd ed. 5 vols. Quito, Ecuador. Quijos, El Chaco, Pizarro, Pineda, Sucumbios.
- Galván, L., M. Olías, T. Izquierdo, J. C. Cerón, and R. Fernández de Villarán. 2014. "Rainfall Estimation in SWAT: An Alternative Method to Simulate Orographic Precipitation." *Journal of Hydrology* 509:257–65. <https://doi.org/10.1016/j.jhydrol.2013.11.044>.
- Gan, Y. 1997. "Effects of Model Complexity and Structure, Data Quality, and Objective Functions on Hydrologic Modeling." *Journal of Hydrology* 192 (1-4): 81–103. [https://doi.org/10.1016/S0022-1694\(96\)03114-9](https://doi.org/10.1016/S0022-1694(96)03114-9).
- Gassman, P. W., J. G. Arnold, R. Srinivasan, and M. R. Reyes. 2010. "The Worldwide Use of the SWAT Model: Networking Impacts, Simulation Trends, and Future Developments." Costa Rica, February 21. Accessed March 10, 2020. <https://swat.tamu.edu/media/39949/gassman.pdf>.
- Gassman, P. W., M. R. Reyes, C. H. Green, and J. G. Arnold. 2007. "THE SOIL and WATER ASSESSMENT TOOL: HISTORICAL DEVELOPMENT, APPLICATIONS, and FUTURE RESEARCH DIRECTIONS."

- 50(4) (0001-2351): 1211–50. https://www.card.iastate.edu/research/resource-and-environmental/items/asabe_swat.pdf. Accessed March 10, 2020.
- Gidey, Eskinder, Oagile Dikinya, Reuben Sebege, Eagilwe Segosebe, and Amanuel Zenebe. 2017. “Cellular Automata and Markov Chain (CA_Markov) Model-Based Predictions of Future Land Use and Land Cover Scenarios (2015–2033) In Raya, Northern Ethiopia.” *Model. Earth Syst. Environ.* 3 (4): 1245–62. <https://doi.org/10.1007/s40808-017-0397-6>.
- Githui, Faith, Wilson Gitau, Francis Mutua, and Willy Bauwens. 2009. “Climate Change Impact on SWAT Simulated Streamflow in Western Kenya.” *Int. J. Climatol.* 29 (12): 1823–34. <https://doi.org/10.1002/joc.1828>.
- Grill, Günther, Bernhard Lehner, Alexander E. Lumsdon, Graham K. MacDonald, Christiane Zarfl, and Catherine Reidy Liermann. 2015. “An Index-Based Framework for Assessing Patterns and Trends in River Fragmentation and Flow Regulation by Global Dams at Multiple Scales.” *Environ. Res. Lett.* 10 (1): 15001. <https://doi.org/10.1088/1748-9326/10/1/015001>.
- Guan, DongJie, HaiFeng Li, Takuro Inohae, Weici Su, Tadashi Nagaie, and Kazunori Hokao. 2011. “Modeling Urban Land Use Change by the Integration of Cellular Automaton and Markov Model.” *ECOL MODEL* 222 (20-22): 3761–72. <https://doi.org/10.1016/j.ecolmodel.2011.09.009>.
- Guo, Hua. 2008. “Annual and Seasonal Streamflow Responses to Climate and Land-Cover Changes in the Poyang Lake Basin, China.” *Journal of Hydrology* 355 (1-4): 106–22. <https://doi.org/10.1016/j.jhydrol.2008.03.020>.
- Hadi, Sinan Jasim, Helmi Z. M. Shafri, and Mustafa D. Mahir. 2014. “Modelling LULC for the Period 2010-2030 Using GIS and Remote Sensing: A Case Study of Tikrit, Iraq.” *IOP Conference Series: Earth and Environmental Science (EES)* 20 (1): 11. http://inis.iaea.org/search/search.aspx?orig_q=RN:47050835.
- Halmy, Marwa Waseem A., Paul E. Gessler, Jeffrey A. Hicke, and Boshra B. Salem. 2015. “Land Use/land Cover Change Detection and Prediction in the North-Western Coastal Desert of Egypt Using Markov-CA.” *Applied Geography* 63:101–12. <https://doi.org/10.1016/j.apgeog.2015.06.015>.
- Hamad, Rahel, Heiko Balzter, and Kamal Kolo. 2018. “Predicting Land Use/Land Cover Changes Using a CA-Markov Model Under Two Different Scenarios.” *Sustainability* 10 (10): 3421. <https://doi.org/10.3390/su10103421>.
- Hargreaves, G. L. 1985. “Agricultural Benefits for Senegal River Basin.” *Journal of Irrigation and Drainage Engineering* 111 (2): 113–24. [https://doi.org/10.1061/\(ASCE\)0733-9437\(1985\)111:2\(113\)](https://doi.org/10.1061/(ASCE)0733-9437(1985)111:2(113)).
- Hasan, M., and G. Wyseure. 2018. “Impact of Climate Change on Hydropower Generation in Rio Jubones Basin, Ecuador.” *Water Science and Engineering* 11 (2): 157–66. <https://doi.org/10.1016/j.wse.2018.07.002>.
- Hassaballah, K., M. Yasir, S. Uhlenbrook, and K. Biro. 2017. “Analysis of Streamflow Response to Land Use and Land Cover Changes Using Satellite Data and Hydrological Modelling: Case Study of Dinder and Rahad Tributaries of the Blue Nile (Ethiopia–Sudan).” *Hydrol. Earth Syst. Sci.* 21 (10): 5217–42. <https://doi.org/10.5194/hess-21-5217-2017>.
- He, Chunyang, Norio Okada, Qiaofeng Zhang, Peijun Shi, and Jingshui Zhang. 2006. “Modeling Urban Expansion Scenarios by Coupling Cellular Automata Model and System Dynamic Model in Beijing, China.” *Applied Geography* 26 (3-4): 323–45. <https://doi.org/10.1016/j.apgeog.2006.09.006>.
- Huang, Jun, Pute Wu, and Xining Zhao. 2013. “Effects of Rainfall Intensity, Underlying Surface and Slope Gradient on Soil Infiltration Under Simulated Rainfall Experiments.” *Catena* 104:93–102. <https://doi.org/10.1016/j.catena.2012.10.013>.
- Hyandye, Canute, and Lawrence W. Martz. 2017. “A Markovian and Cellular Automata Land-Use Change Predictive Model of the Usangu Catchment.” *International Journal of Remote Sensing* 38 (1): 64–81. <https://doi.org/10.1080/01431161.2016.1259675>.
- Iacono, Michael, David Levinson, Ahmed El-Geneidy, and Rania Wasfi. 2015. “A Markov Chain Model of Land Use Change.” 263-276 *Paginazione / Tema. Journal of Land Use, Mobility and Environment, Energy and Mobility: Strategies for Consumptions’ Reduction / Tema. Journal of Land Use, Mobility and Environment, Vol 8, N° 3 (2015): Cities, Energy and Mobility: Strategies for Consumptions’ Reduction. 1* 8 (3): 263–76. <https://doi.org/10.6092/1970-9870/2985>.
- IPCC, ed. 2008. *Climate Change and Water; Technical Paper 4*. IPCC Technical Paper 6. Accessed May 20, 2021. <https://archive.ipcc.ch/pdf/technical-papers/climate-change-water-en.pdf>.
- Jain, Sharad K., Sanjay K. Jain, Neha Jain, and Chong-Yu Xu. 2017. “Hydrologic Modeling of a Himalayan Mountain Basin by Using the SWAT Mode.” *Hydrol. Earth Syst. Sci. Discuss.*, 1–26. <https://doi.org/10.5194/hess-2017-100>.

- Jakeman, A. J. 2003. "Integrated Assessment and Modelling: Features, Principles and Examples for Catchment Management." *Environmental Modelling & Software* 18 (6): 491–501. [https://doi.org/10.1016/S1364-8152\(03\)00024-0](https://doi.org/10.1016/S1364-8152(03)00024-0).
- Jønch-Clausen, Torkil. 2004. "'...Integrated Water Resources Management (IWRM) And Water Efficiency Plans by 2005' Why, What and How?" *Global Water Partnership*, 1–45.
- Juckem, P.F, R.J. Hunt, M.P. Anderson, and Dale M. Robertson. 2008. "Effects of Climate and Land Management Change on Streamflow in the Driftless Area of Wisconsin." *Journal of Hydrology* 355 (1-4): 123–30. <https://doi.org/10.1016/j.jhydrol.2008.03.010UR>.
- Kahn, James, Carlos Freitas, and Miguel Petre. 2014. "False Shades of Green: The Case of Brazilian Amazonian Hydropower." *Energies* 7 (9): 6063–82. <https://doi.org/10.3390/en7096063>.
- Keenan, Rodney J. 2015. "Climate Change Impacts and Adaptation in Forest Management: A Review." *Annals of Forest Science* 72 (2): 145–67. <https://doi.org/10.1007/s13595-014-0446-5>.
- Kendall, Maurice G. 1970. *Rank Correlation Methods*. 4th ed. London: Griffin. <http://worldcatlibraries.org/wcpa/oclc/3827024>.
- Keshkar, Hamidreza, and Winfried Voigt. 2016. "A Spatiotemporal Analysis of Landscape Change Using an Integrated Markov Chain and Cellular Automata Models." *Model. Earth Syst. Environ.* 2 (1): 1–13. <https://doi.org/10.1007/s40808-015-0068-4>.
- Khalid, Khairi, Mohd Fozi Ali, Nor Faiza Abd Rahman, Muhamad Radzali Mispan, Siti Humaira Haron, Zulhafizal Othman, and Mohd Fairuz Bachok. 2016. "Sensitivity Analysis in Watershed Model Using SUFI-2 Algorithm." *Procedia Engineering* 162:441–47. <https://doi.org/10.1016/j.proeng.2016.11.086>.
- Khoi, Dao Nguyen, and Vu Thi Thom. 2015. "Parameter Uncertainty Analysis for Simulating Streamflow in a River Catchment of Vietnam." *Global Ecology and Conservation* 4:538–48. <https://doi.org/10.1016/j.gecco.2015.10.007>.
- Klemes, V. 1986. "Operational Testing of Hydrological Simulation Models." *Hydrological Sciences Journal* 31 (1): 13–24. <https://doi.org/10.1080/02626668609491024>.
- Koch, Franziska, Monika Prash, Heike Bach, Wolfram Mauser, Florian Appel, and Markus Weber. 2011. "How Will Hydroelectric Power Generation Develop Under Climate Change Scenarios? A Case Study in the Upper Danube Basin." *Energies* 4 (10): 1508–41. <https://doi.org/10.3390/en4101508>.
- Kundu, S., D. Khare, and A. Mondal. 2017. "Past, Present and Future Land Use Changes and Their Impact on Water Balance." *Journal of environmental management* 197:582–96. <https://doi.org/10.1016/j.jenvman.2017.04.018>.
- Lambin, Eric F., and Helmut Geist, eds. 2006. *Land-Use and Land-Cover Change: Local Processes and Global Impacts*. Global change. Berlin, New York: Springer.
- Laraque, Alain, Catalina Ceron, E. Armijos, R. Pombosa, Philippe Magat, and Jean-Loup Guyot. 2004. "Sediment Yields and Erosion Rates in the Napo River Basin : An Ecuadorian Andean Amazon Tributary." 288. https://horizon.documentation.ird.fr/exl-doc/pleins_textes/divers17-08/010046799.pdf. Accessed January 09, 2021.
- Latrubesse, Edgardo. 2014. "The Late Pleistocene in Amazonia: A Paleoclimatic Approach." In *Southern Hemisphere Paleo- and Neoclimates: Key Sites, Methods, Data and Models*, edited by Peter Smolka and Wolfgang Volkheimer, 209–24. Berlin, Heidelberg: Springer Verlag. https://www.researchgate.net/profile/Edgardo-Latrubesse/publication/278653145_The_Late_Pleistocene_in_Amazonia_A_Paleoclimatic_Approach/links/5b25e9208ae092e9650669e/The-Late-Pleistocene-in-Amazonia-A-Paleoclimatic-Approach.pdf. Accessed May 21, 2021.
- Latrubesse, Edgardo. 2015. "Large Rivers, Megafans and Other Quaternary Avulsive Fluvial Systems: A Potential "Who's Who" in the Geological Record." *Earth-Science Reviews* 146:1–30. <https://doi.org/10.1016/j.earscirev.2015.03.004>.
- Latrubesse, Edgardo, Eugenio Y. Arima, Thomas Dunne, Edward Park, Victor Baker, Fernando d'Horta, Charles Wright et al. 2017. *Damming the Rivers of the Amazon Basin*.
- Latrubesse, Edgardo, Fernando M. d'Horta, Camila C. Ribas, Florian Wittmann, Jansen Zuanon, Edward Park, Thomas Dunne, Eugenio Y. Arima, and Paul A. Baker. 2021. "Vulnerability of the Biota in Riverine and Seasonally Flooded Habitats to Damming of Amazonian Rivers." *Aquatic Conserv: Mar Freshw Ecosyst* 31 (5): 1136–49. <https://doi.org/10.1002/aqc.3424>.

- Latrubesse, Edgardo, and A. Rancy. 1998. *The Late Quaternary of the Upper Juruá River, Southwestern Amazonia, Brazil: Geology and Vertebrate Paleontology* 11. https://www.researchgate.net/publication/284777523_The_Late_Quaternary_of_the_Upper_Jurua_River_southwestern_Amazonia_Brazil_Geology_and Vertebrate_paleontology.
- Lee, Sangchul, In-Young Yeo, Ali M. Sadeghi, Gregory W. McCarty, Wells D. Hively, Megan W. Lang, and Amir Sharifi. 2018. "Comparative Analyses of Hydrological Responses of Two Adjacent Watersheds to Climate Variability and Change Using the SWAT Model." *Hydrol. Earth Syst. Sci.* 22 (1): 689–708. <https://doi.org/10.5194/hess-22-689-2018>.
- Lees, Alexander C., Carlos A. Peres, Philip M. Fearnside, Maurício Schneider, and Jansen A. S. Zuanon. 2016. "Hydropower and the Future of Amazonian Biodiversity." *Biodivers Conserv* 25 (3): 451–66. <https://doi.org/10.1007/s10531-016-1072-3>.
- Leta, Olkeba Tolessa, Aly I. El-Kadi, Henrietta Dulai, and Kariem A. Ghazal. 2016. "Assessment of Climate Change Impacts on Water Balance Components of Heeia Watershed in Hawaii." *Journal of Hydrology: Regional Studies* 8:182–97. <https://doi.org/10.1016/j.ejrh.2016.09.006>.
- Li, S. H., B. X. Jin, X. Y. Wei, Y. Y. Jiang, and J. L. Wang. 2015. "USING CA-MARKOV MODEL to MODEL the SPATIOTEMPORAL CHANGE of LAND USE/COVER in FUXIAN LAKE for DECISION SUPPORT." *ISPRS Ann. Photogramm. Remote Sens. Spatial Inf. Sci.* II-4/W2:163–68. <https://doi.org/10.5194/isprsannals-II-4-W2-163-2015>.
- Li, Tiejian, Guangqian Wang, Ji Chen, and Hao Wang. 2011. "Dynamic Parallelization of Hydrological Model Simulations." *Environmental Modelling & Software* 26 (12): 1736–46. <https://doi.org/10.1016/j.envsoft.2011.07.015>.
- Liermann, Catherine Reidy, Christer Nilsson, James Robertson, and Rebecca Y. Ng. 2012. "Implications of Dam Obstruction for Global Freshwater Fish Diversity." *BioScience* 62 (6): 539–48. <https://doi.org/10.1525/bio.2012.62.6.5>.
- Lin, Bingqing, Xingwei Chen, Huaxia Yao, Ying Chen, Meibing Liu, Lu Gao, and April James. 2015. "Analyses of Landuse Change Impacts on Catchment Runoff Using Different Time Indicators Based on SWAT Model." *Ecological Indicators* 58:55–63. <https://doi.org/10.1016/j.ecolind.2015.05.031>.
- Lobato, T. C., R. A. Hauser-Davis, T. F. Oliveira, A. M. Silveira, H.A.N. Silva, M.R.M. Tavares, and A.C.F. Saraiva. 2015. "Construction of a Novel Water Quality Index and Quality Indicator for Reservoir Water Quality Evaluation: A Case Study in the Amazon Region." *Journal of Hydrology* 522:674–83. <https://doi.org/10.1016/j.jhydrol.2015.01.021>.
- Lopez-Morrero, T. 2011. "Multicriteria Evaluation and Geographic Information Systems." *Earth & Environmental Science Research & Reviews* 2 (5). https://www.academia.edu/41597149/Multi_Criteria_Evaluation_and_Geographic_Information_Systems_for_Land_Use_Planning_and_Decision_Making.
- Ludwig, F., E. van Slobbe, and W. Cofino. 2014. "Climate Change Adaptation and Integrated Water Resource Management in the Water Sector." *Journal of Hydrology* 518:235–42. <https://doi.org/10.1016/j.jhydrol.2013.08.010>.
- Luo, P., K. Takara, B. He, W. CAO, Y. Yamashiki, and D. Nover. 2011. "CALIBRATION and UNCERTAINTY ANALYSIS of SWAT MODEL in a JAPANESE RIVER CATCHMENT." *J. JSCE* 67 (4): I_61-I_66. https://doi.org/10.2208/jscejhe.67.I_61.
- Mandal, U. K. 2014. "Geo-Information Based Spatio-Temporal Modeling of Urban Land Use and Land Cover Change in Butwal Municipality, Nepal." *Int. Arch. Photogramm. Remote Sens. Spatial Inf. Sci.* XL-8:809–15. <https://doi.org/10.5194/isprsarchives-XL-8-809-2014>.
- Mango, L. M., A. M. Melesse, M. E. McClain, D. Gann, and S. G. Setegn. 2011. "Land Use and Climate Change Impacts on the Hydrology of the Upper Mara River Basin, Kenya: Results of a Modeling Study to Support Better Resource Management." *Hydrol. Earth Syst. Sci.* 15 (7): 2245–58. <https://doi.org/10.5194/hess-15-2245-2011>.
- Mann, Henry B. 1945. "Nonparametric Tests Against Trend." *Econometrica* 13 (3): 245. <https://doi.org/10.2307/1907187>.
- Marengo, J., and J. Espinoza. 2016. "Extreme Seasonal Droughts and Floods in Amazonia: Causes, Trends and Impacts." *Int. J. Climatol.* 36 (3): 1033–50. <https://doi.org/10.1002/joc.4420>.

- Marengo, J., C. Souza, Kirsten Thonicke, Chantelle Burton, Kate Halladay, Richard A. Betts, Lincoln M. Alves, and Wagner R. Soares. 2018. "Changes in Climate and Land Use over the Amazon Region: Current and Future Variability and Trends." *Front. Earth Sci.* 6:228. <https://doi.org/10.3389/feart.2018.00228>.
- Mas, J.F y Sandoval, F. 2011. "Modelacion De Los Cambios De Coberturasuso Del Suelo En Una Region Tropical De Mexico." *Geotrópico*, 1–24.
- Mekonnen, Dagnenet Fenta, Zheng Duan, Tom Rientjes, and Markus Disse. 2018. "Analysis of Combined and Isolated Effects of Land-Use and Land-Cover Changes and Climate Change on the Upper Blue Nile River Basin's Streamflow." *Hydrol. Earth Syst. Sci.* 22 (12): 6187–6207. <https://doi.org/10.5194/hess-22-6187-2018>.
- Memarian, Hadi, Siva K. Balasundram, Karim C. Abbaspour, Jamal B. Talib, Christopher Teh Boon Sung, and Alias Mohd Sood. 2012. "SWAT-Based Hydrological Modelling of Tropical Land Use Scenarios." *Hydrological Sciences Journal* 59 (10): 1808–29. https://www.academia.edu/16145732/SWAT-based_Hydrological_Modelling_of_Tropical_Land_Use_Scenarios?email_work_card=title.
- Mishra, V., P. Rai, and K. Mohan. 2014. "Prediction of Land Use Changes Based on Land Change Modeler (LCM) Using Remote Sensing: A Case Study of Muzaffarpur (Bihar), India." *J geographical I JC* 64 (1): 111–27. <https://doi.org/10.2298/IJGI1401111M>.
- Monteiro, J., M. Strauch, R. Srinivasan, K. Abbaspour, and B. Gücker. 2016. "Accuracy of Grid Precipitation Data for Brazil: Application in River Discharge Modelling of the Tocantins Catchment." *Hydrol. Process.* 30 (9): 1419–30. <https://doi.org/10.1002/hyp.10708>.
- Monteith, J. L. 1965. "Evaporation and Environment." *Symposia of the Society for Experimental Biology* 19: 205–34.
- Mora, D., L. Campozano, F. Cisneros, G. Wyseure, and P. Willems. 2014. "Climate Changes of Hydrometeorological and Hydrological Extremes in the Paute Basin, Ecuadorean Andes." *Hydrol. Earth Syst. Sci.* 18 (2): 631–48. <https://doi.org/10.5194/hess-18-631-2014>.
- Moriasi, D. N. 2007. "MODEL EVALUATION GUIDELINES for SYSTEMATIC QUANTIFICATION of ACCURACY in WATERSHED SIMULATIONS." 50 (ISSN 0001–2351): 885–900.
- Mukherjee, S., S. Shashtri, C. K. Singh, P. K. Srivastava, and M. Gupta. 2009. "Effect of Canal on Land Use/land Cover Using Remote Sensing and GIS." *J Indian Soc Remote Sens* 37 (3): 527–37. <https://doi.org/10.1007/s12524-009-0042-6>.
- Naghbi, Fereydoun, Mahmoud Reza Delavar, and Bryan Pijanowski. 2016. "Urban Growth Modeling Using Cellular Automata with Multi-Temporal Remote Sensing Images Calibrated by the Artificial Bee Colony Optimization Algorithm." *Sensors (Basel, Switzerland)* 16 (12). <https://doi.org/10.3390/s16122122>.
- Nath, Biswajit, Zhihua Wang, Yong Ge, Kamrul Islam, Ramesh P. Singh, and Zheng Niu. 2020. "Land Use and Land Cover Change Modeling and Future Potential Landscape Risk Assessment Using Markov-CA Model and Analytical Hierarchy Process." *IJGI* 9 (2): 134. <https://doi.org/10.3390/ijgi9020134>.
- Neitsch, Susan Lynn. 2002. "Soil and Water Assessment Tool Theoretical Documentation." <https://swat.tamu.edu/media/1290/swat2000theory.pdf>. Accessed March 03, 2020.
- Neitsch, Susan Lynn. 2005. "SWAT 2005 Theoretical Documentation." <https://swat.tamu.edu/media/1292/swat2005theory.pdf>. Accessed March 03, 2020.
- Neitsch, Susan Lynn, J. G. Arnold, J. R. Kiniry, and J. R. Williams. 2011. *Soil and Water Assessment Tool Theoretical Documentation 2009* 406. Texas: Texas A&M University. Accessed March 05, 2020.
- Nie, Wenming, Yongping Yuan, William Kepner, Maliha S. Nash, Michael Jackson, and Caroline Erickson. 2011. "Assessing Impacts of Landuse and Landcover Changes on Hydrology for the Upper San Pedro Watershed." *Journal of Hydrology* 407 (1-4): 105–14. <https://doi.org/10.1016/j.jhydrol.2011.07.012>.
- Nolivos, Indira, Marcos Villacís, Raúl F. Vázquez, Diego E. Mora, Luis Domínguez-Granda, Henrietta Hampel, and Elizabeth Velarde. 2015. "Challenges for a Sustainable Management of Ecuadorian Water Resources." *Sustainability of Water Quality and Ecology* 6:101–6. <https://doi.org/10.1016/j.swaqe.2015.02.002>.
- Notter, B., L. MacMillan, D. Viviroli, R. Weingartner, and H. P. Liniger. 2007. "Impacts of Environmental Change on Water Resources in the Mt. Kenya Region." *JOURNAL OF HYDROLOGY -AMSTERDAM-* 343 (3-4): 266–78.
- Nunes, J., M. Campos, F. Oliveira, and J. Macedo. 2012. "Tolerância De Perda De Solo Por Erosão Na Região Sul Do Amazonas / Soil Loss Tolerance in Southern Amazon." *Ambiência* 8 (3): 859–68. <https://doi.org/10.5777/ambiencia.2012.05.05>.

- Odusanya, Abolanle E., Bano Mehdi, Christoph Schürz, Adebayo O. Oke, Olufiropo S. Awokola, Julius A. Awomeso, Joseph O. Adejuwon, and Karsten Schulz. 2019. “Multi-Site Calibration and Validation of SWAT with Satellite-Based Evapotranspiration in a Data-Sparse Catchment in Southwestern Nigeria.” *Hydrol. Earth Syst. Sci.* 23 (2): 1113–44. <https://doi.org/10.5194/hess-23-1113-2019>.
- Olenin, Sergej. “Čerkasova_PhD Draft_FINAL_edited.”
- Oliveira, Marcos H. Costa, Britaldo S. Soares-Filho, and Michael T. Coe. 2013. “Large-Scale Expansion of Agriculture in Amazonia May Be a No-Win Scenario.” *Environ. Res. Lett.* 8 (2): 24021. <https://doi.org/10.1088/1748-9326/8/2/024021>.
- Omar, N. Q., S. A. M. Sanusi, W. M. W. Hussin, N. Samat, and K. S. Mohammed. 2014. “Markov-CA Model Using Analytical Hierarchy Process and Multiregression Technique.” *IOP Conf. Ser. Earth Environ. Sci.* 20:12008. <https://doi.org/10.1088/1755-1315/20/1/012008>.
- Padilla, Cruz, and Valero. 2015. “Estudio Multitemporal Y Analisis Del Cambio De Uso Del Suelo Y Cobertura Vegetal En La Microcuenca Del Río Cristal Mediante El Uso De Autómatas Celulares.”
- Pahl-Wostl, C. 2002. “Towards Sustainability in the Water Sector – the Importance of Human Actors and Processes of Social Learning.” *Aquat. Sci.* 64 (4): 394–411. <https://doi.org/10.1007/PL00012594>.
- Pahl-Wostl, C. 2007. “Transitions Towards Adaptive Management of Water Facing Climate and Global Change.” *Water Resour Manage* 21 (1): 49–62. <https://doi.org/10.1007/s11269-006-9040-4>.
- Palmeirim, Ana Filipa, Carlos A. Peres, and Fernando C.W. Rosas. 2014. “Giant Otter Population Responses to Habitat Expansion and Degradation Induced by a Mega Hydroelectric Dam.” *Biological Conservation* 174:30–38. <https://doi.org/10.1016/j.biocon.2014.03.015>.
- Pelicice, Valter M. Azevedo-Santos, Jean R. S. Vitule, Mário L. Orsi, Dilermando P. Lima Junior, André L. B. Magalhães, Paulo S. Pompeu, Miguel Petreire, and Angelo A. Agostinho. 2017. “Neotropical Freshwater Fishes Imperilled by Unsustainable Policies.” *Fish Fish* 18 (6): 1119–33. <https://doi.org/10.1111/faf.12228>.
- Pettitt, A. N. 1979. “A Non-Parametric Approach to the Change-Point Problem.” *Applied Statistics* 28 (2): 126. <https://doi.org/10.2307/2346729>.
- Podwojewski, P., and J. Poulencard. 2000. “Los Suelos De Los Paramos Del Ecuador.” (Quito, Ecuador).
- Pontius, Gil R., and Jeffrey Malanson. 2005. “Comparison of the Structure and Accuracy of Two Land Change Models.” *International Journal of Geographical Information Science* 19 (2): 243–65. <https://doi.org/10.1080/13658810410001713434>.
- Premalatha, M., Tabassum-Abbasi, Tasneem Abbasi, and S. A. Abbasi. 2014. “A Critical View on the Eco-Friendliness of Small Hydroelectric Installations.” *The Science of the total environment* 481:638–43. <https://doi.org/10.1016/j.scitotenv.2013.11.047>.
- Priestley, C., and R. Taylor. 1972. “On the Assessment of Surface Heat Flux and Evaporation Using Large-Scale Parameters.” *Mon. Wea. Rev.* 100 (2): 81–92. [https://doi.org/10.1175/1520-0493\(1972\)100<0081:OTAOSH>2.3.CO;2](https://doi.org/10.1175/1520-0493(1972)100<0081:OTAOSH>2.3.CO;2).
- Qi, Junyu, Sheng Li, Charles P.-A. Bourque, Zisheng Xing, and Fan-Rui Meng. 2018. “Developing a Decision Support Tool for Assessing Land Use Change and BMPs in Ungauged Watersheds Based on Decision Rules Provided by SWAT Simulation.” *Hydrol. Earth Syst. Sci.* 22 (7): 3789–3806. <https://doi.org/10.5194/hess-22-3789-2018>.
- Refsgaard, J. van der Sluijs, A. Hojberg, and P. Vanrolleghem. 2007. *Harmoni-CA Guidance Uncertainty Analysis*. Netherlands. Guidance 1.
- Refsgaard, J., and H. Henriksen. 2004. “Modelling Guidelines—terminology and Guiding Principles.” *Advances in Water Resources* 27 (1): 71–82. <https://doi.org/10.1016/j.advwatres.2003.08.006>.
- Refsgaard, J., B. Nilsson, J. Brown, B. Klauer, R. Moore, T. Bech, M. Vurro et al. 2005. “Harmonised Techniques and Representative River Basin Data for Assessment and Use of Uncertainty Information in Integrated Water Management (HarmoniRiB).” *Environmental Science & Policy* 8 (3): 267–77. <https://doi.org/10.1016/j.envsci.2005.02.001>.
- Rimal, Bhagawat, Lifu Zhang, Hamidreza Keshtkar, Nan Wang, and Yi Lin. 2017. “Monitoring and Modeling of Spatiotemporal Urban Expansion and Land-Use/Land-Cover Change Using Integrated Markov Chain Cellular Automata Model.” *IJGI* 6 (9): 288. <https://doi.org/10.3390/ijgi6090288>.
- Rocha, J., and JC. Ferreira. 2007. “Modelling Coastal and Land Use Evolution Patterns Through Neural Network and Cellular Automata Integration.” 827–31.

https://www.academia.edu/6279118/Modelling_Coastal_and_Land_Use_Evolution_Patterns_through_Neural_Network_and_Cellular_Automata_Integration?auto=download.

- Santos, Rangel Eduardo, Ricardo Motta Pinto-Coelho, Maria Auxiliadora Drumond, Rogério Fonseca, and Fabrício Berton Zanchi. 2020a. "Damming Amazon Rivers: Environmental Impacts of Hydroelectric Dams on Brazil's Madeira River According to Local Fishers' Perception." *Ambio* 49 (10): 1612–28. <https://doi.org/10.1007/s13280-020-01316-w>.
- Santos, Rangel Eduardo, Ricardo Motta Pinto-Coelho, Maria Auxiliadora Drumond, Rogério Fonseca, and Fabrício Berton Zanchi. 2020b. "Damming Amazon Rivers: Environmental Impacts of Hydroelectric Dams on Brazil's Madeira River According to Local Fishers' Perception." *Ambio* 49 (10): 1612–28. <https://doi.org/10.1007/s13280-020-01316-w>.
- Sayemuzzaman, Mohammad, and Manoj K. Jha. 2014. "MODELING of FUTURE LAND COVER LAND USE CHANGE in NORTH CAROLINA USING MARKOV CHAIN and CELLULAR AUTOMATA MODEL." *American Journal of Engineering and Applied Sciences* 7 (3): 295–306. <https://doi.org/10.3844/ajeassp.2014.295.306>.
- Schoups, G., N. C. van de Giesen, and H. C. Savenije. 2008. "Model Complexity Control for Hydrologic Prediction." *Water Resour. Res.* 44 (12): 203. <https://doi.org/10.1029/2008WR006836>.
- Sen, P. K. 1968. "Estimates of the Regression Coefficient Based on Kendall's Tau." 1968. <https://www.eea.europa.eu/data-and-maps/indicators/oxygen-consuming-substances-in-rivers/sen-pranab-kumar-1968>.
- SENPLADES. 2014. *Planificación Hídrica Nacional*. With the assistance of Secretaria Nacional de Planificación y Desarrollo. 1st ed. 1 vol. Quito, Ecuador: CISPDR.
- Sierra, Rodrigo. 2013. *Patrones Y Factores De Deforestación En El Ecuador Continental, 1990-2010. Y Un Acercamiento a Los Próximos 10 Años*. With the assistance of GeoIS Consultores. Quito, Ecuador.
- Sloan, P., I. Moore, G. Coltharp, and J. Eigel. 1983. "Modeling Surface and Subsurface Stormflow on Steeply-Sloping Forested Watersheds." *KWRRRI Research Reports*. <https://doi.org/10.13023/kwrrri.rr.142>.
- Stickler, Claudia M., Michael T. Coe, Marcos H. Costa, Daniel C. Nepstad, David G. McGrath, Livia C. P. Dias, Hermann O. Rodrigues, and Britaldo S. Soares-Filho. 2013. "Dependence of Hydropower Energy Generation on Forests in the Amazon Basin at Local and Regional Scales." *Proceedings of the National Academy of Sciences of the United States of America* 110 (23): 9601–6. <https://doi.org/10.1073/pnas.1215331110>.
- Stonestrom, D., B. Scanlon, and L. Zhang. 2009. "Introduction to Special Section on Impacts of Land Use Change on Water Resources." *Water Resour. Res.* 45 (7). <https://doi.org/10.1029/2009WR007937>.
- Strauch, Michael, and Martin Volk. 2013. "SWAT Plant Growth Modification for Improved Modeling of Perennial Vegetation in the Tropics." *Ecological Modelling* 269:98–112. <https://doi.org/10.1016/j.ecolmodel.2013.08.013>.
- Subedi, Praveen, Kabiraj Subedi, and Bina Thapa. 2013. "Application of a Hybrid Cellular Automaton – Markov (CA-Markov) Model in Land-Use Change Prediction: A Case Study of Saddle Creek Drainage Basin, Florida." *AEES* 1 (6): 126–32. <https://doi.org/10.12691/aees-1-6-5>.
- Surabuddin Mondal, M., Nayan Sharma, Martin Kappas, and P. K. Garg. 2013. "Modeling of Spatio-Temporal Dynamics of Land Use and Land Cover in a Part of Brahmaputra River Basin Using Geoinformatic Techniques." *Geocarto International* 28 (7): 632–56. <https://doi.org/10.1080/10106049.2013.776641>.
- Tamm, Ottar. 2016. "Modeling Future Changes in the North-Estonian Hydropower Production by Using SWAT." *Hydrology Research* 47 (4): 835–46. <https://doi.org/10.2166/nh.2015.018>.
- The State of World Fisheries and Aquaculture 2018: Meeting the Sustainable Development Goals*. 2018. State of world fisheries and aquaculture 2018. Rome: Food and Agriculture Organization of the United Nations. Accessed May 20, 2021. <http://www.fao.org/3/i9540en/i9540en.pdf>.
- Timpe, Kelsie, and David Kaplan. 2017. "The Changing Hydrology of a Dammed Amazon." *Science Advances* 3 (11): e1700611. <https://doi.org/10.1126/sciadv.1700611>.
- Tundisi, J. G., J. Goldemberg, T. Matsumura-Tundisi, and A.C.F. Saraiva. 2014. "How Many More Dams in the Amazon?" *Energy Policy* 74:703–8. <https://doi.org/10.1016/j.enpol.2014.07.013>.
- Tuo, Ye, Zheng Duan, Markus Disse, and Gabriele Chiogna. 2016. "Evaluation of Precipitation Input for SWAT Modeling in Alpine Catchment: A Case Study in the Adige River Basin (Italy)." *Science of The Total Environment* 573:66–82. <https://doi.org/10.1016/j.scitotenv.2016.08.034>.

- UN Water, GWP. 2007. *Roadmapping for Advancing Integrated Water Resources Management (IWRM) Processes: UN-Water and the Global Water Partnership*.
- UN Water, GWP. 2013. "Integrated Water Resources Management." https://unece.org/fileadmin/DAM/env/water/publications/NPD_IWRM_study/ECE_MP.WAT_44_en.pdf. Accessed May 24, 2021.
- UN WCED. 1987. *United Nations World Commission on Environment and Development*. 17 vols. Energy 7. https://idl-bnc-idrc.dspacedirect.org/bitstream/handle/10625/152/wced_v17_doc149.pdf.
- Urrutia, R., and M. Vuille. 2009. "Climate Change Projections for the Tropical Andes Using a Regional Climate Model: Temperature and Precipitation Simulations for the End of the 21st Century." *J. Geophys. Res.* 114 (D2). <https://doi.org/10.1029/2008JD011021>.
- USDA, S.C.S. 1972. *National Engineering Handbook Section 4 Hydrology*. Accessed March 12, 2020. <https://directives.sc.egov.usda.gov/OpenNonWebContent.aspx?content=18393.wba>.
- Valero, O., A. Padilla, and M. Cruz. 2012. "Estudio Multitemporal Y Análisis Prospectivo De Cambio De Uso Del Suelo Y Cobertura Del Río Cristal."
- van der Keur, P., H. J. Henriksen, J. C. Refsgaard, M. Brugnach, C. Pahl-Wostl, A. Dewulf, and H. Buiteveld. 2008. "Identification of Major Sources of Uncertainty in Current IWRM Practice. Illustrated for the Rhine Basin." *Water Resour Manage* 22 (11): 1677–1708. <https://doi.org/10.1007/s11269-008-9248-6>.
- van der Sluijs, J. et al. 2004. "RIVM/MNPGuidance ForUncertaintyAssessment AndCommunication Tool Catalogue ForUncertainty Assessment." <http://www.nusap.net/sections.php?op=viewarticle&artid=17>.
- van Griensven, A., P. Ndomba, S. Yalaw, and F. Kilonzo. 2012. "Critical Review of SWAT Applications in the Upper Nile Basin Countries." *Hydrol. Earth Syst. Sci.* 16 (9): 3371–81. <https://doi.org/10.5194/hess-16-3371-2012>.
- Vanrolleghem, P., J. Refsgaard, J. van der Sluijs, and A. Hojberg. 2010. *Modelling Aspects of Water Framework Directive Implementation*. London, New York: IWA Pub.
- Verburg, P. H., G.H.J. de Koning, K. Kok, A. Veldkamp, and J. Bouma. 2002. "A Spatial Explicit Allocation Procedure for Modelling the Pattern of Land Use Change Based Upon Actual Land Use." *ECOL MODEL* 116 (1): 45–61. [https://doi.org/10.1016/S0304-3800\(98\)00156-2](https://doi.org/10.1016/S0304-3800(98)00156-2).
- Verburg, Peter H., Kasper Kok, Robert Gilmore Pontius, and A. Veldkamp. 2006. "Modeling Land-Use and Land-Cover Change." In *Land-Use and Land-Cover Change: Local Processes and Global Impacts*, edited by Eric F. Lambin and Helmut Geist, 117–35. Global change. Berlin, New York: Springer.
- Vilaysane, Bounhieng, Kaoru Takara, Pingping Luo, Inthavy Akkharath, and Weili Duan. 2015. "Hydrological Stream Flow Modelling for Calibration and Uncertainty Analysis Using SWAT Model in the Xedone River Basin, Lao PDR." *Procedia Environmental Sciences* 28:380–90. <https://doi.org/10.1016/j.proenv.2015.07.047>.
- Volk, M. 2016. "Application of the Soil and Water Assessment Tool (SWAT) To Predict the Impact of Alternative Management Practices on Water Quality and Quantity." https://www.academia.edu/5056123/Application_of_the_Soil_and_Water_Assessment_Tool_SWAT_to_predict_the_impact_of_alternative_management_practices_on_water_quality_and_quantity?email_work_card=view-paper.
- Volk, M., S. Lorz, and M. Strauch. 2012. "Using Precipitation Data Ensemble for Uncertainty Analysis in SWAT Streamflow Simulation." https://www.academia.edu/5056061/Using_precipitation_data_ensemble_for_uncertainty_analysis_in_SWAT_streamflow_simulation.
- Vuille, M., R. Bradley, M. Werner, and F. Keimig. 2003. "20th Century Climate Change in the Tropical Andes: Observations and Model Results." *Climatic Change* 59 (1/2): 75–99. <https://doi.org/10.1023/A:1024406427519>.
- Walker, W. E., P. Harremoës, J. Rotmans, J. P. van der Sluijs, M.B.A. van Asselt, P. Janssen, and M. P. Krayen von Krauss. 2003. "Defining Uncertainty: A Conceptual Basis for Uncertainty Management in Model-Based Decision Support." *Integrated Assessment* 4 (1): 5–17. <https://doi.org/10.1076/iaij.4.1.5.16466>.
- Wang, X.Q. Zheng, X.B. Zang, S. Q. Wang, X. Q. Zheng, and X. B. Zang. 2012. "Accuracy Assessments of Land Use Change Simulation Based on Markov-Cellular Automata Model." *Procedia Environmental Sciences* 13. <https://cyberleninka.org/article/n/896081>.

- WFS. 2004. "Common Implementation Strategy for the Water Framework Directive." *WFD Common Implementation Strategy*. <http://forum.europa.eu.int/Members/irc/env/wfd/home>.
- Winchell, M., R. Srinivasan, M. Di Luzio, and J. G. Arnold. 2013. "Arcswat Interface for SWAT2012: User's Guide." 1–464.
- Winemiller, P. B. McIntyre, L. Castello, E. Fluet-Chouinard, T. Giarrizzo, S. Nam, I. G. Baird et al. 2016. "DEVELOPMENT and ENVIRONMENT. Balancing Hydropower and Biodiversity in the Amazon, Congo, and Mekong." *Science (New York, N.Y.)* 351 (6269): 128–29. <https://doi.org/10.1126/science.aac7082>.
- Worku, T., D. Khare, and S. Tripathi. 2017. "Modeling Runoff–sediment Response to Land Use/land Cover Changes Using Integrated GIS and SWAT Model in the Beressa Watershed." *Environ Earth Sci* 76 (16). <https://doi.org/10.1007/s12665-017-6883-3>.
- Yang, Jing, Yongbo Liu, Wanhong Yang, and Yaning Chen. 2012. "Multi-Objective Sensitivity Analysis of a Fully Distributed Hydrologic Model WetSpa." *Water Resour Manage* 26 (1): 109–28. <https://doi.org/10.1007/s11269-011-9908-9>.
- Yang, Xin, Xin-Qi Zheng, and Rui Chen. 2014. "A Land Use Change Model: Integrating Landscape Pattern Indexes and Markov-CA." *Ecological Modelling* 283 (C): 1–7. https://econpapers.repec.org/article/eeeecomod/v_3a283_3ay_3a2014_3ai_3ac_3ap_3a1-7.htm.
- Ye, Baoying, and Zhongke Bai. 2008. "Simulating Land Use/Cover Changes of Nenjiang County Based on CA-Markov Model." In *Computer and Computing Technologies in Agriculture, Volume I: First IFIP TC 12 International Conference on Computer and Computing Technologies in Agriculture (CCTA 2007), Wuyishan, China, August 18-20, 2007*, edited by Daoliang Li, 321–29. The International Federation for Information Processing 258. Boston, MA: International Federation for Information Processing.
- Yirsaw, Eshetu, Wei Wu, Xiaoping Shi, Habtamu Temesgen, and Belew Bekele. 2017. "Land Use/Land Cover Change Modeling and the Prediction of Subsequent Changes in Ecosystem Service Values in a Coastal Area of China, the Su-Xi-Chang Region." *Sustainability* 9 (7): 1204. <https://doi.org/10.3390/su9071204>.
- Yuanyuan Yang, Shuwen Zhang, Jiuchun Yang, Xiaoshi Xing, Dongyan Wang, Yuanyuan Yang, Shuwen Zhang, Jiuchun Yang, Xiaoshi Xing, and Dongyan Wang. 2015. "Using a Cellular Automata-Markov Model to Reconstruct Spatial Land-Use Patterns in Zhenlai County, Northeast China." *Energies* 8 (5). <https://cyberleninka.org/article/n/338568>.
- Yusuf, Yusuf Ahmed, Biswajeet Pradhan, and Mohammed O. Idrees. 2014. "Spatio-Temporal Assessment of Urban Heat Island Effects in Kuala Lumpur Metropolitan City Using Landsat Images." *J Indian Soc Remote Sens* 42 (4): 829–37. <https://doi.org/10.1007/s12524-013-0342-8>.
- Zahar, Y., A. Ghorbel, and J. Albergel. 2008. "Impacts of Large Dams on Downstream Flow Conditions of Rivers: Aggradation and Reduction of the Medjerda Channel Capacity Downstream of the Sidi Salem Dam (Tunisia)." *Journal of Hydrology* 351 (3-4): 318–30. <https://doi.org/10.1016/j.jhydrol.2007.12.019>.

Acknowledgments

Quem me der também apanha.

- Mestre Burguês

This research would not have been possible without the support and goodwill of several extraordinary persons - I will be eternally grateful to all of them for making this thesis possible.

First, I would like to express my deep gratitude to my supervisor Dr.-Ing. Uwe Ehret. Thank you for your incredible support, both academically and personally. Thank you for your guidance along with the whole process, and thank you very much for this opportunity.

Without the help of the wonderful people that work at the KIT's Institute of Water and River Basin Management – Chair of Hydrology, this study would not have been possible. I would like to thank Prof. Dr. Erwin Zehe, Dr. Jan Wienhöfer, Sibylle Hassler, Franziska Villinger, Rik van Pruijssen, Lucas Reid, Malte Neuper, Mirko Mälicke, Svenja Hoffmeister, Jan Bondy, Samuel Schroers, Nicolas Rodriguez, Maria Rieger, Raziye Fiden and Jutta Szabadics, for their general support, and for all the good moments we had in the last years playing Kubb.

A special thank goes to Stephanie Thiesen, Ralf Loritz, and Alcides Aybar, for your support and expertise, which helped me to improve my research.

I gratefully acknowledge the DAAD-STIBET – doctoral candidates Program, and the KIT-INTL for partly funding my Ph.D. thesis. Furthermore, I would like to express my gratitude to the National Secretary of Science, Technology, and Innovation of Ecuador (SENESCYT) for the scholarship that I was granted to start my Ph.D. program.

I would also like to deeply thank my partner Hana and her family, for pushing me to be better, for being by my side during all this journey with unconditional support, and for cheering me up under difficult situations. I also want to thank my faithful companions Knut and Baloo, for reminding me that happiness lies in enjoying the little things in life. Last but not least, I want to thank my family in Ecuador, because, despite the distance and the difficulties, they always gave me their support in any possible way.

The life path is not easy, it takes time, and something often gets in the way. Still...Get it done.

Author's declaration

This dissertation was prepared without any illegal assistance, and it has not been submitted for any other degree or at any other University for examination, neither in Germany nor elsewhere.

Karlsruhe, Germany, 2021.

Carlos Zuleta Salmon